



Yvonne Moritz, BSc

# **Effect of Cyclometalation on the Photophysical Properties of Luminescent Dyes**

## **MASTER'S THESIS**

to achieve the university degree of

Diplom-Ingenieurin

Master's degree programme: Technical Chemistry

submitted to

**Graz University of Technology**

Supervisor

Assoc. Prof. kand. Sergey Borisov

Institute of Analytical Chemistry and Food Chemistry

Graz, September, 2018



---

## Abstract

The aim of this thesis was to investigate the effect of cyclometalation on the photophysical properties of luminescent dyes, whereby special focus was placed on porphyrin dyes. During the experimental work, a novel Pd-porphyrin complex, which was cyclometalated on the porphyrin core, was synthesized. Compared to the non-cyclometalated analogous dye, the complex showed a significant red-shift of absorption and emission spectra. Furthermore, as expected the lifetime was decreased by a factor of 100 from 0.69 ms to 9.8  $\mu$ s of the cyclometalated porphyrin. Unfortunately, quantum yields were determined to be significantly lower in respect to the non-cyclometalated dye. Besides cyclometalation on the porphyrin core, also peripheral cyclometalation of porphyrins and of anthraquinone-based dyes was attempted.

Additionally, improvement of the reaction conditions for the platination of  $\pi$ -extended porphyrins was aimed during this thesis. Two new Pt-precursors including (1,5-cyclooctadiene)dimethylplatinum(II) and bis[dimethyl( $\mu$ -dimethyl sulfide)platinum(II)] were synthesized. Both precursors were found to be suitable for platination reactions, whereby especially the latter allowed platination of benzoporphyrins under much milder reaction conditions than those known in literature.

---

## Kurzfassung

Das Ziel dieser Arbeit war es, den Effekt der Cyclometallierung auf die photophysikalischen Eigenschaften von lumineszierenden Farbstoffen zu untersuchen; hierbei wurde der Fokus im Speziellen auf Porphyrin-Farbstoffe gelegt. Während der experimentellen Arbeit war es möglich, einen neuen - direkt am Porphyrin Gerüst cyclometallierten - Pd-Porphyrin-Komplex zu synthetisieren. Im Vergleich mit dem nicht cyclometallierten analogen Farbstoff zeigte sich, dass dieser Komplex eine signifikante Rot-Verschiebung des Absorptions- und Emissionsspektrums aufwies. Des Weiteren, verringerte sich die Lebenszeit der cyclometallierten Komponente wie erwartet um einen Faktor 100 von 0.69 ms auf 9.8  $\mu$ s. Die gemessenen Quantenausbeuten zeigten einen deutlich niedrigeren Wert verglichen mit dem nicht cyclometallierten Komplex. Außerdem wurde die periphere Cyclometallierung von Porphyrinen sowie Anthraquinon-basierten Farbstoffen untersucht.

Ein weiteres Ziel dieser Master-Arbeit war es, die Reaktionsbedingungen für die Platinierung von  $\pi$ -expandierten Porphyrinen (z. B. Benzoporphyrine) zu optimieren. Zwei unterschiedliche Platin-Reagenzien, (1,5-Cyclooctadien)dimethylplatin(II) und bis[Dimethyl( $\mu$ -dimethylsulfid)platin(II)] wurden zu diesem Zweck synthetisiert. Beide Reagenzien erwiesen sich als gute Alternative für die Durchführung von Platinierungsreaktionen; im Speziellen das letzte genannte Reagenz machte die Platinierung von Benzoporphyrinen unter deutlich mildereren Bedingungen als bisher in der Literatur bekannten möglich.

---

## EIDESSTATTLICHE ERKLÄRUNG

Ich erkläre an Eides statt, dass ich die vorliegende Arbeit selbstständig verfasst, andere als die angegebenen Quellen/Hilfsmittel nicht benutzt, und die den benutzten Quellen wörtlich und inhaltlich entnommenen Stellen als solche kenntlich gemacht habe. Das in TUGRAZonline hochgeladene Textdokument ist mit der vorliegenden Masterarbeit identisch.

## AFFIDAVIT

I declare that I have authored this thesis independently that I have not used other than the declared sources/resources, and that I have explicitly indicated all material which has been quoted either literally or by content from the sources used. The text document uploaded to TUGRAZonline is identical to the present master's thesis.

---

09.09.2018

Datum/Date

---

*Yvonne Moritz*

Unterschrift/Signature

---

## Danksagung

Auf diesem Wege möchte ich mich bei all jenen Personen bedanken, die mich während meiner Master Arbeit und auch während des gesamten Studiums unterstützt und begleitet haben.

Vielen Dank Sergey, für die großartige Unterstützung während meiner gesamten Master Arbeit. Du hast mir stets bei jeder Fragestellung weitergeholfen und mir viele neue Ansätze aufgezeigt, wenn ich einmal nicht weiter wusste. Aufgrund deines fundierten Wissens und vor allem deiner immensen Begeisterung für die Welt der Farbstoffe, könnte ich mir keinen besseren Betreuer für die Verfassung einer Master Arbeit vorstellen. Großer Dank gilt auch Ingo, für die Möglichkeit, meine Master Arbeit in deiner Arbeitsgruppe durchführen zu dürfen.

Dankeschön Andi, dass du mir als quasi Zweit-Betreuer stets bei jeglichen Fragen sofort weiter geholfen hast, mir immer wieder Vorschläge gebracht hast, welche weiteren Ansätze ich verfolgen könnte und mir durch Verbesserungsvorschläge ermöglicht hast, mein experimentelles Arbeiten weiterzuentwickeln.

Großer Dank gilt auch der gesamten Arbeitsgruppe für das Schaffen eines so lustigen und gleichzeitig produktiven und hilfreichen Arbeitsumfeldes. Bei jeglichen Problemen und Fragestellungen habt ihr mir stets sofort weitergeholfen; durch die vielen lustigen Kaffeepausen und "Kuchentreffen" kam auch der Spaß nicht zu kurz.

Danke an meine Freundinnen und Studienkolleginnen Carina, Kathi und Elli; es war eine unglaublich lustige und schöne Erfahrung, mit euch die letzten fünf Jahre zu verbringen und jegliche Herausforderungen mit euch gemeinsam zu meistern.

Außerdem möchte ich mich bei meiner Familie und vor allem bei meinen Eltern bedanken, die mir überhaupt erst dieses Studium ermöglichten und ohne deren Unterstützung ich niemals so weit gekommen wäre. Danke Jenny, dass du die beste Zwillingsschwester bist, die man sich nur vorstellen kann und mir während meines Studiums stets Mut zugesprochen hast, wenn ich mal vor scheinbar unlösbaren Schwierigkeiten stand. Flo, danke dass du mich im letzten Abschnitt meines Studiums so wundervoll unterstützt hast, mir stets geduldig weitergeholfen hast wenn mich die LaTeX-Software zum Verzweifeln brachte und an mich geglaubt hast wenn ich selbst an mir zweifelte.

Abschließend möchte ich mich bei meinem ehemaligen Chemie Prof. Herrn Dipl.-Ing. Manfred Sussitz bedanken, ohne welchen ich möglicherweise nie meine Begeisterung für die Welt der Chemie entdeckt hätte.

Yvonne Moritz, BSc

Graz, September, 2018

---

# Contents

<b>1</b>	<b>Introduction</b>	<b>1</b>
<b>2</b>	<b>Theoretical Part</b>	<b>3</b>
2.1	Principle of luminescence . . . . .	3
2.2	Physical background of light absorption . . . . .	4
2.2.1	Forbidden transitions . . . . .	4
2.2.2	Franck-Condon principle . . . . .	5
2.3	Jablonski-diagram . . . . .	5
2.3.1	Internal conversion . . . . .	6
2.3.2	Fluorescence . . . . .	6
2.3.3	Intersystem Crossing . . . . .	7
2.3.4	Phosphorescence . . . . .	7
2.3.5	Delayed fluorescence . . . . .	7
2.4	Lifetime and quantum yields . . . . .	8
2.4.1	Effect on temperature . . . . .	9
2.5	Optical sensors in analytical chemistry . . . . .	9
2.5.1	Sensing methodologies . . . . .	9
2.6	Optical oxygen sensing . . . . .	11
2.6.1	Important indicator dyes for oxygen sensing . . . . .	11
2.7	Quenching of Luminescence . . . . .	11
2.7.1	Static quenching . . . . .	12
2.7.2	Dynamic quenching . . . . .	12
2.8	Optical pH-sensing . . . . .	13
2.8.1	pH-Indicator dyes . . . . .	13
2.9	State-of-the-art of porphyrins in optical sensing . . . . .	15
2.9.1	NIR-indicators . . . . .	16
2.9.2	UV-VIS spectra of porphyrins . . . . .	18
2.10	Platination of metal-free porphyrins . . . . .	19
2.11	Cyclometalated indicator dyes . . . . .	21
2.11.1	Tuning of photophysical properties of porphyrins by cyclometalation . . . . .	22
<b>3</b>	<b>Chemicals and Methods</b>	<b>24</b>
3.1	Chemicals . . . . .	24
3.2	Solvents . . . . .	24
3.2.1	NMR solvents . . . . .	25
3.3	Chromatography . . . . .	25
3.3.1	Thin layer chromatography (TLC) . . . . .	25
3.3.2	Flash column chromatography . . . . .	25
3.4	Photophysical measurements . . . . .	26
3.4.1	Absorption spectra . . . . .	26
3.4.2	Emission and excitation spectra . . . . .	26

3.4.3	Lifetime measurements . . . . .	26
3.4.4	Relative quantum yields . . . . .	26
3.5	Structural characterization . . . . .	26
3.5.1	Nuclear magnetic resonance spectroscopy (NMR) . . . . .	26
3.5.2	High resolution mass spectrometry (MALDI-TOF) . . . . .	27
<b>4</b>	<b>Experimental</b>	<b>28</b>
4.1	Synthesis of Pt-precursors for platination and cyclometalation reactions . . . . .	28
4.1.1	Potassium tetrachloroplatinate (II) $K_2PtCl_4$ . . . . .	28
4.1.2	Synthesis of Bis[Dimethyl( $\mu$ -Dimethyl Sulfide)Platinum(II)] (2) . . . . .	29
4.1.3	Synthesis of [Pt(acac)Cl(DMSO)] (4) . . . . .	31
4.1.4	[Synthesis of PtMe <sub>2</sub> (COD)] (7) . . . . .	32
4.2	Platination reactions with synthesized Pt-precursors . . . . .	34
4.2.1	Synthesis of PtTPTBP (8) using compound 2 as a precursor . . . . .	34
4.2.2	Attempted synthesis of PtTFPP (9) using compound 2 as a precursor . . . . .	34
4.2.3	Synthesis of PtTPTBP (8) using compound 7 as a precursor . . . . .	35
4.3	Synthesis of suitable structures for cyclometalation reactions . . . . .	36
4.3.1	Porphyrins for peripheral cyclometalation . . . . .	36
4.3.2	Synthesis of porphyrins suitable for cyclometalation at the porphyrin core . . . . .	38
4.3.3	Synthesis of other dyes besides porphyrins suitable for cyclometalation (16) . . . . .	40
4.4	Synthesis of cyclometalated complexes . . . . .	41
4.4.1	Attempted synthesis of cyclometalated compound 17 . . . . .	41
4.4.2	Synthesis of cyclometalated compound 18 . . . . .	42
4.5	Characterization of the cyclometalated complex (18) . . . . .	43
4.5.1	Excitation and emission spectra . . . . .	43
4.5.2	Lifetime measurements . . . . .	43
<b>5</b>	<b>Results and Discussion</b>	<b>44</b>
5.1	Synthetic considerations . . . . .	44
5.1.1	Synthesis of new platinum-precursors for platination reactions . . . . .	45
5.1.2	Improvement of the reaction conditions for platination reactions of benzoporphyrins . . . . .	47
5.1.3	Dyes with structures suitable for cyclometalation . . . . .	50
5.1.4	Cyclometalation reactions . . . . .	53
5.1.5	Characterization of the cyclometalated Pd-porphyrin-dye (18) . . . . .	65
<b>6</b>	<b>Conclusion and Outlook</b>	<b>67</b>
<b>7</b>	<b>Bibliography</b>	<b>69</b>
<b>8</b>	<b>List of Figures</b>	<b>77</b>
<b>9</b>	<b>List of Tables</b>	<b>80</b>
<b>10</b>	<b>Appendix</b>	<b>81</b>
10.1	NMR-spectra of synthesized compounds . . . . .	81
10.1.1	<i>Cis/trans</i> -dichlorobis(dimethyl sulfide)platinum(II) (compound (1)) . . . . .	81
10.1.2	Bis[dimethyl( $\mu$ -dimethyl sulfide)platinum(II)] (compound 2) . . . . .	82
10.1.3	[PtMe <sub>2</sub> (COD)] (compound (7)) . . . . .	83

---

10.1.4	2-(Tributylstannyl)pyridine (compound (10)) . . . . .	84
10.1.5	Disubstituted compound 12 (compound (12a)) . . . . .	85
10.1.6	Monosubstituted compound 12 (compound (12b)) . . . . .	86
10.1.7	Porphyrin ligand (compound (13)) . . . . .	87
10.1.8	Pd-porphyrin-complex (compound (14)) . . . . .	88
10.1.9	Monosubstituted compound (16 a) . . . . .	89
10.1.10	Disubstituted compound (16 b) . . . . .	90
10.1.11	Cyclometalated complex (compound 18) . . . . .	91
10.2	MS-Data . . . . .	92
10.2.1	Cyclometalated complex (compound 18) . . . . .	92
10.3	Supporting information for synthetic considerations . . . . .	93
10.3.1	Cyclometalation attempts using $K_2PtCl_4$ . . . . .	93
10.3.2	Cyclometalation attempts using $Pt(BN)_2Cl_2$ . . . . .	94
10.3.3	Cyclometalation attempts using newly synthesized Pt-precursors . . . . .	94
10.3.4	Attempted optimization of reaction conditions for the cyclometalation of compound 14 . . . . .	95
10.3.5	Further attempted cyclometalation reactions using compound 4 as a precursor . . . . .	96
10.4	Abbreviations . . . . .	97



---

# 1 Introduction

During the last decades, optical sensors have gained more and more attention in analytical chemistry, as they are inexpensive, miniaturizable and allow contact-less measurement [1–3]. Typically, measurements with optical sensors are based on absorption and luminescence. A large variety of indicator dyes may be used that show a change of luminescence intensity depending on the analyte concentration. Usually, these dyes are embedded in a polymer matrix; depending on the type of indicator and matrix material, optical sensors can be used for a large variety of applications [1].

One of the analytes of high interest is oxygen, due to the reason that optical oxygen sensors find – amongst other fields – applications in medicine [4], chemical industry and environmental sciences (e.g. marine research) [5]. Several years ago, the Clark electrode [6] was considered the standard technique for measurement of oxygen concentrations, however in comparison to optical sensors the electrode shows electrical interference and does not allow contact-less measurement [7]. Optical oxygen sensors rely on quenching of luminescence of the respective indicator dye in the presence of oxygen. Hereby, measurements can be based on intensity or lifetime, however lifetime tends to be the preferred parameter, as it is not affected by external perturbations [8]. Typical classes of indicator dyes for oxygen sensing include ruthenium complexes such as  $[\text{Ru}(\text{bpy})_3]$  [9–11], metallo-porphyrins and polycyclic aromatic hydrocarbons [12, 13], whereby latter are not commonly used anymore.

Metallo-porphyrins - especially platinum (II) and palladium (II) porphyrins - are highly interesting for oxygen sensing applications, due to their chemical stability, high luminescence, large Stoke's shift and long lifetimes [7, 14]. Examples for this class of indicators are Pt(II) and Pd(II) octaethylporphyrins (PtOEP, PdOEP) [15] or Pt(II) and Pd(II) tetrakis(pentafluorophenylporphyrins) (PdTFPP, PtTFPP) [16, 17]. While OEP exhibit poor photostability, TFPP are able to overcome this drawback, however both types of indicator dyes suffer from the disadvantage of only absorbing light in the visible region. Due to this problem, measurements of biological samples, which show autofluorescence or measurements in scattering media, such as marine sediments, can hardly be performed using UV-VIS indicators [7]. Indicators that are better suitable for applications in biological samples are dyes that emit in the NIR-region (780 nm - 3  $\mu\text{m}$ ).

NIR-dyes tend to be especially useful for light-conversion applications such as OLEDs [18–20], due to the reason that nearly half of the sun's energy reaching the earth is NIR-radiation [21, 22]. However, also sensing of oxygen with NIR-indicators is of enormous value [7, 23, 24]. In order to obtain porphyrin dyes that emit in the NIR region, a bathochromic shift of absorption and emission bands is required, which can be achieved by different structural changes on the porphyrin macrocycle.

For instance, Pt(II) and Pd(II) porphyrin ketones [25] and lactones [26] show emission in the NIR-region, however their brightness is rather low. Another group are  $\pi$ -extended porphyrins, such as Pd(II) and Pt(II) benzo- and naphthoporphyrins, which are widely used for oxygen sensing. They can be obtained by extension of the porphyrin structure with various aromatic

moieties.

However, besides  $\pi$ -extension of porphyrins, adjustment of the spectral properties of these dyes tends to be difficult, as simple structural modification only show limited influence. Nevertheless, close control over these properties would be highly favourable for a variety of applications.

Besides porphyrins, several cyclometalated Ir(III) [27–29] and Pt(II) [30, 31] complexes are known in literature that can be used as indicators for optical sensing. These dyes typically exhibit strong luminescence, high quantum yields and good photostability. However, they suffer from the drawbacks of showing rather short decay times and low molar absorption coefficients in the visible region, wherefore they are often unsuitable for certain applications [7].

In the course of this Master's thesis, it was attempted to alter the spectral properties of porphyrins by the method of cyclometalation. Combination of porphyrin dyes with the concept of cyclometalation might lead to several advantageous properties such as tuneable emissive lifetimes, high absorption coefficients and bathochromic shifts of absorption and emission. The introduction of heavy atoms leads to strong spin-orbit coupling and therefore typically to reduced lifetimes and higher quantum yields. During the experimental work of this thesis it was tried to investigate the effect of cyclometalation on luminescent dyes such as porphyrins and to establish a structure-property relationships.

---

## 2 Theoretical Part

Most of the content of this chapter is based on references [32–34]. Therefore, only additional references will be displayed separately.

### 2.1 Principle of luminescence

Luminescence describes the process of the emission of photons (ultraviolet, visible or infrared) from electronically excited species. Depending on the excitation mechanism, different types of luminescence such as chemiluminescence, electroluminescence or photoluminescence exist. Regarding the process of photoluminescence, absorption of a photon takes place, leading to an electronic excited state, which can then undergo a de-excitation process by photon emission. There are different types of luminescent compounds which are divided into three groups: organic compounds (e.g. aromatic hydrocarbons, fluorescein, coumarins), inorganic compounds (e.g. lanthanide ions such as  $\text{Eu}^{3+}$  or crystals such as ZnS) and organometallic compounds (e.g. ruthenium complexes, complexes with fluorogenic chelating agents).

Two very important cases of luminescence are phosphorescence and fluorescence. These two radiative processes can be distinguished regarding the excited state from which photons are emitted, which is a singlet excited state for fluorescence and a triplet excited state for phosphorescence. Furthermore, many other de-excitation pathways can occur: internal conversion, vibrational relaxation, intersystem crossing (which might be followed by the occurrence of phosphorescence), conformational changes or intramolecular charge transfer. (figure 2.1) Moreover, it is possible that interactions between other molecules and the species in the excited state take place, which can then compete with de-excitation; examples for this processes are electron/proton/energy transfer, or exciplex and excimer formation.

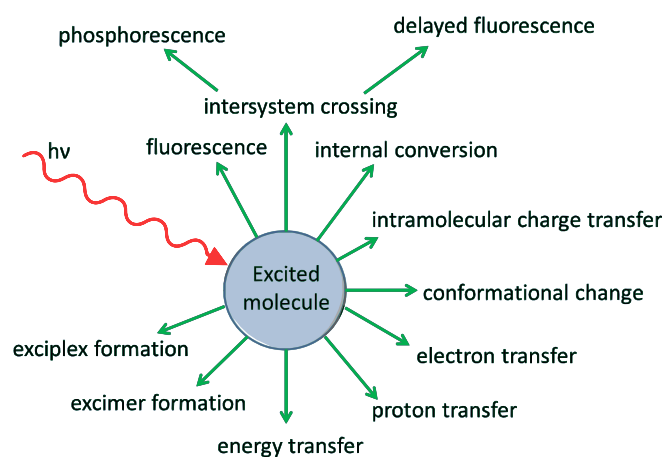


**Figure 2.1:** Possible de-excitation processes for excited molecules

## 2.2 Physical background of light absorption

In order to understand electronic transitions in molecules, one needs to take a closer look at the respective orbitals. Typically, an electronic transition is the movement of an electron from an orbital of a molecule that is located in the ground state to another unoccupied orbital. Regarding absorption and fluorescence spectroscopy there are two types of orbitals, which are of high importance: the Lowest Unoccupied Molecular Orbitals (LUMO) and the Highest Occupied Molecular Orbitals (HOMO), whereby both refer to the ground state of the respective molecule.

If one of the two electrons with opposite spin of a molecular orbital in the ground state is promoted to an orbital of a higher energy, its spin remains unchanged, leading to a total spin quantum number of zero and an excited singlet state. ( $S = \sum s_i$ , whereby  $s_i = +\frac{1}{2}$  or  $-\frac{1}{2}$ )

Besides the singlet-singlet transition mentioned above, it is possible that the promoted electron might change its spin, leading to two electrons with parallel spins. In this case, the total spin quantum number equals to 1 and the multiplicity is 3 ( $M = 2S + 1$ ), wherefore this state is called a triplet state. In figure 2.2 the different spin orientations for an excited singlet or triplet state are displayed.

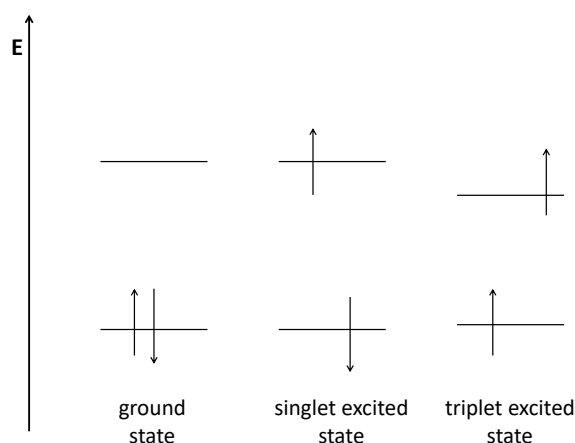


**Figure 2.2:** Difference in spin orientation for excited singlet or triplet states

It can be observed that the triplet state, which indicates three states of equal energy, has a lower energy compared to that of a singlet state. (Hund's Rule)

### 2.2.1 Forbidden transitions

Two important selection rules apply for absorption transitions, which are called spin-forbidden transitions and symmetry-forbidden transitions.

The first selection rule (spin-forbidden transitions) states that between states of different multiplicities no transitions are allowed. (e.g. singlet-triplet transitions) However, as a matter of fact there is still a weak interaction between wavefunctions of different multiplicities present, which is a result of the so-called spin-orbit coupling. For example, the process of intersystem crossing (from singlet excited state  $S_1$  to triplet state  $T_1$ ) is only occurring due to spin-orbit coupling. Intersystem crossing can be enhanced by the introduction of heavy atoms, as the intensity of the coupling depends on the fourth power of the atomic number.

The second selection rule states that transitions may also be forbidden for symmetry reasons. However, it is nevertheless possible to observe these types of transitions due to vibronic coupling, meaning that the vibrations of the molecule lead to a departure from perfect symmetry.

### 2.2.2 Franck-Condon principle

According to the Franck-Condon principle, nuclei show an extensively higher mass than electrons, leading to the circumstance that nuclei cannot respond as fast as the electronic transitions take place. Therefore, electronic transitions occur most likely without a change in the nuclear framework. The transition can be imagined to take place along a vertical line, wherefore the expression vertical transition is commonly used, meaning that no change of nuclear geometry occurred.

Typically, most molecules are located in the lowest vibrational level of the ground state at room temperature, however besides the 0-0 electronic transitions also vibronic transitions can take place, which are dependent on the relative horizontal positions of the potential energy curves (figure 2.3).

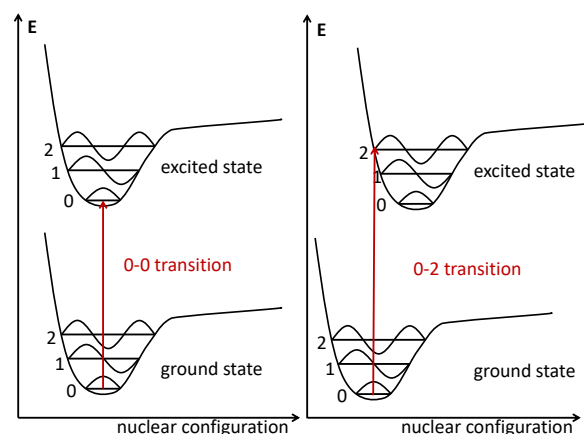


**Figure 2.3:** Potential energy diagrams for different vertical transitions

## 2.3 Jablonski-diagram

All processes that might occur between the excitation and de-excitation of a molecule can be visualized with help of the Jablonski-diagram. (figure 2.4 ) The most important processes occurring are absorption, internal conversion, fluorescence, vibrational relaxations, intersystem crossing, phosphorescence and delayed fluorescence. The ground state and the excited singlet states are depicted by  $S_0$ ,  $S_1$  and  $S_2$ , the triplet state is shown with the abbreviation  $T_1$ . Each of the electronic energy levels consists of various vibrational energy levels. The time required for transitions lies within the range of  $10^{-15}$  s; as mentioned above according to the Franck-Condon principle, this time is too short to lead to a displacement of the nuclei. The most important radiative and non-radiative processes that occur between the different electronic states will be discussed in more detail in the following.

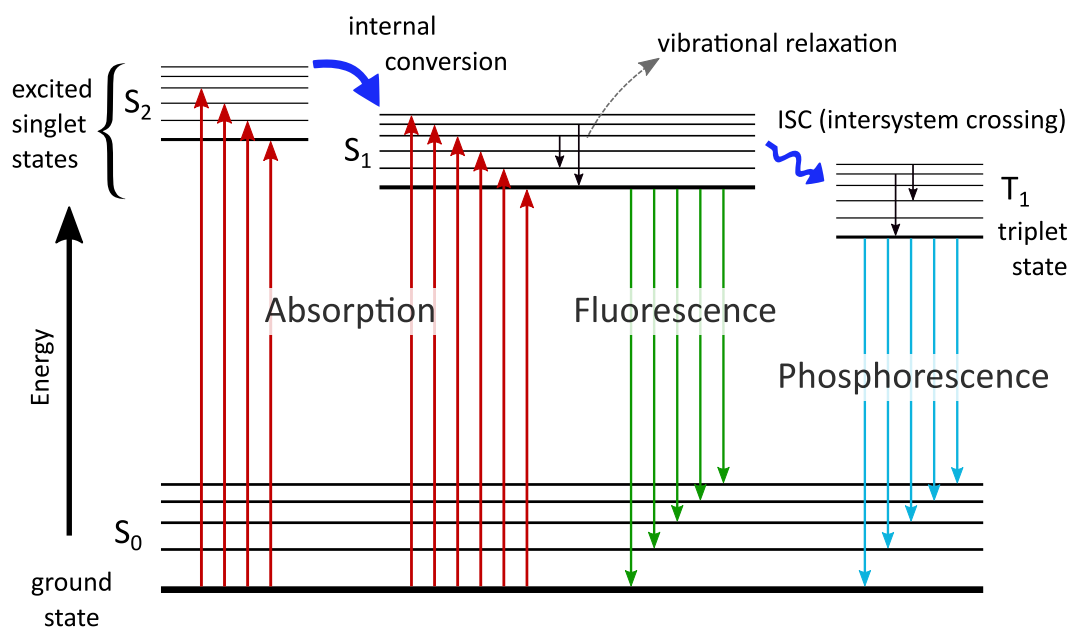


**Figure 2.4:** Jablonski-diagram for radiative and non-radiative processes

### 2.3.1 Internal conversion

Typically, internal conversion takes place as a non-radiative transition between two electronic states that have the same spin multiplicity, e.g. from a higher excited singlet state to a lower singlet state ( $S_2$  to  $S_1$ ). Vibrational relaxation to the 0 vibrational level can take place if the excitation of a molecule reaches a higher energy level than the lowest vibrational level of the respective electronic state. Internal conversion is not only possible for  $S_2$  to  $S_1$  transitions, but also for a transition from the  $S_1$  electronic state to the ground level  $S_0$ , however this process is less likely due to the larger energy gap.

### 2.3.2 Fluorescence

If an excited molecule relaxates under emission of photons from the  $S_1$  to the  $S_0$  ground state the process is called fluorescence. In comparison to an absorption spectrum, a fluorescence spectrum is shifted to higher wavelengths, which is due to the energy loss caused by vibrational relaxation. Often, an overlap can be observed between both spectra. This is resulting from the circumstance that at room temperature some molecules are in a higher vibrational level than 0 (ground state and excited state). The difference in wavelength between the maximum of absorption and emission peak is called *Stokes shift*. Excited molecules do not immediately return to the ground state, but stay in the  $S_1$  state for a specific amount of time, before emission of a photon can occur; lifetime is a measure for this time span. Depending on the lifetime of a molecule in the  $S_1$  state, the fluorescence intensity decay takes place exponentially.

### 2.3.3 Intersystem Crossing

Another non-radiative transition besides the internal conversion is the intersystem crossing (ISC) that takes place between electronic states with different multiplicities. For example, it is possible that an excited molecule in the  $S_1$  state can move to a vibrational level of the triplet state with the same energy. This is followed by vibrational relaxation to the 0 vibrational level of the triplet state  $T_1$ . In general, as already discussed in section 2.2.1, the transition between states of a different multiplicity is not allowed, however it can still be observed due to spin-orbit coupling. By introduction of heavy atoms into the molecule, intersystem crossing can be drastically enhanced, due to the large atomic number of these atoms.

### 2.3.4 Phosphorescence

There are two possible de-excitation processes from the triplet state  $T_1$ , the radiative transition, which is called phosphorescence and the non-radiative transition, which is typically favoured over the occurrence of phosphorescence. As the transition from the  $T_1$  to the  $S_0$  state is forbidden, the radiative process is very slow. Phosphorescence can be favourably observed at low temperatures. The lifetime of a molecule in the triplet state is much longer than in the singlet state (fluorescence), due to the forbidden transition to the ground state. Therefore, phosphorescence might be observed up to minutes or longer. In comparison to a fluorescence spectrum, the phosphorescence spectrum is shifted to higher wavelengths, which can be explained by an energetically lower lying zero vibrational level of the  $T_1$  compared to the singlet state  $S_1$ .

### 2.3.5 Delayed fluorescence

There are two different mechanisms that can lead to delayed fluorescence.

- Thermally activated delayed fluorescence: If the energy difference between the excited singlet state  $S_1$  and the triplet state  $T_1$  is rather small and the lifetime of the triplet state is sufficiently long, a process called reverse intersystem crossing can take place. (transition from  $T_1$  to  $S_1$ ) As the molecule first rests in the triplet state before returning to the singlet state via reverse ISC, the decay time is much longer compared to normal fluorescence. The efficiency of this type of fluorescence can be enhanced by increasing the temperature, wherefore it is called thermally activated delayed fluorescence.
- Triplet-triplet annihilation: The second possibility for the occurrence of delayed fluorescence is the triplet-triplet annihilation, which means that collisions between two molecules in the triplet state lead to the return of one of the molecules to the  $S_1$  state and the other one to the  $S_0$  level. This effect can mainly be observed in very concentrated solutions.

## 2.4 Lifetime and quantum yields

Two very important parameters for the characterization of luminophores are the luminescent lifetime ( $\tau$ ) and the quantum yield ( $Q$ ). The quantum yield is a parameter for the brightness (which is a product of the quantum yield  $Q$  and the molar absorption coefficient  $\epsilon$ ) and describes the relation of emitted photons to the number of absorbed photons. Meanwhile, the lifetime gives information about the amount of time a molecule remains in the excited state. Both parameters can be expressed by the rate constants of radiative ( $\Gamma$ ) and non-radiative ( $k_{nr}$ ) deactivation. (figure 2.5)

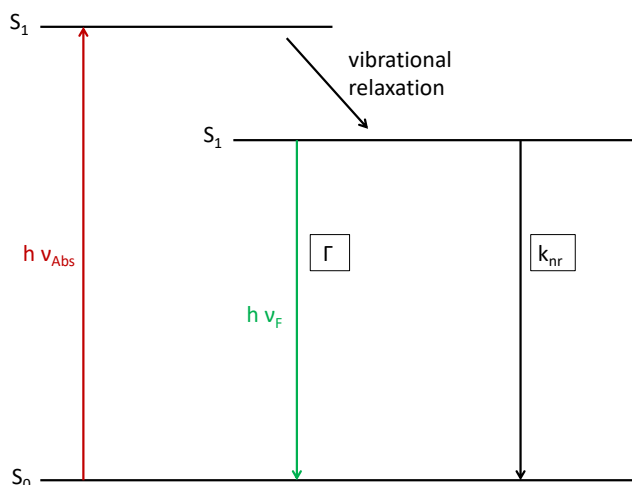


**Figure 2.5:** Simplified Jablonski-diagram showing the emissive rate of a fluorophore and the rate of non-radiative decay

The quantum yield can be determined according to equation 2.1.

$$Q = \frac{\Gamma}{\Gamma + k_{nr}} \quad (2.1)$$

If the non-radiative decay is much smaller compared to the radiative decay, the quantum yield reaches a value close to 1. However, regarding fluorescence emissions, the quantum yield always reaches a value  $< 1$ , due to Stokes losses. One exception of this rule is the process of singlet fission, where a singlet exciton is converted to a pair of triplet excitons. This step is followed by a diffusion process and the formation of two free triplet excitons. Regarding singlet fission processes, the quantum yield is able exceed 100 % [35].

The lifetime of a molecule is described by equation 2.2.

$$\tau = \frac{1}{\Gamma + k_{nr}} \quad (2.2)$$

The lifetime of an excited luminophore is thus described by the time a molecule stays in the excited state (e.g.  $S_1$  for fluorescence or  $T_1$  for phosphorescence emission), before returning to the ground state  $S_0$ . Typically, phosphorescence lifetimes tend to be much longer (range from microseconds to seconds) than fluorescence lifetimes (picoseconds to nanoseconds), which is due to the spin-forbidden transition from the triplet state to the ground state for phosphorescence.

### 2.4.1 Effect on temperature

Quantum yields and lifetimes of molecules can be strongly influenced by variation of temperature. In general, increasing the temperature leads to lower fluorescence quantum yields and to shorter lifetimes. This is related to the fact that some non-radiative processes (e.g. intramolecular vibrations, collisions with solvent molecules) take place more efficiently at higher temperature. As already mentioned before, phosphorescence shows a longer lifetime than fluorescence and is even more easily deactivated by collisions with solvent molecules, wherefore it can be observed best at low temperature or when molecules are embedded in a rigid matrix. Quantum yields for phosphorescence can be increased up to a factor of  $10^3$  when cooling, while for fluorescent molecules the factor is typically not higher than 10.

Besides the temperature also other factors such as polarity, pH or the presence of quenchers might have an impact on the quantum yields and the lifetime.

## 2.5 Optical sensors in analytical chemistry

A sensor is per definition a device that detects the change of a specific physical parameter and converts it into a more easily measurable second parameter, which then provides the necessary information for the respective measurement [36]. Nowadays, especially optical sensors play an important role as they allow contact-less measurement, are miniaturizable and typically inexpensive [1–3]. These advantages have led to the preparation of various fiber-optic

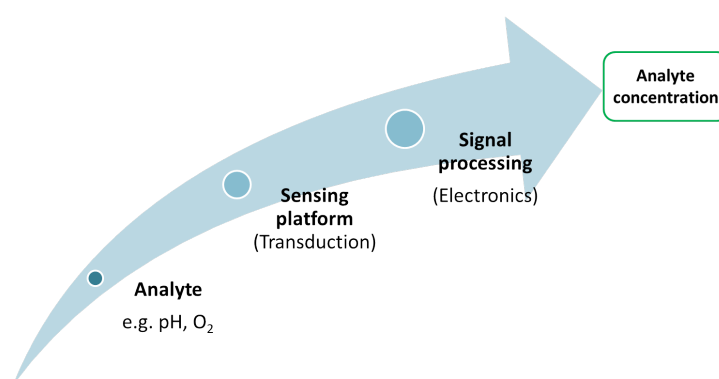


**Figure 2.6:** Components of a typical chemical optical sensor

sensors which can be applied in multiple fields for the detection of physical parameters such as temperature, pH-value, pressure or oxygen concentrations [1, 36]. In analytical chemistry, measurements with optical sensors are typically based on absorption and luminescence, however also chemical sensors based on other optical parameters have already been developed. (figure 2.6) Fiber optical based sensors often rely on specific indicator dyes that show a change of luminescence in respect to the analyte concentration [1]. Dependent on the type of indicator dye and the matrix of the sensors they can be used for a large variety of applications.

### 2.5.1 Sensing methodologies

Typically, sensing of oxygen relies on luminescence quenching of a suitable indicator dye. Hereby, it is required that the indicator changes its spectral properties in presence of oxygen. Changes of different parameters can be measured, such as luminescence intensity, emission spectrum

or lifetime. The easiest way of oxygen detection is by measuring the change in luminescence intensity, however this method suffers from a serious drawback. Often intensity-based measurements are influenced by external parameters such as light source intensity or luminophore concentration, wherefore the results of the measurement might be distorted. Thus, it is of high interest to use measuring methods that are independent of such factors, for instance ratiometric or lifetime-based measurements. In general, the best suitable method is chosen depending on expenditure, application and availability of the indicator [7]. Regarding ratiometric methods, the sensor usually consists of an oxygen-sensitive dye and a reference dye which are embedded into a matrix. Requirements for this type of measurement are that the reference dye must not be quenched in presence of oxygen, no overlap of the emission spectra of indicator and reference dye should occur and no energy transfer between the two dyes should take place. It is then possible to detect oxygen concentrations by measuring the intensities of indicator and reference dye at two different emission wavelengths. For this purpose bandpass filters or also tailor-made indicators can be used [7]. The latter show dual emission, meaning that they exhibit oxygen-sensitive phosphorescence but oxygen-insensitive fluorescence, however the synthesis of these dyes tends to be challenging and only few examples are known in literature so far [7, 31, 37, 38]. Ratiometric oxygen sensors can be used for a variety of biological and medicinal applications such as non-invasive oxygen detection in cancer cells [39].

As already mentioned above, besides ratiometric measurements, also lifetime-based ( $\tau$ ) measurements are used for a large variety of applications. The lifetime of a luminophore can be determined via two different methods, either in time domain or in frequency domain (figure 2.7). Time domain means that the time-dependent intensity is monitored after excitation of a sample

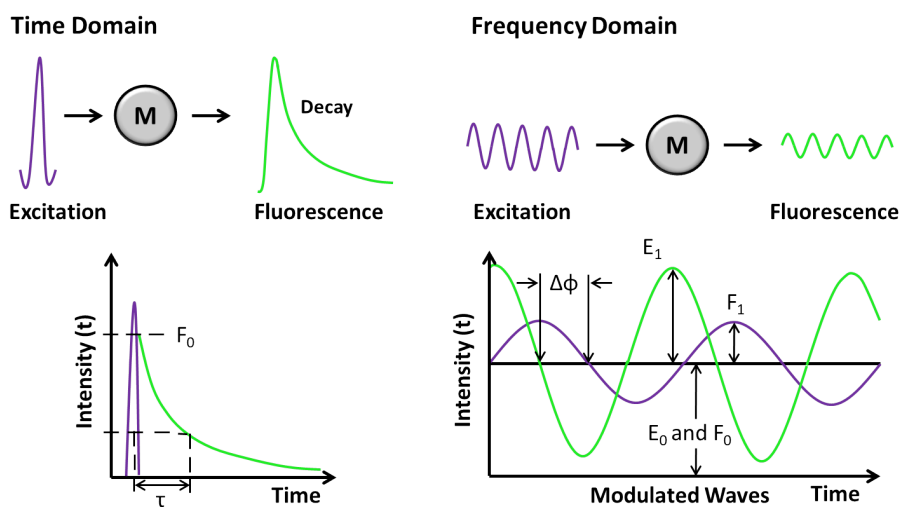


**Figure 2.7:** Principles of Frequency-Domain and Lifetime-Domain Measurements

with a light pulse. Then,  $I(t)$  can be plotted versus  $t$ , whereby the exponential decay gives information about the lifetime of the sample (exponential fit). An advantage of this method is that the delay between the light pulse and the measurement eliminates background fluorescence [7]. Regarding the frequency domain method, an intensity-modulated light source is used for excitation of the sample. A time delay between the excitation and emission of the luminophore takes place, which is measured as physical quantity called phase shift ( $\phi$ ) [7]. The phase shift

can then be used to calculate the lifetime via the following equation:

$$\tau = \frac{\tan\phi}{2\pi f} \quad (2.3)$$

Here,  $f$  represents the modulation frequency of the light source. A very convenient approach for oxygen detection in plant tissues is the two-frequency phase modulation. This method is able to differ between the lifetime of autofluorescence of the tissue and the phosphorescence of the indicator [40].

In general, pulse and phase techniques lead to the same information but show different advantages and disadvantages [7].

## 2.6 Optical oxygen sensing

Today, oxygen counts to the analytes of highest interest [41], as optical oxygen sensors can be used for biotechnological and medical applications [4], in chemical industry and also for environmental analysis (e.g. marine research) [5].

Before the emergence of optical sensors, several other methods for oxygen detection were available, including electrochemical (e.g. potentiometric), optical (luminescence, absorption) and chemical (Winkler titration) analysis techniques. For a long period of time, the Clark electrode [6] was considered an optimal method for oxygen detection, until optical sensors conquered the world of chemical sensing, as they do not show electrical interference, are inexpensive and allow contactless measurement [7].

The working principle of an optical oxygen sensor is based on quenching of the luminescence of the respective indicator dye by oxygen. The general set-up comprises a luminescent dye that is entrapped in a polymeric matrix on a solid support (e.g. optical fiber) [7]. Both, intensity-based and lifetime-based measurements are possible, however often lifetime is the preferred parameter, as these measurements are independent of external perturbations [8].

### 2.6.1 Important indicator dyes for oxygen sensing

Typical indicator dyes for optical sensing of oxygen include polycyclic aromatic hydrocarbons [12, 13] (today not used anymore), ruthenium complexes (e.g.  $[\text{Ru}(\text{bpy})_3]$  or  $[\text{Ru}(\text{dpp})_3]$ ) [9–11] and various metallo-porphyrin compounds.

These molecules have the advantage of showing a high solubility in various organic solvents and in a wide range of polymers such as polymethylmethacrylate (PMMA) or silicone rubber. As ruthenium complexes tend to show a limited sensitivity towards oxygen, current research focuses on porphyrin complexes due to their chemical stability, high luminescence, longer lifetimes and large Stokes's shifts. Oxygen detection with porphyrins as indicator dyes works by quenching of the photoexcited triplet state by oxygen and subsequent measurement of the phosphorescence intensity change or lifetime [14]. More detailed information about the use of porphyrins for optical sensing will be provided later on.

## 2.7 Quenching of Luminescence

Quenching of luminescence describes all processes that lead to a decrease in luminescence intensity. Among these processes are molecular rearrangements, excited state reactions, energy transfer, collisional quenching (dynamic quenching) and ground state complex formation (static

quenching). The last two mechanisms, dynamic and static quenching, will be discussed in more detail. Both processes require contact between a luminescent molecule  $M^*$  and a quencher molecule  $Q$  [42].

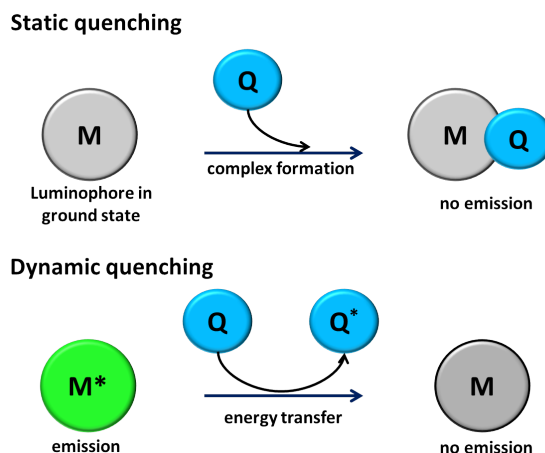


**Figure 2.8:** Mechanisms for dynamic and static quenching

### 2.7.1 Static quenching

Static quenching is a result of complex formation between a fluorescent molecule in the ground state  $M$  and a quencher  $Q$  (figure 2.8). As the resulting complex  $MQ$  does not show fluorescence emission, the complex formation leads to reduction of the concentration of the fluorophore and thus to a lower intensity [43]. Static quenching is described by the following formula:

$$\frac{I_0}{I} - 1 = K_a[Q] \quad (2.4)$$

Hereby,  $K_a$  represents the association constant and  $[Q]$  the concentration of the quencher molecule. Due to the reason that static quenching results from binding of the quencher to the fluorophore an association constant is involved, which decreases with increasing temperature. Regarding equation 2.4 it can be seen that the lifetime of the fluorophore stays unaffected by the mechanism of static quenching [43].

### 2.7.2 Dynamic quenching

Dynamic quenching is a diffusion controlled process that describes collisions between a fluorophore in the excited state  $M^*$  and a quencher  $Q$  (figure 2.8). Hereby, an energy transfer from the excited molecule to the quencher takes place and the fluorophore is relaxed radiationless to the ground state. Therefore, another rate constant for non-radiative decay from the excited state is the rate of quenching. This means that in comparison to static quenching, dynamic quenching decreases both the fluorescence intensity and the lifetime [42]. Dynamic quenching can be described by:

$$\frac{I_0}{I} - 1 = \frac{T_0}{T} - 1 = k_q\tau_0[Q] = K_{SV}[Q] \quad (2.5)$$

Here,  $k_q$  represents the bimolecular quenching constant and  $\tau_0$  the lifetime of the fluorophore,  $K_{SV}$  is the Stern-Volmer constant.  $I_0$  and  $I$  represent the intensities of the luminescence in

presence and absence of the analyte (e.g.  $O_2$ ) [14]. The bimolecular quenching constant is dependent on the number of collisions between fluorophores and quenchers and also on the efficiency of quenching [42]. As already stated above, dynamic quenching, in contrast to static quenching, also influences the lifetime of the fluorophore, which is shown by equation 2.5.

Due to the reason that the lifetime of molecules in the triplet state is typically much longer than in an excited singlet state, interactions with molecules such as oxygen have a higher probability to occur. Porphyrins are very prone to react with oxygen in the excited triplet state, which is due to the reason that the energy level of the triplet state is close to the lowest unoccupied molecular orbital of oxygen. By this means, oxygen is converted into a singlet oxygen species ( $^1O_2$ ), which requires a transfer of energy from the porphyrin. Regarding cyclometalated complexes, also a superoxide anion radical species ( $O_2^-$ ) may be formed. The decay of the triplet state is then directly related to the concentration of oxygen, as these are first order reactions [14].

In general it can be said that phosphorescent lifetime measurements are a suitable method for the determination of oxygen concentration by optical sensors.

## 2.8 Optical pH-sensing

Besides oxygen, another important parameter in optical sensing is the pH. Determination of pH-values is applied in a broad variety of scientific and technological fields, such as biotechnology, chemistry or medicine [44, 45]. Generally, a pH-optode consists of a pH-sensitive dye and a polymeric matrix [46]. A required property of an indicator dye is that it needs to show different optical properties for its protonated and deprotonated structure [47]. Therefore, the absorption or fluorescence emission of the dye correlates with the concentration of hydrogen ions [46].

The polymer host matrix of pH-optodes meets the requirement of being hydrophilic in order to allow proton diffusion and needs to display a high chemical, mechanical and thermal stability. Furthermore, before development of an optical pH-sensor, a suitable sensor sensitivity for the respective application needs to be considered. For example, pH sensors for measurements in the marine environment need to show a high sensitivity around pH 8.0; bioprocesses however, usually require a high sensitivity around pH 6.0. Regarding biological applications, the pH indicator dye should show optical properties in the red/infrared region, because at these wavelengths only a low background fluorescence (e.g. from solvents, substrates) is expected [48].

### 2.8.1 pH-Indicator dyes

There are two main principles of pH-sensing, which are the absorption- and fluorescence based sensing. (figure 2.9) Absorption-based pH sensors work by a color change of the indicator dye, depending on if the protonated or deprotonated form is present [48]. Typical examples of absorption-based pH indicators include compounds such as phenolphthalein [49] or phenol red [50].

Luminescence-based chemical pH-sensors tend to be of even higher interest than absorption based sensors, due to their excellent sensitivity and selectivity [51]. Widely used fluorescent pH indicators are fluorescein and its derivatives [52, 53], coumarin-based indicators [54], 1-hydroxypyrene-3,6,8-trisulfonic acid (HPTS) [55, 56] and seminaphthofluorescein (SNAFL) [57]. While fluorescein and SNAFL indicators show poor photostability, the opposite is the case for HPTS, however its pH-response is strongly dependent on ionic strength [48]. Until now, most indicator dyes mentioned only allow pH-sensing based on intensity, however sensing based on

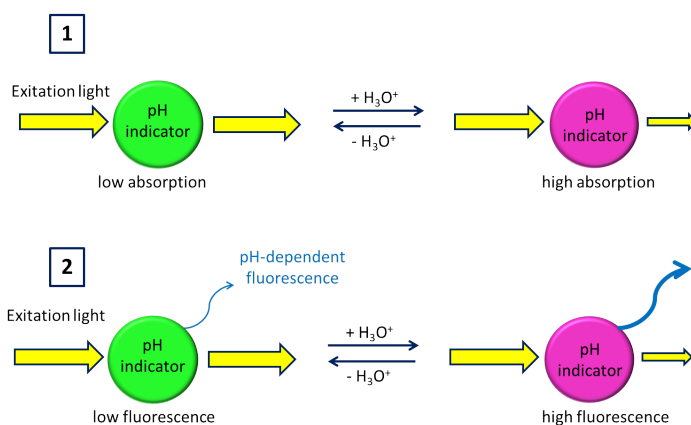


**Figure 2.9:** Mechanisms of absorption-based (1) and fluorescence-based (2) pH-sensing

luminescence decay times would be highly favoured. New attempts include the use of lanthanide complexes [58, 59] (e. g. Eu(III)) and sensitive ruthenium metal-ligand complexes [60, 61] as pH indicators for optical sensing. A problem which could not be solved entirely until now is the oxygen cross-sensitivity of metal-ligand complexes for pH-sensing with oxygen, due to rather long decay times.

## 2.9 State-of-the-art of porphyrins in optical sensing

Porphyrins are macrocyclic compounds with single-double conjugated bonds and a planar structure that can contain a metal atom in the core center. (figure 2.10)

Amongst others, they can be found in natural compounds such as hemoglobin or chlorophyll [62].

Luminophores of high interest for oxygen sensing are Pt(II) and Pd(II) porphyrins. They exhibit excellent properties for optical sensing – especially oxygen sensing [63–66]– such as large Stokes' shifts, strong phosphorescence and high molar absorption coefficients. Furthermore, the phosphorescence lifetimes of these complexes can be varied depending on the metal in the core center. In general, palladium porphyrins show significantly longer lifetimes than platinum porphyrins [67], which is related to the fact that platinum is a heavier metal and therefore facilitates spin-orbit coupling. However, platinum complexes have the advantage of exhibiting higher quantum yields than the palladium analogue [7]. In the following, a short overview will be given about the most important different types of Pt(II) and Pd(II) porphyrins.

The first class of porphyrins that is still commonly used for oxygen sensing are platinum and palladium octaethylporphyrins (PtOEP, PdOEP). They exhibit a strong phosphorescence at room temperature, high quantum yields and also long lifetimes [15]. Typically, these complexes are dispersed in different polymer matrices for optical oxygen sensing, such as poly(1-trimethylsilyl-1-propyne) (TMSP) [68], polystyrene (PS) [69], fluorine containing poly(aryl ether ketones) [70] and polyethylene glycol (PEG) combined with polystyrene (PS) or ethyl cellulose (EC) [71]. However, one drawback of the mentioned complexes is their limited photostability [7]. Another

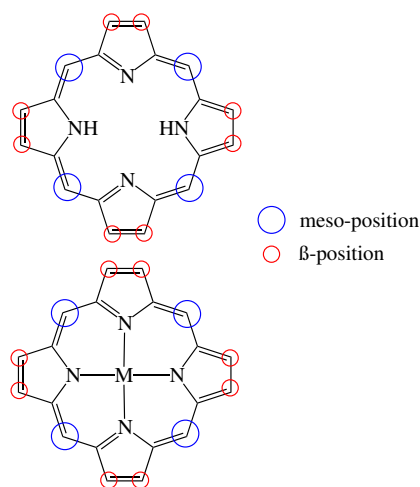


**Figure 2.10:** Typical porphyrin ligand and porphyrin compound including a metal atom in the core

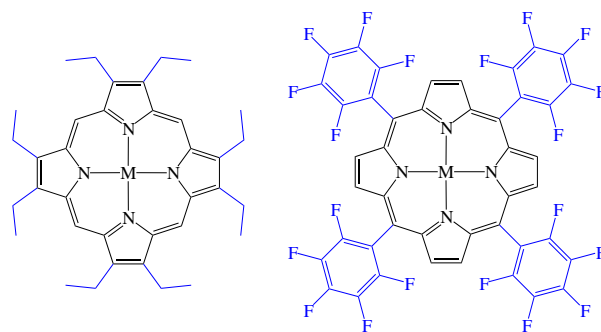


**Figure 2.11:** Structure of octaethylporphyrin (left) and tetrakis(pentafluorophenylporphyrin) (right) containing a central metal atom ( $M = \text{Pt(II)}, \text{Pd(II)}$ )

class of Pt(II) and Pd(II) porphyrins for oxygen sensing – which show a significantly higher photostability than octaethylporphyrins – are tetrakis(pentafluorophenylporphyrins) (TFPP). The two porphyrin classes show different properties due to their functional groups (figure 2.11), which are perfluorophenyl (meso-position) and ethyl ( $\beta$ -position) for TFPP and OEP, respectively. In comparison, ethyl groups have a smaller size and are less rigid, which affects

the efficiency of collision with oxygen molecules. Furthermore, the fluorine functional groups are electron-withdrawing and therefore decrease the electron density on the porphyrin ring, leading to a reduced probability of undergoing an oxidation reaction with singlet oxygen [72]. PtTFPP is commonly used for applications requiring high light intensities, e.g. in microscopy or in fiber-optic microsensors. PdTFPP however, stands out due to its long lifetime (at room temperature 1 ms) and is frequently used to determine trace levels of oxygen [7]. The Pt(II) and Pd(II) OEP and TFPP entail the disadvantage of only absorbing light in the UV-Vis region. This can lead to problems, especially regarding biological samples, as a high level of autofluorescence is present in the UV-Vis region, which is due to fluorescent compounds such as FAD or NAD. Furthermore, UV-Vis indicators cannot easily be used in scattering media (e.g. marine sediments) or in implantable sensors, as blood absorbs mostly in the visible region. Therefore, indicators that emit in the NIR-region (780 nm - 3  $\mu\text{m}$ ) are of high interest, because these sensors can be applied in scattering media or biological samples such as blood, tissues or cells [7].

### 2.9.1 NIR-indicators

Metal complexes that are able to be excited in the red part of the spectrum and show emission in the NIR-region have become more and more popular, due to their large variety of applications. Typically, these dyes can be found in organic light emitting diodes (OLEDs) [18–20] and in optical sensors, for example for oxygen detection [7, 23, 24]. Regarding light conversion applications, NIR-excitable complexes are of special interest, as nearly half of the sun's energy that reaches the earth is NIR radiation [21, 22].

In order to obtain a bathochromic shift of the absorption and emission bands, different synthetic approaches can be followed that include modifications of the porphyrin structure. The first groups of NIR-indicators that were commonly used for oxygen sensing are platinum(II) and palladium(II) porphyrin lactones [26] (figure 2.12) and porphyrin ketones [25] (figure 2.12). Pt(II) complexes of porphyrin ketones, for instance, show strong phosphorescence at room temperature, have a high photochemical stability and exhibit long wave spectral characteristics [25]. However, although porphyrin lactone and ketone complexes show strong absorption bands within a range of 580-600 nm, they suffer from moderate to low brightness and cannot be applied for measurements in blood or subcutaneous tissue, as the transmittance of the excitation-light is rather low [73].

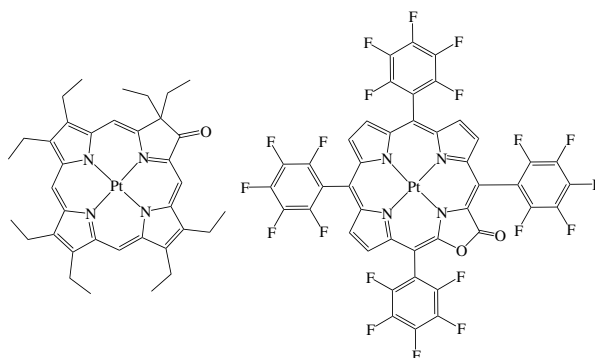


**Figure 2.12:** Structure of Pt(II) octaethylporphyrinketone (PtOEPK) (left) and Platinum(II)-5,10,15,20-tetrakis-(2,3,4,5,6-pentafluorophenyl)porpholactone (PtTFPPL) (right)

## Benzo- and naphthoporphyrins

Another important group of NIR-indicators for oxygen sensing consists of  $\pi$ -extended porphyrins, such as Pd(II) and Pt(II) benzo- and naphthoporphyrins (figure 2.13). These complexes are obtained by extension of the porphyrin macrocycle with various aromatic moieties, which leads to a bathochromic shift of the emission spectra (figure 2.14). Popular representative of this type of NIR-indicators are platinum(II) and palladium(II) tetraphenyltetrabenzoporphyrins (PtTPTBP, PdTPTBP). These complexes exhibit excellent absorption coefficients with  $200,000 \text{ M}^{-1} \text{ cm}^{-1}$  for the blue region and  $130,000 \text{ M}^{-1} \text{ cm}^{-1}$  for the red region. Furthermore, they show good emission quantum yields with values of 0.50 and 0.20, respectively [7]. Benzoporphyrins

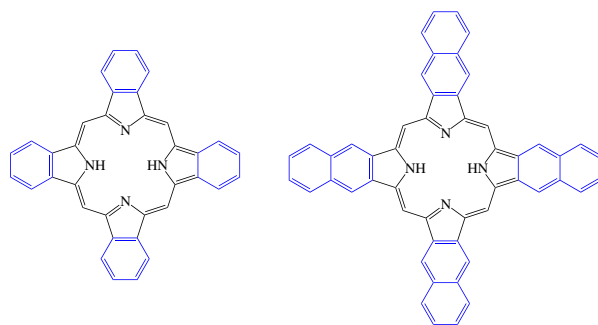


**Figure 2.13:** Structure of TBP (right) and TNP (left) ligands

that are substituted at their meso-positions show a non-planar structure and therefore exhibit good solubility and no tendency for aggregation, which is an important factor considering the use of polymer matrices (e.g. polystyrene [74]) for optical sensing [75]. If embedded in polystyrene, platinum (II) meso-substituted benzoporphyrins can be ideally used as oxygen sensors in a range from 0 to 100 % air saturation. Meanwhile, the analogous Pd (II) complexes exhibit longer lifetimes of approximately  $300 \mu\text{s}$ , wherefore they are more suitable for trace oxygen sensing, since strong luminescence quenching takes place at high air saturation. One possibility to make these palladium complexes suitable for oxygen detection at air saturation would be entrapment of the dyes in a polymer matrix that shows low oxygen permeability [7]. Furthermore, meso-substituted

porphyrins can be altered by introduction of fluorine atoms instead of hydrogen on the phenyl-rings in meso-position. This modification leads to PtTPTBPF or PdTPTBPF complexes showing enhanced quantum yields and photostabilities due to the electron-withdrawing groups [73]. As already mentioned above another group of  $\pi$ -extended porphyrins are the so-called naphthoporphyrins. In comparison to benzopor-

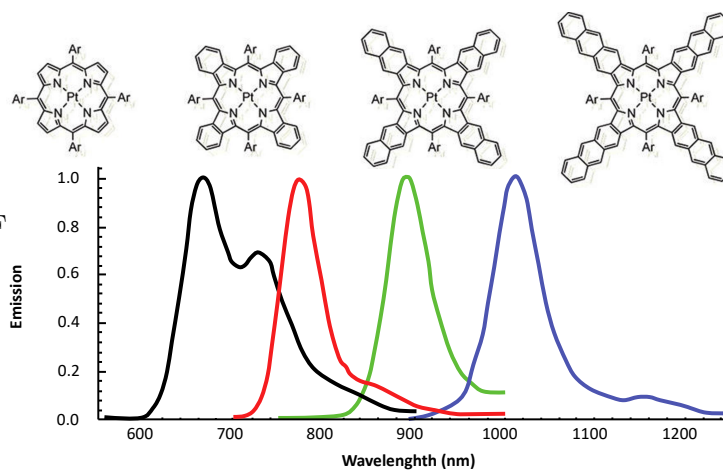


**Figure 2.14:** Emission spectra of various  $\pi$ -extended porphyrins in toluene [76]

phyrins, these complexes contain an additional benzene ring at the  $\beta$ -pyrrole positions, which leads to an increased bathochromic shift of absorption and emission bands of approximately 80 nm [7]. Although emission at higher wavelengths would be favoured, these dyes suffer of decreasing quantum yields and low photostability [75, 77, 78], leading to problems regarding the use in light conversion applications (e.g. OLEDs, photovoltaics). For example, the quantum yields for PtTPTNP and PdTPTNP have shown to be 0.22 [79] and 0.079 [80] respectively, while the quantum yields of the benzoporphyrin analogue complexes are 0.51 for PtTPTBP and 0.21 for PdTPTBP [73].

### 2.9.2 UV-VIS spectra of porphyrins

Usually, the absorption spectrum of porphyrin ligands without metal center shows an intense Soret band at a wavelength of approximately 380 -500 nm and four Q-bands between 500 and 700 nm. Metalloporphyrins containing central atoms such as Pt(II) or Zn(II) however, exhibit a Soret band and only two Q-bands due to their symmetrical structure [81].

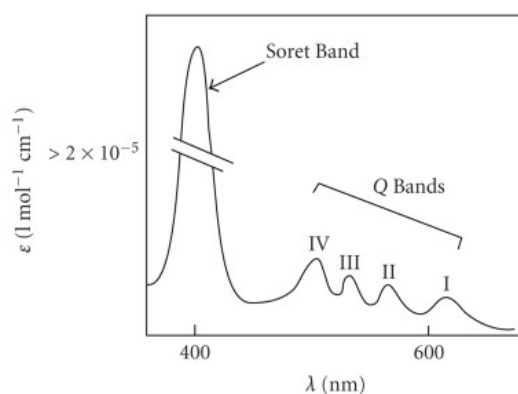


**Figure 2.15:** Absorption spectrum of a porphyrin without metal ion [82]

Absorption spectra of porphyrins were first explained by Martin Gouterman in 1959 [83] by the so-called "four-orbital" model [84, 85], which describes the two lowest unoccupied  $\pi^*$  and highest occupied  $\pi$  orbitals. This model states that the absorption bands of porphyrins are a result of transitions between the two HOMOs and LUMOs, whereby the type of central atom and substituents on the porphyrin ring lead to different energies of transitions. The Soret band of a porphyrin complex is a result of a transition from the ground state to the second excited singlet state ( $S_0$  to  $S_2$ ), while the Q bands originate from a transition from the ground state to the first excited state ( $S_0$  to  $S_1$ ). Due to the reason that the transition to the first singlet state is weaker, Q bands show a much lower absorption intensity compared to the Soret band [86]. The relative intensity of all Q bands depends on the substituents on the porphyrin ring; e.g. if the intensities of the Q bands decrease in the order of  $IV > III > II > I$ , generally six or more substituents without  $\pi$ -electrons (e.g. alkyl groups) are located at the  $\beta$ -positions. However, if substituents with  $\pi$ -electrons are present at the  $\beta$ -positions, the Q band decrease in the order of  $III > IV > II > I$ , which is called a rhodo-type spectrum. This name results from the fact that the substituents with  $\pi$ -electrons cause a "reddening" effect, meaning that the spectrum is shifted to longer wavelengths [86].

Therefore, as variations of the substituents on a porphyrin ring and also insertion of metal atoms into the porphyrin ligand lead to changes in the absorption spectra, UV-VIS spectroscopy represents an ideal technique for monitoring of these processes [86].

## 2.10 Platination of metal-free porphyrins

As already mentioned above, platinum(II) and palladium(II) porphyrins have shown to be excellent indicator dyes for optical sensors, because they show strong phosphorescence at room temperature and large Stoke's shifts [7]. Extending the porphyrin core with aromatic moieties at the  $\beta$ -pyrrole positions leads to compounds such as tetrabenzoporphyrins [87] or tetranaphthaloporphyrins [75], which are of high interest due to a bathochromic shift of their absorption and emission spectra and the possibility of emission in the NIR region [88]. However, although  $\pi$ -extended platinum(II) and palladium(II) porphyrins are a luminophore class of high interest – for example for medical or therapeutic applications [89] – especially the synthesis of these compounds containing a platinum central atom remains a challenging task.

So far, the typical synthetic procedure (figure 2.16) for the preparation of  $\pi$ -extended Pt(II) porphyrins consists of the addition of  $\text{PtCl}_2$  to the porphyrin ligand in benzonitrile under reflux for several hours at a temperature of 190 - 200°C [75, 90–92]. It is assumed

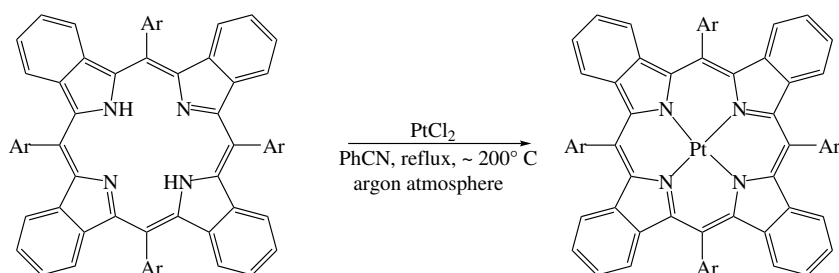


**Figure 2.16:** Typical platination procedure for  $\pi$ -extended porphyrins

that a reaction between the  $\text{PtCl}_2$  and the solvent PhCN takes place, leading to a Pt(II)-benzonitrile complex, which is capable of improving the solubility of the platinum reagent. However, large drawbacks of these reaction conditions are long reaction times (up to 24 hours) and moderate yields, due to no quantitative conversion of the porphyrin ligands [76].

An improvement of the typical platination process of tetraphenyltetrabenzoporphyrins (TPTBP) was achieved by Borisov et al. by using the non-coordinating diphenylether (figure 2.17) instead of benzonitrile as a solvent. It was assumed that a large excess of coordinating benzonitrile could possibly disfavour the metallation process, wherefore diphenylether was thought to be a promising alternative. Results showed that by using diphenylether the platination process could be performed in tens of minutes at 190 °C without decomposition of the ligand. One drawback of this synthetic attempt were the resulting purification processes, as it is not possible to remove diphenylether under vacuum [93]. Another synthetic route for the preparation of  $\pi$ -extended Pt(II) porphyrins, which is now commonly used, includes the usage of the precursor  $\text{Pt}(\text{C}_6\text{H}_5\text{CN})_2\text{Cl}_2$  in 1,2,4-trimethylbenzene as a solvent; depending on the exact structure of the porphyrin, yields for this procedure also tend to be rather moderate [24, 89].

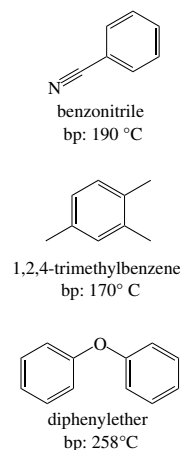


**Figure 2.17:** Typical high-boiling point solvents for the platination of porphyrins

Recently, another mild method for the synthesis of platinum(II) porphyrin complexes was reported, which is shown in figure 2.18. Free-base porphyrins were treated with 1.5 equivalents of  $[\text{PtCl}_2(\text{PhCN})_2]$  in presence of the base sodium propionate in refluxing chlorobenzene. The

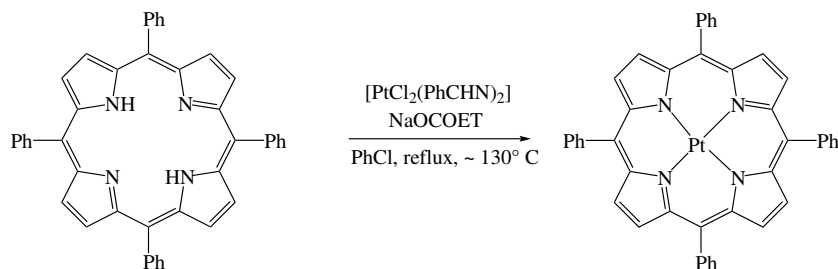


**Figure 2.18:** Recently reported platinumation reaction using sodium propionate as a base

reaction resulted in good yields of the respective Pt(II) complexes. It needs to be pointed out that the work-up process of this method was easier compared to earlier reported synthesis, due to the reason that chlorobenzene can be removed by rotary evaporation (bp:  $131^\circ \text{C}$ ) [94]. In conclusion, it is still a field of great interest to improve the platinumation reactions for  $\pi$ -extended porphyrins, e.g. benzoporphyrins. Therefore, the synthesis of new Pt-precursors that might enhance currently applied reaction conditions was also investigated during the experimental work of this master's thesis.

## 2.11 Cyclometalated indicator dyes

Besides the mentioned ruthenium(II) polypyridyl complexes and the extensively discussed metalloprophyrins, another class of indicator dyes are cyclometalated Ir(III) and Pt(II) complexes. These compounds are characterised by strong luminescence, high quantum yields, a large Stokes' shift and good photostability. However, cyclometalated complexes generally suffer from the drawbacks of showing relatively short decay times (several microseconds) and low molar absorption coefficients in the visible region, which makes them often unsuitable for applications in optical sensing [7, 95].

Typical representatives of this group of indicators are phenylpyridine based  $[\text{Ir}(\text{ppy})_3]$  [27], cyclometalated iridium complexes with coumarins with the formula  $\text{Ir}(\text{C}_x)_2(\text{acac})$  (with  $X = \text{N}, \text{O}, \text{S-Me}$  or  $\text{S}$ ) [28, 29], platinum(II) complexes with thienylpyridine ligands  $\text{Pt}(\text{thpy})_2$  [30] and platinum(II) compounds coordinated with acetylacetonate  $\text{C}^{\wedge}\text{NPt}(\text{acac})$  [31].

Upon the mentioned compounds cyclometalated iridium(III) complexes with coumarins are able to overcome the drawback of low absorption in the visible region. Typically these indicators yield absorption coefficients up to  $90,000 \text{ M}^{-1} \text{ cm}^{-1}$  and exhibit strong phosphorescence. Another advantage of these compounds is the possibility of altering the spectral properties by variation of the substituent of the coumarin, whereby the spectrum shows a bathochromic shift in the order of  $X = \text{S} > \text{O} > \text{N}$  [7, 28]. Cyclometalated iridium(III) coumarin complexes have already been used for optical oxygen sensing by embedding the dye in a polystyrene film. One large drawback of these indicators however is that they show a poor photostability and are therefore only suitable for short-term measurements [28].

Another attempt was the use of dimeric iridium coumarin complexes with the formula  $(\text{C}_x)_2\text{Ir}(\mu\text{-Cl})_2\text{Ir}(\text{C}_x)_2$ . It was shown that these compounds exhibit lower emission quantum yields in comparison to the monomeric complexes; the absorption and emission bands are shifted bathochromically regarding the dimeric compounds [28].

As already mentioned above, besides iridium(III) complexes also platinum(II) cyclometalated complexes have been investigated as indicator dyes for optical sensing. The platinum compounds suffer from the same drawbacks of showing low absorption coefficients in the visible part of the spectrum [7].

Some years ago, cyclometalated Pt(II) complexes were discovered that are able to exhibit dual

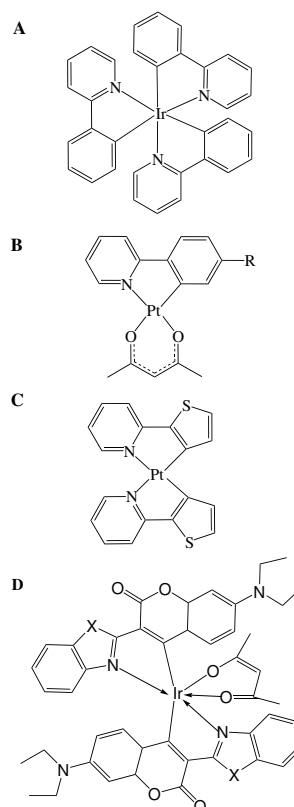


**Figure 2.19:** Examples of cyclometalated indicator dyes such as  $[\text{Ir}(\text{ppy})_3]$  (A), acetylacetonato based Pt (II) complex (B), thienylpyridine based  $\text{Pt}(\text{thpy})_2$  (C) and iridium complex with coumarin ligands  $\text{Ir}(\text{C}_x)_2(\text{acac})$  (with  $X = \text{N}, \text{O}, \text{S-Me}$  or  $\text{S}$ ) (D)

fluorescence and phosphorescence emissions. They contain the general formula  $C^{\wedge}NPt(acac)$ , whereby the photophysical properties are strongly related to the  $C^{\wedge}N$  ligand [31, 96].

Besides mononuclear cyclometalated complexes, also bi- and trinuclear Pt and Ir complexes have been reported (figure 2.20). These compounds experience a stronger heavy atom effect, and therefore enhanced spin-orbit coupling. In general, multinuclear complexes exhibit significantly redshifted absorption and emission spectra, which is a result of the stabilization of the LUMO by presence of additional metal centers [97].

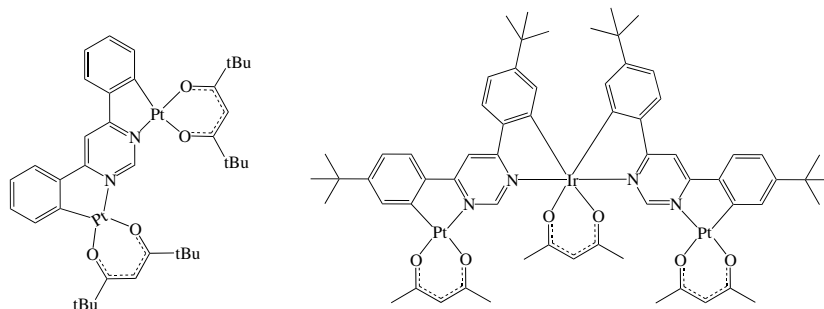


**Figure 2.20:** Structures of a binuclear platinum(II) complex (left) and a hybrid trinuclear complex with two Pt and one Ir center (right)

### 2.11.1 Tuning of photophysical properties of porphyrins by cyclometalation

As already mentioned above in section 2.9.1, a common strategy of alternating the photophysical properties of porphyrins is the  $\pi$ -extension of the macrocycle, which however only shows limited influence. Furthermore, different central atoms lead to strongly varying spectral properties; nevertheless, it needs to be considered that only a small amount of atoms such as Ir (III), Pt (II), and Pd (II) have shown to be suitable for optical sensing by showing bright phosphorescence [7]. It would be a topic of high interest to be able to tune the photophysical properties of porphyrins in a controlled manner, in order to be able to use them for a larger variety of applications. For example, currently life-time based pH sensing remains a difficult task due to the quenching of phosphorescence by molecular oxygen. This problem could be avoided if the lifetimes of the complexes were reduced drastically.

One possibility to alter the photophysical properties of luminescent dyes might be cyclometalation of the respective compound.

#### Principle of cyclometalation - heavy atom effect

Cyclometalation is a possibility for the introduction of heavy atoms such as Pt (II) or Ir(III), which enhance the process of spin-orbit coupling.

According to spin selection rules, the transition between states showing different multiplicity is forbidden. Nevertheless, these transitions can often be observed in organic molecules which is due to spin-orbit coupling. This phenomenon is a result of quantum mechanical mixing of states showing different multiplicity, meaning that no pure states are present. Regarding the theoretical background, spin-orbit coupling is a result of the interaction of spin magnetic moments of electrons and the magnetic field that arises from motion of the nucleus [98]. Spin-orbit coupling increases proportionally with higher atomic number, due to the reason that the magnitude

of the magnetic field rises with the nuclear charge and therefore the atomic number. This means that by introduction of heavy atoms the rates of spin-forbidden transitions (radiative and non-radiative) can increase significantly, which is known as the so-called heavy-atom (H-A) effect [99].

The heavy-atom effect was first noticed and described by McClure et al. in 1949 [100]. It was observed that the introduction of heavy atoms could alter the phosphorescence lifetimes of luminescent compounds, whereby a decrease in lifetime was measured with increasing atomic number of the heavy atom. Later on it was discovered by Ermolaev et al. that besides the decrease of lifetime of the triplet state an increase of the ratio of phosphorescence to fluorescence quantum yields  $\phi_P/\phi_F$  occurs. The decrease in phosphorescent lifetime is a result of both the increasing rate of phosphorescence and intersystem crossing for  $T_1$  to  $S_0$ . However, the increase in  $\phi_P/\phi_F$  is due to an enhanced rate of intersystem crossing for  $S_1$  to  $T_1$ . Therefore, it was concluded that heavy atoms have a significant impact on the rate of triplet decay and also on the rate of population of the triplet state [99].

### Effect of cyclometalation on porphyrin dyes

As already stated above controlling the photophysical properties of porphyrin dyes by cyclometalation would be highly favourable in order to generate a larger range of applications.

As described in section 2.11 cyclometalated complexes often suffer from the drawback of poor molar absorption coefficients in the visible region. Porphyrin dyes show good molar absorption coefficients, however these indicators often exhibit only moderate quantum yields [7]. Therefore, one strategy of achieving dyes showing high quantum yields and good molar absorption coefficients could be the method of cyclometalation. Furthermore, a change of spectral properties such as a bathochromic shift of absorption and emission would be expected. The expected properties for cyclometalated porphyrin dyes are shown in figure 2.21.

It is known that due to the heavy-atom effect an increase of radiative deactivation  $\Gamma$  can occur, leading to a shorter lifetime ( $\tau = \frac{1}{\Gamma+k_{nr}}$ ) [99]. However, the impact of cyclometalation on quantum yields, which is given by equation  $Q = \frac{\Gamma}{\Gamma+k_{nr}}$ , might be positive or negative, as cyclometalation also affects the rate constant of the non-radiative deactivation  $k_{nr}$  from the triplet state.

To enable a cyclometalation process, suitable structures of porphyrins need to be synthesized. This can be done, for instance, by introduction of a pyridine at the meso position of the macrocycle or by introduction of 2-phenylpyridine groups (figure 2.21). The aim of this master's thesis was to establish a structure-property relationship for newly synthesized cyclometalated porphyrin complexes.

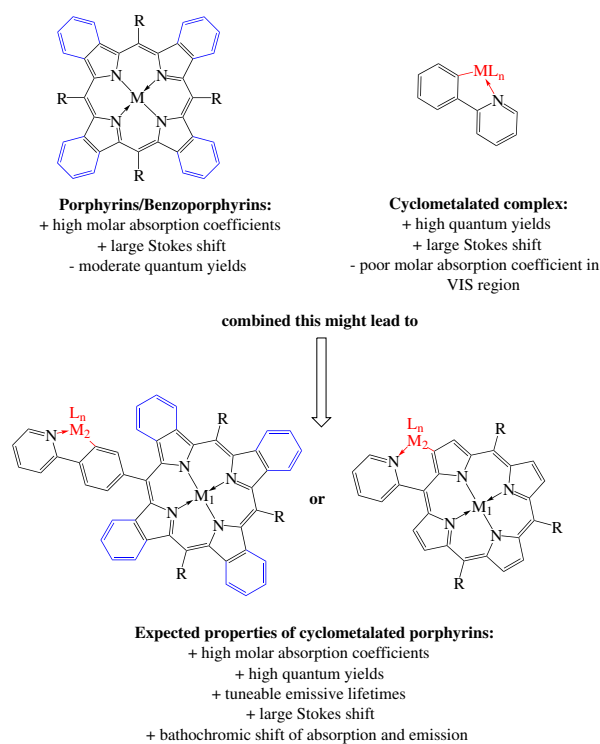


**Figure 2.21:** Expected advantages for the cyclometalation of porphyrin dyes

---

## 3 Chemicals and Methods

The chemicals and solvents that were used during the experimental work of this masters's thesis are listed in the tables below.

### 3.1 Chemicals

**Table 3.1:** List of used chemicals

<b>Chemical</b>	<b>Supplier</b>	<b>CAS-Number</b>
Platinum	Ögussa	7440-06-4
Hydrochloric acid	Merck	7647-01-0
Nitric acid	Merck	7697-37-2
Hydrazine dihydrochloride	SIGMA-ALDRICH	5341-61-7
Potassium chloride	Merck	7447-40-7
Dimethylsulfide	Alfa Aesar	75-18-3
Sodium sulfate	Merck	7757-82-6
Methyl lithium	Aldrich	917-54-4
Ammonium chloride	Merck	12125-02-9
Decolorizing charcoal	Kremer Pigmente	7782-42-5
Acetylacetone	SIGMA-ALDRICH	123-54-6
Potassium hydroxide	Merck	1310-58-3
1,5-Cyclooctadiene	Aldrich	111-78-4
Tin chloride	Merck	7772-99-8
Sodium Iodide	Aldrich	7681-82-5
2-Bromopyridine	Alfa Aesar	109-04-06
n-Butyl lithium	Acros	109-72-8
Tributyltin chloride	Alfa Aesar	1461-22-9
Propionic acid	Roth	79-09-4
Pyrrole	Aldrich	109-97-7
2-Pyridine carboxaldehyde	TCI	1121-60-4
Pentafluorobenzaldehyde	ABCR	653-37-2

### 3.2 Solvents

Solvents were used as bought from the supplier, unless it is indicated in the experimental section that a solvent was dried before the respective synthesis. In this case, solvents were dried for 24 hours over 4 Å molecular sieve.

**Table 3.2:** List of used solvents

Solvent	Supplier	CAS-Number
Dichloromethane	Fisher chemicals	75-09-2
Diethylether	Fisher chemicals	60-29-7
DMSO	Roth	67-68-5
Methanol	Fisher chemicals	67-56-1
2-Propanol	Fisher chemicals	67-63-0
Ethanol	Fisher chemicals	64-17-5
Acetone	Fisher chemicals	67-64-1
Toluene	Fisher chemicals	108-88-3
1,2,4-Trimethylbenzene	Aldrich	95-63-6
THF	Fisher chemicals	109-99-9
Ethyl acetate	Fisher chemicals	141-78-6
Cyclohexane	Fisher chemicals	110-82-7
n-Heptane	Roth	142-82-5
3M Novec 7200	3M	163702-05-4

### 3.2.1 NMR solvents

**Chloroform D:** + 0.03 % TMS, 99.80 % D, supplier: Eurisotop

**Methylene chloride D2:** 99.90 % D, supplier: Eurisotop

**Benzene D6:** 99.50 % D, water content < 0.02 %, supplier: VWR

## 3.3 Chromatography

### 3.3.1 Thin layer chromatography (TLC)

Most reactions performed were monitored using thin layer chromatography. Hereby, TLC plates from Merck (Silica gel 60 F<sub>254</sub>, 20 x 20 cm) were used. The solvent used for TLC was dependent on the respective product. The spots on the TLC plate were detected using an UV lamp ( $\lambda = 254$  nm or  $\lambda = 366$  nm).

### 3.3.2 Flash column chromatography

Some products were purified and separated from side-products by flash column chromatography. Silica gel purchased from Roth (0.04-0.063 mm, 60 Å) was utilized. As a general rule for the amount of required silica gel, approximately the 100-fold amount of the product was needed. The solvents used for column chromatography strongly depend on the respective product. Typically, an  $R_f$ -value between 0.2 and 0.4 was aimed to achieve. During the process of purification via column chromatography often the polarity of the eluent mixture was increased slowly. The exact solvent mixtures for each product are described in the experimental section of this thesis.

## 3.4 Photophysical measurements

### 3.4.1 Absorption spectra

Absorption spectra were recorded using a *Varian Cary 50 conc* UV-VIS spectrophotometer. The used cuvettes were precision cells of special optical glass by Hellma Analytics (type 100-OS, 10 mm). All spectra were recorded in scan mode "fast" and the baseline was corrected depending on the respective solvent (blank sample).

### 3.4.2 Emission and excitation spectra

The emission and excitation spectra were measured on a *Fluorolog®3* spectrofluorometer from Horiba Scientific which was equipped with a *R2658* photomultiplier by Hamamazu. Regarding the cuvettes, fluorescence cuvettes from Hellma (type 100-QS, 10 mm) with screw-caps were utilized.

### 3.4.3 Lifetime measurements

Phosphorescence decay times were measured with a *Fluorolog®3* spectrofluorometer from Horiba Scientific. Excitation was achieved with two different SpectraLEDs ( $\lambda = 395$  nm or  $\lambda = 450$  nm), whereby additionally filters were used (OG570 or RG665). The dyes were diluted in toluene until the absorption spectrum showed an absorption intensity below 0.1. Afterwards, the solution was degassed for 10 minutes with argon and the excitation/emission spectra were recorded using a DAS-6 Analysis software.

### 3.4.4 Relative quantum yields

The relative quantum yields were determined by using references with known quantum yields for each dye. The dyes were diluted until an absorption intensity below 0.1 was achieved. Then, emission spectra were recorded on the *Fluorolog®3* spectrofluorometer. Afterwards, the emission spectra were integrated with the Origin-Software and the relative quantum yields were calculated according to equation 3.1 [101].

$$\Phi_C = \Phi_R \frac{E_C}{E_R} \frac{B_R}{B_C} \frac{n_C^2}{n_R^2} \quad (3.1)$$

Hereby,  $\Phi$  represents the quantum yield,  $E$  is the integrated area of the respective emission spectrum,  $B$  represents the absorption related term ( $1 - 10^{-A}$ ) and  $n$  is the refractive index of the solvent. The subscripts  $C$  and  $R$  indicate the investigated compound and the reference dye, respectively.

## 3.5 Structural characterization

### 3.5.1 Nuclear magnetic resonance spectroscopy (NMR)

$^1\text{H}$ -NMR spectra were measured on a *Bruker AVANCE III* instrument (300.36 MHz) which was equipped with an autosampler. As a reference for the measured chemical shifts  $\delta$  (ppm), the signal of the respective deuterated solvent (e.g.  $\text{C}_6\text{D}_6$ ) was used. The software MestReNova NMR was utilized for analysis of the recorded spectra. The chemical shifts  $\delta$  (in ppm), the multiplicity (e.g. singlet (s), doublet (d)), the coupling constant  $J$  and the number of protons are displayed for each measured compound.

### 3.5.2 High resolution mass spectrometry (MALDI-TOF)

Structural measurements via mass spectrometry were carried out with a *Micromass ToFSpec 2E* on a MALDI-TOF/TOF from *Bruker Ultraflex Extreme*. This type of analysis was performed by Prof. Saf's group at the Institute for Chemistry and Technology of Materials at Graz University of Technology. External calibration was achieved by usage of a mixture of poly(ethyleneglycol) standards. Analysis of the received data was performed with *MassLynx<sup>TM</sup> V4.1* software from *Waters*.

---

## 4 Experimental

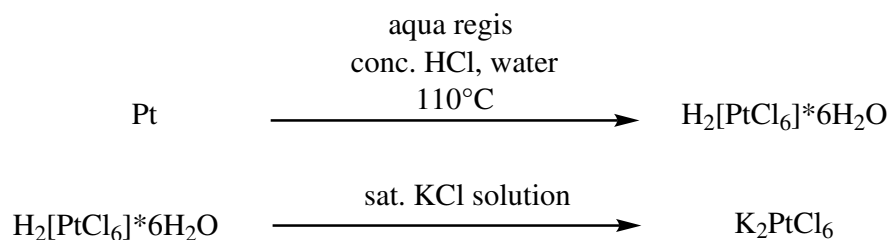
In the following, the experimental procedures for the synthesis that were carried out successfully during the course of this master's thesis will be described. Synthesis that did not yield the desired product will be discussed in chapter 'results and discussion' and the respective experimental procedure will be shown in the appendix of this thesis.

### 4.1 Synthesis of Pt-precursors for platination and cyclometalation reactions

#### 4.1.1 Potassium tetrachloroplatinate (II) $K_2PtCl_4$

The synthesis of  $K_2PtCl_6$  and the subsequently prepared  $K_2PtCl_4$  were performed analogously to reference [102].

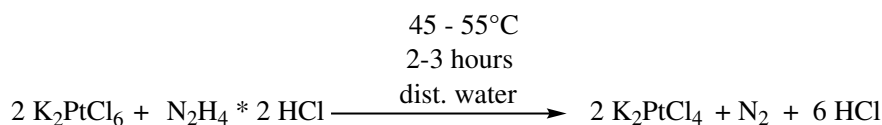
#### Potassium hexachloroplatinate



**Figure 4.1:** Synthesis of  $K_2PtCl_6$  from pure platinum metal

Platinum metal (3.00 g, 15.4 mmol) was dissolved in aqua regia in a beaker in an oil bath at 70 °C. The temperature was increased to 110°C and the evaporated volume was filled up with HCl (3 x 15 ml). Then, after further evaporation, the volume was filled up with distilled water (3 x 20 ml). After a final volume reduction to 3 ml, approximately 5 ml of saturated KCl solution were added, which resulted in a strong yellow colour of the suspension. In the next step, the mixture was centrifuged and washed with saturated KCl solution four times (4000 rpm, 2 min). Then, another washing step, using ice-cold distilled water (2 x 10 ml) was performed and the mixture was centrifuged again (4000 rpm, 2 min), in order to eliminate remaining traces of KCl. Afterwards, the residue was dried in the vacuum drying cabinet at 65 °C for 48 hours, yielding a bright yellow solid ( $K_2PtCl_6$ ).

Yield: 7.26 g (97 %)

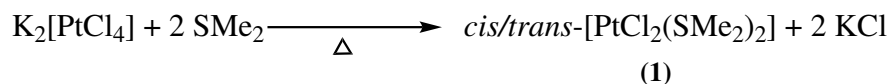
**Potassium tetrachloroplatinate (II)****Figure 4.2:** Preparation of  $\text{K}_2\text{PtCl}_4$  from potassium hexachloroplatinate using hydrazine dihydrochloride

$\text{K}_2\text{PtCl}_6$  (6.00 g, 12.3 mmol, 1 equ.) was suspended in distilled water (55 ml) in a beaker at 45 °C. Hydrazine dihydrochloride (0.68 g, 12.9 mmol, 1.05 eq.) was dissolved in distilled water (5 ml) and added dropwise to the suspension. After addition of hydrazine, the temperature was increased to 55 °C. The solution was stirred for approximately two more hours, until a red clear solution with traces of elemental platinum was obtained. The mixture was filtered, in order to remove traces of platinum; the filtrate was evaporated to a final volume of about 10 ml. The solution was then allowed to slowly evaporate in the heating cabinet, leading to red, crystalline  $\text{K}_2\text{PtCl}_4$ .

Yield: 4.12 g (81 %)

**4.1.2 Synthesis of Bis[Dimethyl( $\mu$ -Dimethyl Sulfide)Platinum(II)] (2)**

Both, compound **1** and compound **2** were synthesized according to reference [103].

**Cis/trans-Dichlorobis(Dimethyl Sulfide)Platinum(II) (1)****Figure 4.3:** Synthesis of compound **1**

To a 100 ml three-necked-round bottom flask with rubber septum,  $\text{N}_2$  inlet and gas outlet, was added a solution of the earlier synthesized  $\text{K}_2\text{PtCl}_4$  (1.00 g, 2.41 mmol, 1 eq.) in distilled water (15 ml). Dimethylsulfide (1.3 ml, 17.6 mmol, 7.3 eq.) was added slowly to the stirred solution, which resulted in a yellow/orange precipitate. Then, the mixture was heated using a heating mantle for 30 minutes, until a bright yellow precipitate appeared. In the next step, the mixture was allowed to cool to room temperature and was extracted with dichloromethane (2 x 50 ml). The organic phases were combined, dried over anhydrous  $\text{Na}_2\text{SO}_4$  and the solvent was evaporated by rotary evaporation. The product was obtained as a yellow solid and was not further purified for following synthesis.

Yield: 0.76 g (86 %)

The NMR spectrum is shown in the appendix as figure 10.1. Analysis data are in accordance with literature.

$^1\text{H}$  NMR (300 MHz, Chloroform- $d$ ):  $\delta = 2.53 - 2.40$  (m, 12H, S-Me with  $^{195}\text{Pt}$  satellites), 2.66 - 2.49 (m, 12H, S-Me with  $^{195}\text{Pt}$  satellites); *cis-* and *trans* isomers

**Bis[Dimethyl( $\mu$ -Dimethyl Sulfide)Platinum(II)] (2)**

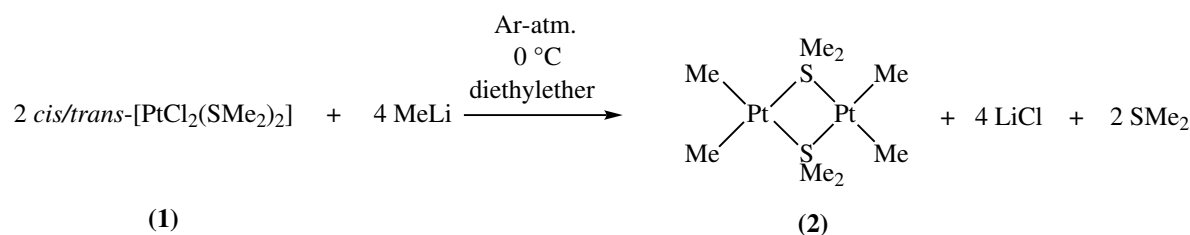


**Figure 4.4:** Synthesis of compound **2**

A 100 ml Schlenk flask under argon atmosphere was charged with finely powdered and vacuum-dried compound **1** (0.71 g, 2.00 mmol, 1 eq.). The complex was then suspended in 30 ml of dry diethylether and the mixture was cooled in an ice-bath for approximately 40 min. Over a period of 10 minutes, a 1.5 M solution of methyl lithium in diethylether (2.7 ml, 4.07 mmol, 2 eq.) was added dropwise. The mixture was stirred for 20 minutes while being cooled in an ice-bath; then cooled saturated  $\text{NH}_4\text{Cl}$ -solution (1 ml) and cooled distilled water (20 ml) were added, which led to a light brown colour of the suspension. In the next step, the mixture was extracted with ice-cold diethylether (2 x 40 ml). The organic phases were combined, cooled to 0 °C and dried over  $\text{Na}_2\text{SO}_4$ . A small amount of decolorizing charcoal (0.3 g) was added and the mixture was filtered. The solvent was evaporated under reduced pressure without using a hot water bath, due to temperature instability of the compound, leading to a slightly yellow solid. The product (compound **2**) was stored in a Schlenk flask in the freezer under Ar-atmosphere.

Yield: 0.22 g (25 %)

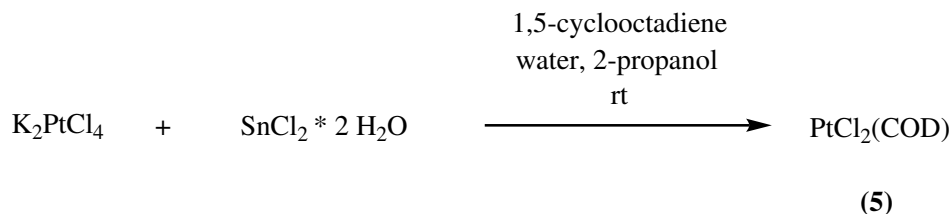
The NMR spectrum is shown in the appendix as figure 10.2. Analysis data are in accordance with literature.

$^1\text{H}$  NMR (300 MHz,  $\text{CDCl}_3$ ):  $\delta = 2.85 - 2.67$  (m, 12H, S- $\text{Me}_2$  ligand), 0.59 (s, 12H, Pt-Me with  $^{195}\text{Pt}$  satellite signals)



4.1.4 [Synthesis of PtMe<sub>2</sub>(COD)] (7)

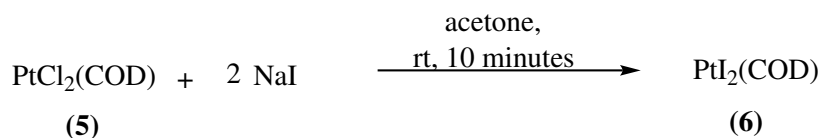
Compound **7** and its previous stages (compound **5** and **6**) were synthesized analogously to reference [105].

PtCl<sub>2</sub>(COD) (**5**)

**Figure 4.7:** Synthesis of compound **5**

K<sub>2</sub>PtCl<sub>4</sub> (0.51 g, 1.22 mmol, 1 eq.) was dissolved in distilled water (8 ml) in a one-neck round bottom flask. 2-Propanole (5.5 ml), 1,5-cyclooctadiene (1 ml, 8.13 mmol, 6.7 eq.) and tin chloride (9.1 mg, 0.041 mmol, 0.03 eq.) were added and the solution was stirred over night. After 48 hours the mixture was filtered and washed with distilled water (10 ml) and ethanol (3 ml) and the solid product was allowed to dry at air.

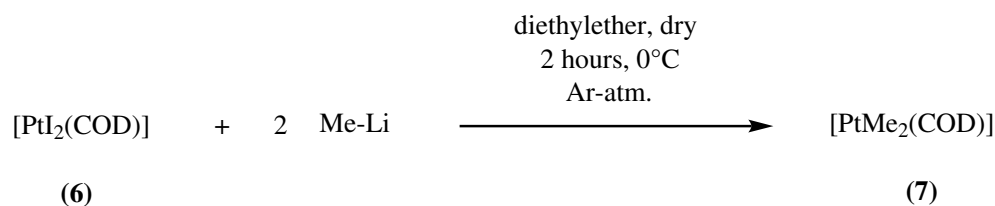
Yield: 0.35 g (77 %)

PtI<sub>2</sub>(COD) (**6**)

**Figure 4.8:** Synthesis of compound **6**

Compound **5** (0.35 g, 0.94 mmol, 1 eq.) was suspended in acetone (25 ml) under continuous stirring. NaI (0.295 g, 1.97 mmol, 2 eq.) was added and the solution was stirred for approximately 10 minutes. The solvent was evaporated under reduced pressure by rotary evaporation. The residue was washed with distilled water (3 x 5 ml), yielding a bright yellow solid (compound **6**), which was air-dried for several hours.

Yield: (0.40 g, 77 %)

**PtMe<sub>2</sub>(COD) (7)****Figure 4.9:** Synthesis of compound **7**

PtI<sub>2</sub>(COD) (0.40 g, 0.72 mmol, 1 eq.) was dissolved in dry diethylether (8 ml) in an ice-bath and stirred continuously. A 1.2 M methyl lithium solution (1.65 ml, 1.98 mmol, 2.75 eq.) was added slowly and the mixture was stirred for two hours at 0 °C. The solution was hydrolysed by addition of saturated aqueous NH<sub>4</sub>Cl solution (20 ml). Then, the mixture was extracted with ice-cold diethylether and the organic fractions were combined and dried over anhydrous sodium sulfate. A spatula tip of decolourising charcoal was added and the mixture was filtered. The solvent was removed by rotary evaporation, yielding a light brown solid.

Yield: (0.10 g, 44 %)

The NMR spectrum is shown in the appendix as figure 10.3. Analysis data are in accordance with literature.

<sup>1</sup>H NMR (300 MHz, C<sub>6</sub>D<sub>6</sub>): δ = 4.68 – 4.46 (m, 4H, COD, CH), 1.90 – 1.58 (m, 8H, COD, CH<sub>2</sub>), 1.26 (s, 6H, Pt-Me with <sup>195</sup>Pt satellite signals)

## 4.2 Platination reactions with synthesized Pt-precursors

### 4.2.1 Synthesis of PtTPTBP (8) using compound 2 as a precursor

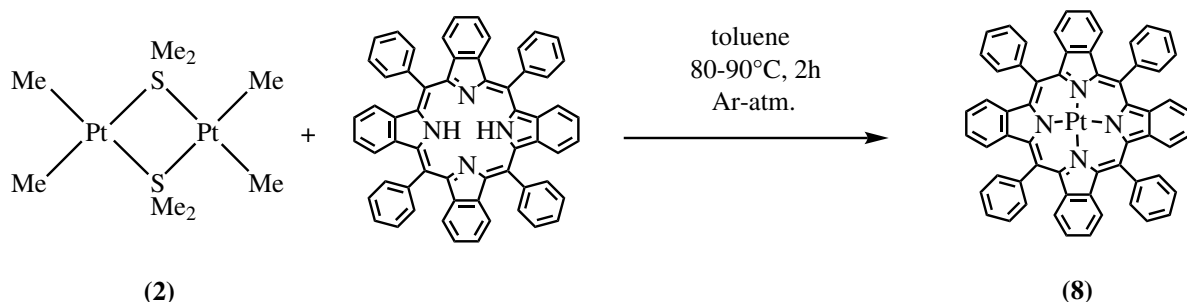


**Figure 4.10:** Synthesis of compound 8

H<sub>2</sub>TPTBP (3.0 mg, 3.56  $\mu$ mol, 1 eq.) was dissolved in toluene (2 ml) in a Schlenk flask under argon atmosphere. A gas bubbler was used in order to allow the methane formed during this procedure to escape from the reaction vessel. The solution was heated up to 80 °C in an oil bath and the platinum precursor (compound 2) (6.3 mg, 11.0  $\mu$ mol, 3 eq.) was added. After increasing the reaction temperature to 90 °C and stirring for two hours, full conversion of the porphyrin ligand to the Pt complex (compound 8) could be observed in the UV-VIS spectrum.

UV-VIS spectra of educt and product are shown in chapter 'results and discussion' as figure 5.3

$\lambda_{max}$  (nm) educt in DCM: 463

$\lambda_{max}$  (nm) product in DCM: 430

### 4.2.2 Attempted synthesis of PtTFPP (9) using compound 2 as a precursor

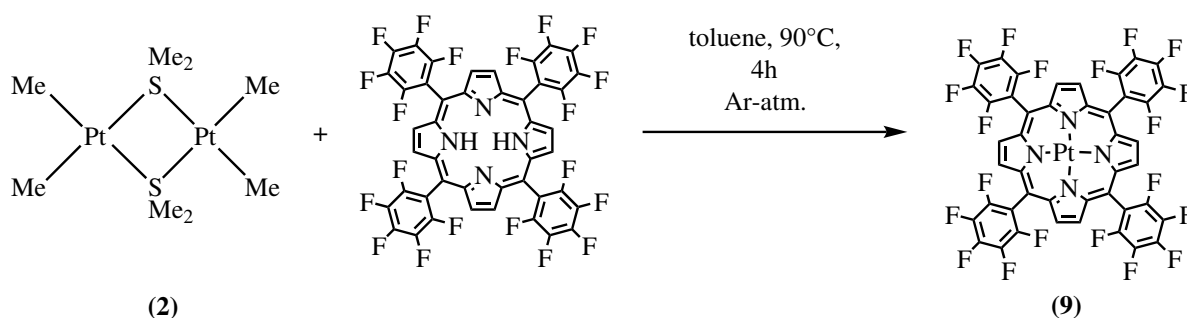


**Figure 4.11:** Synthesis of compound 9

H<sub>2</sub>TFPP (3.0 mg, 3.1  $\mu$ mol, 1 eq.) was dissolved in toluene (2 ml) in a Schlenk flask under argon atmosphere. The solution was heated up to 90 °C and the Pt-precursor (compound 2) (4.4 mg, 7.7  $\mu$ mol, 2.5 eq) was added. A conversion of the educt to the Pt-complex could be observed after approximately 10 minutes. The percentage of converted ligand to the desired Pt-complex increased constantly by addition of more equivalents of the Pt-precursor. An amount of 4.5 eq.

of the precursor led to a conversion of approximately 50 %; further progress would be expected by addition of more equivalents of compound 2.

UV-VIS spectra of educt and product are shown in chapter 'results and discussion' as figure 5.5.

$\lambda_{max}$  (nm) educt in DCM: 411

$\lambda_{max}$  (nm) product in DCM: 392

#### 4.2.3 Synthesis of PtTPTBP (8) using compound 7 as a precursor

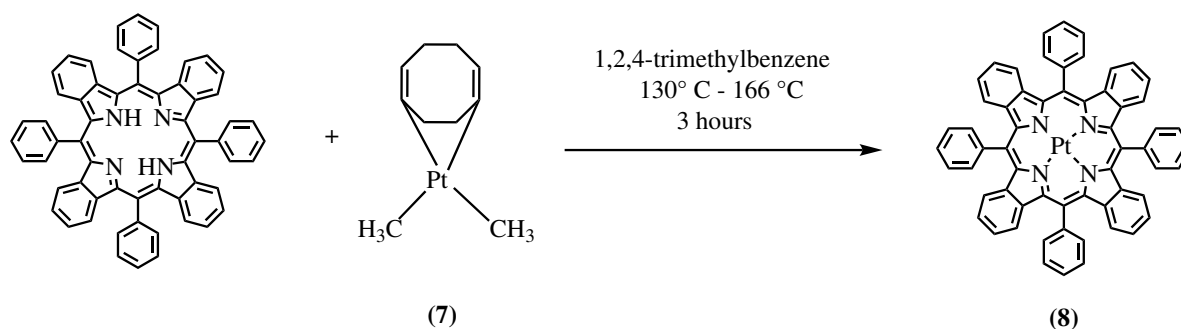


**Figure 4.12:** Synthesis of compound 8 using PtMe<sub>2</sub>COD (7) as a precursor

H<sub>2</sub>TPTBP (3.1 mg, 3.8  $\mu$ mol, 1 eq.) was dissolved in 1,2,4-trimethylbenzene (5 ml) in a Schlenk flask under argon atmosphere. PtMe<sub>2</sub>COD (compound 7) (1.9 mg, 5.7  $\mu$ mol, 1.5 eq) was added as a platination reagent. The solution was stirred and heated up to 166 °C for three hours. Full conversion of the educt to the desired product could be observed in the UV-VIS spectrum.

UV-VIS spectra of educt and product are shown in chapter 'results and discussion' as figure 5.4.

$\lambda_{max}$  (nm) educt in DCM: 463

$\lambda_{max}$  (nm) product in DCM: 430

### 4.3 Synthesis of suitable structures for cyclometalation reactions

Different structures of porphyrins that allow peripheral cyclometalation or cyclometalation on the porphyrin core were synthesized. The respective procedures are described in the following section.

#### 4.3.1 Porphyrins for peripheral cyclometalation

##### Synthesis of 2-(tributylstannyl)pyridine (10)

This synthesis was performed analogously to reference [106]. A solution of 2-bromopyridine

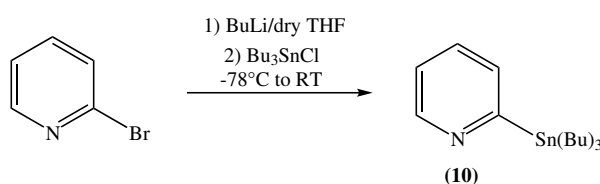


**Figure 4.13:** Synthesis of compound **10**

(1.3 ml, 12.5 mmol, 1 eq.) in dry THF (5 ml) in a Schlenk flask under argon atmosphere was stirred and cooled down to -78 °C in a mixture of ethanol and liquid N<sub>2</sub>. n-Buli (5.4 ml, 2.34 M in hexane, 12.5 mmol, 1 eq.) was added dropwise and the mixture was stirred for 1 hour. Tributyltin chloride (3.4 ml, 12.6 mmol, 1 eq.) was added quickly at -78 °C, then the solution was allowed to stir for 3 more hours followed by 35 minutes of stirring at room temperature. The reaction mixture was quenched using saturated aqueous NH<sub>4</sub>Cl solution (10 ml). After extraction with ethyl acetate (3 x 25 ml) the combined organic layers were washed with brine (2 x 25 ml) and water (2 x 20 ml) and dried over anhydrous Na<sub>2</sub>SO<sub>4</sub>. Then, the solvent was evaporated under reduced pressure yielding a dark brown liquid. The product was not further purified for following synthesis.

Yield: 3.2 g (72 %)

The NMR spectrum is shown in the appendix as figure 10.4.

<sup>1</sup>H NMR (300 MHz, CDCl<sub>3</sub>): δ = 8.73 (d, *J* = 4.2 Hz, 1H, pyridine), 7.48 (dt, *J* = 8.0 Hz, 1H, pyridine), 7.40 (d, *J* = 7.4 Hz, 1H, pyridine), 7.11 (t, 1H, pyridine), 1.56 (t, 6H, butyl, CH<sub>2</sub>), 1.37 - 1.27 (m, *J* = 14.7, 7.3 Hz, 6H, butyl CH<sub>2</sub>), 1.16 - 1.07 (m, 6H, butyl CH<sub>2</sub>), 0.88 (t, *J* = 9.0, 5.5 Hz, 9H, butyl CH<sub>3</sub>)

## Synthesis of compound 12

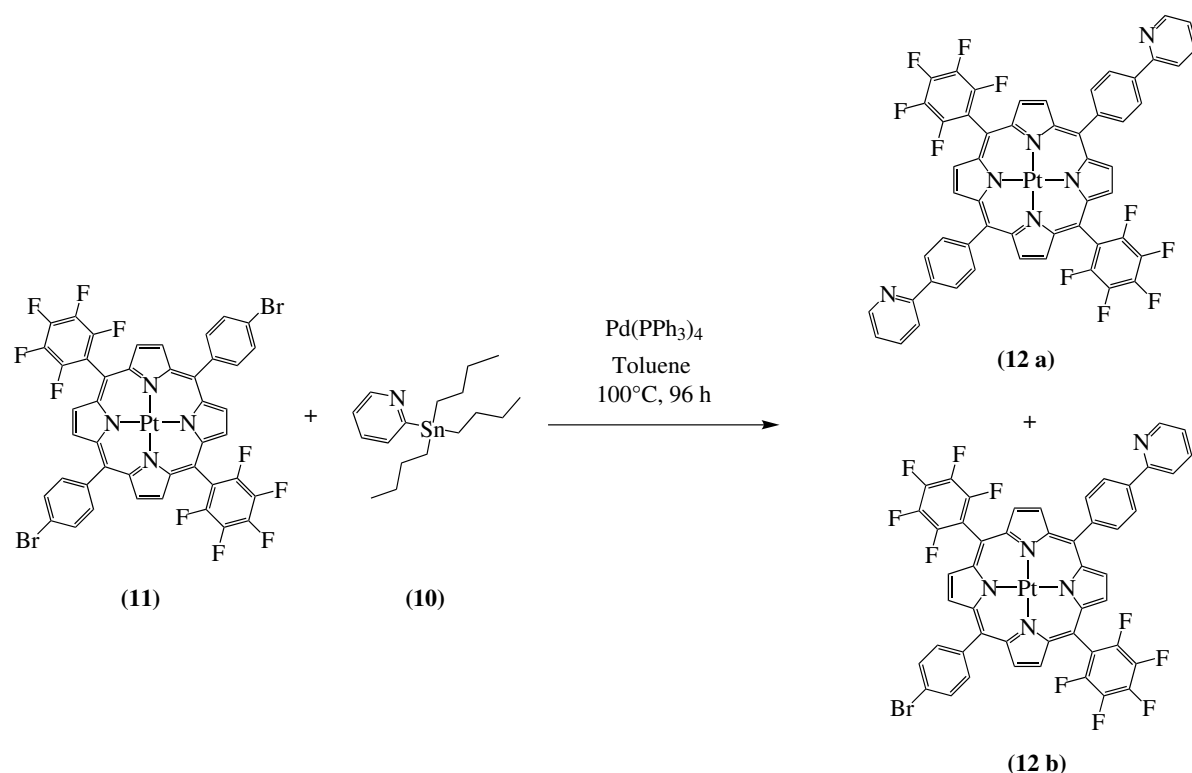


Figure 4.14: Synthesis of compound 12

The reaction was conducted according to reference [107]. A 25 ml Schlenk flask under argon atmosphere was charged with dry toluene (7 ml), the Pt-porphyrin (11) (45.0 mg, 39.4  $\mu\text{mol}$ , 1 eq.), the catalyst Pd(PPh<sub>3</sub>)<sub>4</sub> (11.7 mg, 10.1  $\mu\text{mol}$ , 0.25 eq) and the tin-reagent 2-(tributylstannyl)pyridine (10) (37.3 mg, 97.7  $\mu\text{mol}$ , 2.5 eq.). The reaction mixture was heated up to 100 °C and stirred for 96 hours. The reaction progress was monitored via TLC, which still showed traces of educt after stirring for 96 hours. Nevertheless, the reaction mixture was filtered over aluminium-oxide and washed with ethyl acetate (2 x 20 ml). The product was purified via column chromatography (silica, CH+EE 6+1) to yield the monosubstituted (12 b) and disubstituted (12 a) product.

Yield (monosubstituted, 12 b): 26.6 mg (59 %)

Yield (disubstituted, 12 a): 5.3 mg (12 %)

R<sub>f</sub> value (monosubstituted) (CH+EE 3+1): 0.65

R<sub>f</sub> value (disubstituted) (CH+EE 3+1): 0.49

The NMR spectra are shown in the appendix as figure 10.5 and 10.6.

monosubstituted (12 b): <sup>1</sup>H NMR (300 MHz, CDCl<sub>3</sub>):  $\delta$  = 8.95 (d, *J*=5.4Hz, 1H, pyridine), 8.84 (d, *J*=5.1Hz, 4H, porphyrin, beta-H), 8.73 (d, *J*=5.0 Hz, 4H, porphyrin, beta-H), 8.41 (d, *J*=8.3Hz, 2H, arom. CH), 8.28 (d, *J*=8.4Hz, 2H, arom. CH), 8.09 - 8.00 (m, 3H, pyridine),

7.98 - 7.87 (m,  $J=8.2\text{Hz}$ , 4H, arom. CH)

disubstituted (12 a):  $^1\text{H}$  NMR (300 MHz,  $\text{CDCl}_3$ ):  $\delta = 8.95$  (d,  $J=5.1\text{Hz}$ , 4H, porphyrin, beta-H), 8.87 (d,  $J=4.5\text{Hz}$ , 2H, pyridine), 8.73 (d,  $J=5.1\text{ Hz}$ , 4H, porphyrin, beta-H), 8.40 (d,  $J=8.0\text{Hz}$ , 4H, arom. CH), 8.29 (d,  $J=8.1\text{Hz}$ , 4H, arom. CH), 8.05 (d,  $J=7.8\text{Hz}$ , 2H, pyridine), 7.93 (t,  $J=7.6\text{Hz}$ , 2H, pyridine), 7.82 (t, 2H, pyridine)

### 4.3.2 Synthesis of porphyrins suitable for cyclometalation at the porphyrin core

#### Synthesis of porphyrin ligand (compound 13)

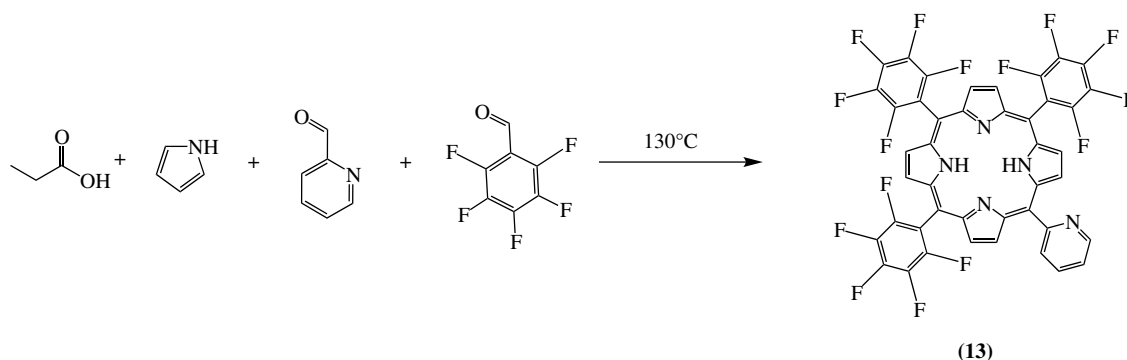


**Figure 4.15:** Synthesis of compound 13

In a one-neck round-bottom-flask, propionic acid (270 ml, 3.61 mol) was heated up to 130 °C. Pyrrole (5 ml, 72 mmol, 5.9 eq.), 2-pyridinecarboxaldehyde (1.2 ml, 12.2 mmol, 1 eq.) and pentafluorobenzaldehyde (7.51 ml, 60.8 mmol, 5 eq.) were added to the hot acid and the dark brown mixture was stirred for 30 minutes. An UV-VIS spectrum was measured that showed that the desired porphyrin ligand (**13**) had formed. Furthermore, the reaction progress was monitored via TLC (Tol+DCM 5+4), which indicated full conversion to the ligand. The propionic acid was evaporated on the rotary evaporator and the product mixture was purified via column chromatography (silica, Tol+DCM 5+4). The product fractions obtained from column chromatography were dried and dissolved in a minimum amount of DCM. Cyclohexane (10 ml) and 3M Novec 7200 (3 ml) were added. DCM was allowed to evaporate over night and the precipitated dye was filtered through cotton and washed with cyclohexane (5 ml), in order to yield a pure dark violet ligand. Unfortunately, it was not possible to achieve quantitative precipitation of the dye, wherefore also one fraction of the product showing slight impurities was obtained.

Yield (without impurities): 389 mg (4 %)

Yield (fraction containing slight impurities): 81 mg (1 %)

$R_f$  value (product) (Tol+DCM 5+4): 0.31

The NMR spectrum is shown in the appendix as figure 10.7.

$^1\text{H}$  NMR (300 MHz,  $\text{CDCl}_3$ ):  $\delta = 9.17$  (d,  $J = 4.6\text{ Hz}$ , 1H, pyridine), 9.02 – 8.82 (m, 8H, porphyrin, beta-H), 8.27 (d,  $J = 7.7\text{ Hz}$ , 1H, pyridine), 8.16 (t,  $J = 7.6\text{ Hz}$ , 1H, pyridine), 7.78 (t, 1H, pyridine), -2.88 (s, 2H, N-H)

## Synthesis of Pd-porphyrin compound 14

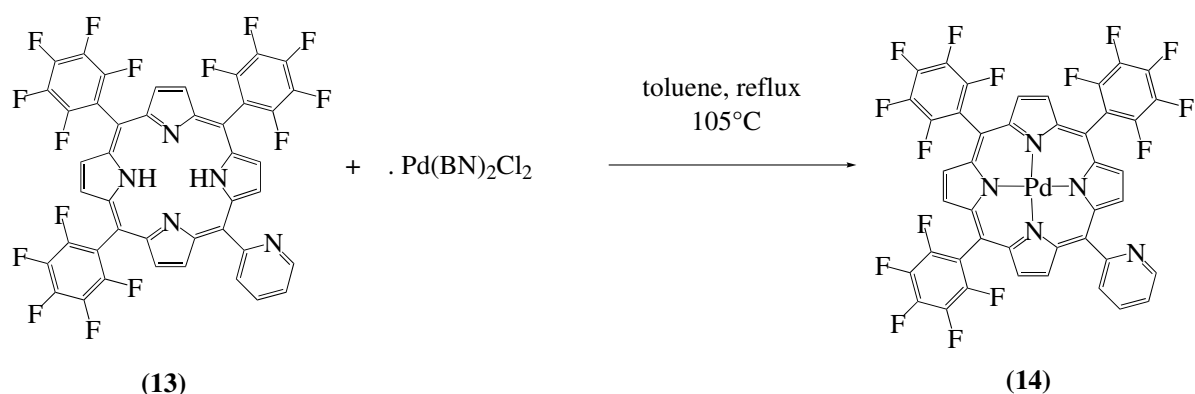


Figure 4.16: Synthesis of compound 14

The porphyrin ligand (compound 13) (160 mg, 0.18 mmol) was dissolved in toluene (30 ml) in a Schlenk flask under argon atmosphere.  $\text{Pd(BN)}_2\text{Cl}_2$  (104 mg, 0.27 mmol, 1.5 eq.) was added and the solution was stirred at 105 °C for 3 hours. An UV-VIS spectrum showed full conversion to the desired Pd-complex (14). The solvent was evaporated under reduced pressure and the residue was cleaned via column chromatography (silica, Tol+DCM 5+4). TLCs and  $^1\text{H}$ NMRs confirmed that despite the purification step still benzonitrile was coordinated to the dye. Therefore, small portions of the dye were washed and centrifuged with 5 ml of ethanol, 500  $\mu\text{l}$  of pyridine and 5 ml of distilled water. Afterwards, each fraction was washed three times with distilled water in order to remove traces of pyridine. Then, another column chromatography (silica, Tol+DCM 5+4) was performed, which yielded the pure Pd-porphyrin-complex (14) as a pink solid.

Yield: 43 mg (24 %)

$R_f$  value (product) (Tol+DCM 5+4): 0.15

The NMR spectrum is shown in the appendix as figure 10.8.

$^1\text{H}$  NMR (300 MHz,  $\text{CDCl}_3$ ):  $\delta = 9.13$  (d,  $J = 4.1$  Hz, 1H, pyridine), 8.94 – 8.79 (m, 8H, porphyrin, beta position), 8.25 (d,  $J = 7.6$  Hz, 1H, pyridine), 8.15 (t,  $J = 7.6$  Hz, 1H, pyridine), 7.77 (t, 1H, pyridine)

### 4.3.3 Synthesis of other dyes besides porphyrins suitable for cyclometalation (16)

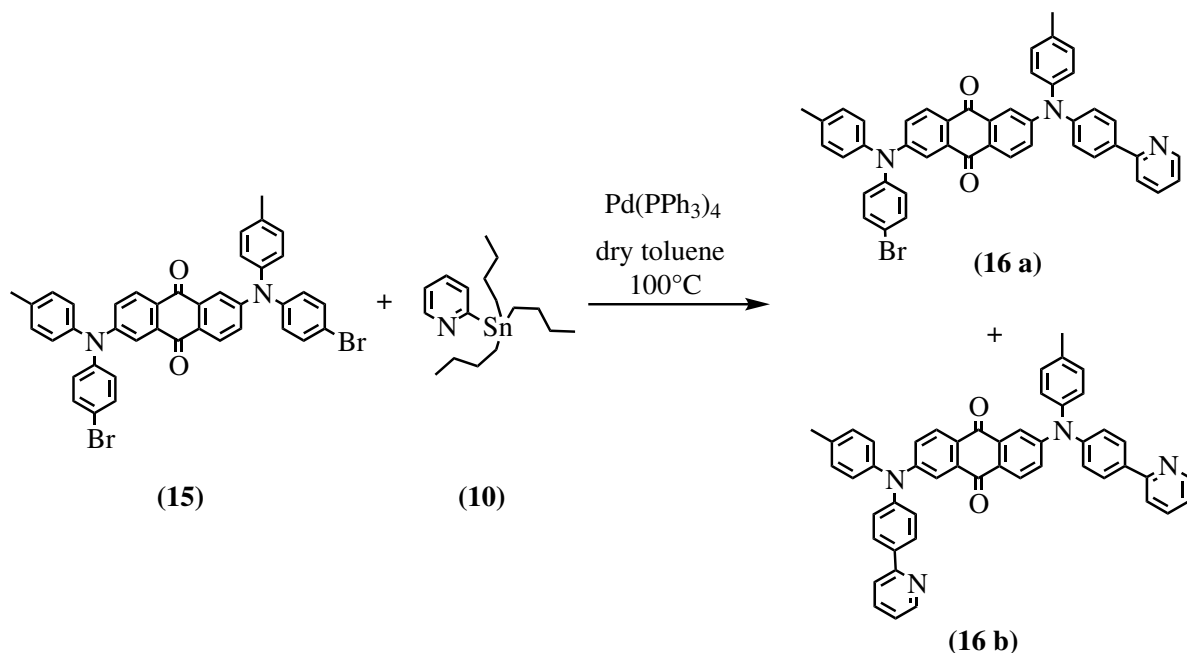


**Figure 4.17:** Synthesis of compound **16**

2,6-Bis((4-bromophenyl)(p-tolyl)amino)anthracene-9,10-dione (compound **15**) (30 mg, 40.8  $\mu\text{mol}$ , 1 eq.) was dissolved in dry toluene (12 ml) in a 25 ml Schlenk flask under argon atmosphere. The catalyst  $\text{Pd(PPh}_3)_4$  (13.1 mg, 11.3  $\mu\text{mol}$ , 0.25 eq.), and tin compound (**10**) (18.1 mg, 52.1  $\mu\text{mol}$ , 1.2 eq.) were added and the solution was heated up to 100  $^\circ\text{C}$  and stirred for 24 hours. A TLC (CH+EE 3+1) was performed to investigate the reaction progress. It was shown that not all educt was converted, nevertheless the reaction work-up was proceeded. The reaction mixture was filtered over aluminium-oxide and washed with ethyl acetate (2 x 20 ml). After evaporation of the solvent under reduced pressure, the crude product was purified via column chromatography (silica, CH+EE 6+1). After solvent evaporation, the monosubstituted (**16 a**) and the disubstituted product (**16 b**) were obtained as red solids.

Yield (monosubstituted, **16 a**): 12.3 mg (41 %)

Yield (disubstituted, **16 b**): 5.8 mg (20 %)

$R_f$  value (monosubstituted) (CH+EE 3+1): 0.58

$R_f$  value (disubstituted) (CH+EE 3+1): 0.26

The NMR spectra are shown in the appendix as figure 10.9 and 10.10.

monosubstituted (**16 a**):  $^1\text{H NMR}$  (300 MHz,  $\text{CDCl}_3$ ):  $\delta$  = 8.73 – 8.65 (m, 1H, pyridine), 8.03 (d,  $J$  = 12.3 Hz, 2H, Anq), 7.96 (d,  $J$  = 10.3 Hz, 2H, pyridine), 7.83 – 7.78 (m, 1H, pyridine), 7.78 – 7.68 (m, 4H, Ph), 7.50 – 7.42 (m, 2H, Ph), 7.24 – 7.17 (m, 6H, Ph+Anq), 7.16 – 7.01 (m,  $J$  = 16.2, 7.6 Hz, 8H, Ph), 2.37 (d,  $J$  = 2.7 Hz, 6H,  $\text{CH}_3$ )

disubstituted (16 b):  $^1\text{H}$  NMR (300 MHz,  $\text{CDCl}_3$ ):  $\delta = 8.72 - 8.65$  (m,  $J = 4.9$  Hz, 2H, pyridine), 8.04 (d,  $J = 8.6$  Hz, 2H, Anq.), 7.96 (d,  $J = 8.5$  Hz, 4H, pyridine), 7.82 (d,  $J = 2.2$  Hz, 2H, pyridine), 7.78 – 7.68 (m,  $J = 17.6, 7.4$  Hz, 4H, Ph), 7.25 – 7.19 (m, 8H, Ph+Anq), 7.18 – 7.01 (m, 8H, Ph), 2.38 (s, 6H,  $\text{CH}_3$ )

## 4.4 Synthesis of cyclometalated complexes

### 4.4.1 Attempted synthesis of cyclometalated compound 17

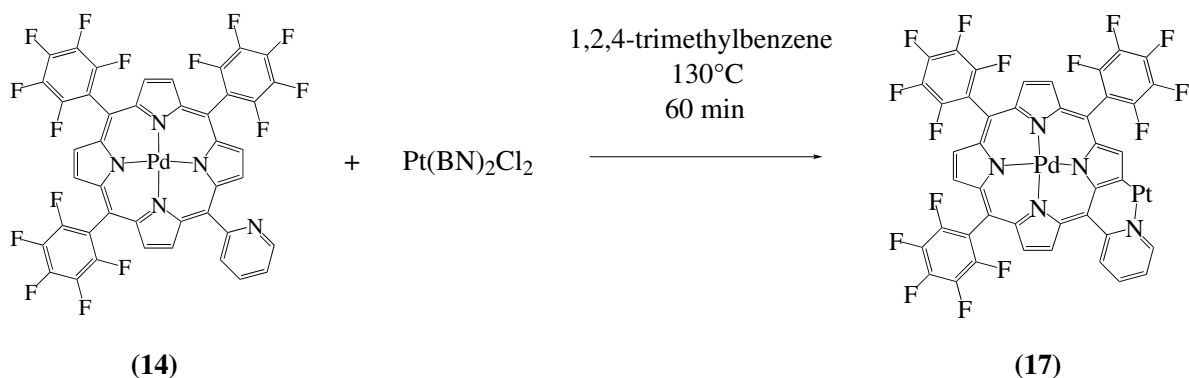


**Figure 4.18:** Synthesis of compound 17

The Pd-porphyrin complex (**14**) (4 mg,  $4.0 \mu\text{mol}$ , 1 eq.) was dissolved in 1,2,4-trimethylbenzene (3 ml) in a Schlenk flask under argon-atmosphere.  $\text{Pt}(\text{BN})_2\text{Cl}_2$  (19.1 mg,  $40.4 \mu\text{mol}$ , 10 eq.) was added and the solution was heated up to  $120^\circ\text{C}$  in an oil bath and stirred for 60 minutes. After 1 hour an UV-VIS spectrum was measured that showed the formation of a new product. The reaction mixture was cooled down to room temperature and acetylacetonone ( $10 \mu\text{l}$ ,  $97.9 \mu\text{mol}$ ) and triethylamine ( $10 \mu\text{l}$ ,  $72.0 \mu\text{mol}$ ) were added. After 20 minutes of stirring, a slight shift of the product peak was observed in the UV-VIS spectrum. The solvent was removed on the rotary evaporator and the residue was purified via column chromatography (silica,  $\text{DCM}+\text{THF}$  10+1). However, TLCs showed that even after purification via column chromatography a complex mixture of various products was present, that could not be separated. It was assumed that no acetylacetonate-ligand was attached to the platinum atom. Preliminary lifetime measurements of the mixed product fractions showed a drastically reduced lifetime of the dye of  $11 \mu\text{s}$ .

$\lambda_{\text{max}}$  (nm) educt in DCM: 412

$\lambda_{\text{max}}$  (nm) product in DCM without addition of acetylacetonone: 434

$\lambda_{\text{max}}$  (nm) product in DCM after addition of acetylacetonone: 429

## 4.4.2 Synthesis of cyclometalated compound 18

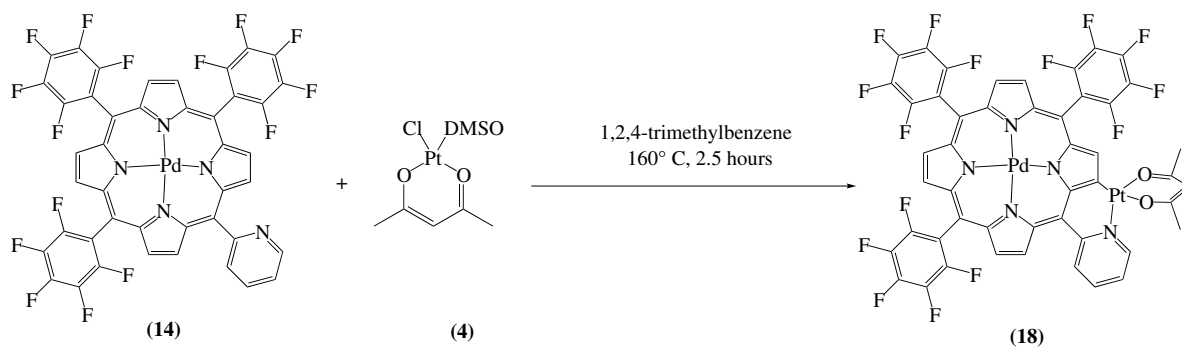


**Figure 4.19:** Synthesis of compound 18

The Pd-porphyrin complex (**14**) (25 mg, 25.2  $\mu\text{mol}$ , 1 eq.) was dissolved in 1,2,4-trimethylbenzene (15 ml) in a Schlenk flask under Ar-atmosphere. The Pt-precursor (compound 4) (18.5 mg, 45.4  $\mu\text{mol}$ , 1.8 eq.) was added and the mixture was stirred at 160 °C for 2 hours in an oil bath. UV-VIS spectra showed full conversion of the educt. The reaction mixture was distilled under reduced pressure at 50 °C; the residue was purified via column chromatography (silica, CH+EE 3+1). The different fractions were collected and a TLC was performed (CH+EE 3+1) in order to identify the desired product fractions. These fractions were evaporated to dryness and washed with 3M Novec 7200 (5 ml) and heptane (5 ml). The residue was dried in the vacuum drying cabinet, yielding a dark green-brownish solid.

Yield: 3.3 mg (10 %)

$R_f$  value (product) (CH+EE 3+1): 0.33

The NMR spectrum is shown in the appendix as figure 10.11.

$^1\text{H}$  NMR (300 MHz,  $\text{CD}_2\text{Cl}_2$ ):  $\delta$  = 9.78 (d,  $J$  = 5.8 Hz, 1H, pyridine), 9.28 (d,  $J$  = 5.0 Hz, 1H, pyridine), 8.90 – 8.65 (m, 7H, porphyrin, beta-H), 7.99 (t,  $J$  = 7.3 Hz, 1H, pyridine), 7.58 – 7.41 (m,  $J$  = 13.6, 7.6 Hz, 1H, pyridine), 5.66 (s, 1H, acac, CH), 2.17 (s, 3H, acac,  $\text{CH}_3$ ), 2.05 (s, 3H, acac,  $\text{CH}_3$ )

MALDI TOF:  $m/z$ :  $[\text{M}^+]$  calc.: 1282.99, found: 1282.97

## 4.5 Characterization of the cyclometalated complex (18)

In order to characterize the photophysical properties of the synthesized cyclometalated complex (18), excitation/emission spectra, relative quantum yields and the phosphorescence lifetime were measured.

### 4.5.1 Excitation and emission spectra

Excitation spectra were measured of the Pd-porphyrin educt (compound 14) and of the cyclometalated product (compound 18) on the *Fluorolog@3* spectrofluorometer. Due to the reason that the relative quantum yields of the dye had to be determined, emission spectra were not only measured of educt and product compound, but also of a reference for each dye. The same measurement parameters were used for the investigated dye and the respective reference. Each dye was dissolved in toluene until an absorption intensity below 0.1 was obtained. The solution was degassed for 10 minutes before the respective measurements.

#### Measurement parameter:

##### **Pd-porphyrin-complex (educt) (compound 14) and reference PtOEP:**

*Emission spectrum:* excitation: 395 nm, 3 nm slit width, emission start: 570 nm, emission end: 900 nm, increment: 1.00, filter OG570

*Excitation spectrum:* emission: 652 nm, 3 slit band width, excitation start: 350 nm, excitation end: 650 nm, increment: 1.00, filter OG570

*Absorption Pd-porphyrin-educt (14):* 0.092

*Absorption PtOEP refernce:* 0.097

##### **Cyclometalated Pd-porphyrin (product) (compound 18) and reference PtTPTBP:**

*Emission spectrum:* excitation: 430 nm, 7 nm slit width, integration time: 0.25, emission start: 700 nm, emission end: 1000 nm, increment: 0.40, slit width: 7 nm, filter RG665

*Excitation spectrum:* emission: 765 nm, 12 nm slit width, integration time: 0.25, excitation start: 350 nm, excitation end: 700 nm, increment: 0.40, 6.0 nm slit width, filter RG665

*Absorption cyclometalated Pd-porphyrin-product (14):* 0.087

*Absorption PtTPTBP reference:* 0.069

### 4.5.2 Lifetime measurements

Lifetime measurements for the Pd-porphyrin educt and the cyclometalated compound were also performed on the *Fluorolog@3* spectrofluorometer. Decay times were evaluated with a Data Station Software. A biexponential fit was used for the decay times of the educt and product.

#### Measurement parameter:

*Pd-porphyrin educt (compound 14):* 392 nm LED, PMT 1350 V, Emission mono 670 nm

*Cyclometalated Pd-porphyrin product (compound 18):* 456 nm LED, PMT 1450 V, Emission mono 778 nm

---

## 5 Results and Discussion

All synthetic and characterization experiments that were carried out within the scope of this Master's thesis will be discussed in the following section.

### 5.1 Synthetic considerations

The aims of this thesis were, on the one hand, the synthesis of new Pt-precursors that might improve the currently applied reaction conditions for platination reactions for  $\pi$ -extended porphyrins. On the other hand, the effect of cyclometalation on the photophysical properties of luminescent dyes had to be investigated, whereby the main focus was placed on porphyrin dyes. In literature, various cyclometalated Ir- and Pt-complexes are known, which typically exhibit a large Stokes shift and high quantum yields but a poor molar absorption coefficient in the VIS region [7]. Combination of the method of cyclometalation with porphyrin dyes might lead to favourable properties such as high quantum yields and tuneable emissive lifetimes. Therefore, it was attempted to establish a structure-property relationship for newly synthesized cyclometalated porphyrin complexes within the experimental work of this thesis.

Firstly, dyes containing a structure suitable for cyclometalation reactions were synthesized. Therefore, 2-phenylpyridine ligands or pyridines at the meso-position of the macro-cycle of porphyrins were successfully introduced. A palladium-porphyrin complex containing a pyridine in meso-position (compound 14), a platinum porphyrin complex with a 2-phenylpyridine ligand in meso-position for peripheral cyclometalation (compound 12) and an anthraquinone-based-dye bearing a 2-phenylpyridine group (compound 16) were synthesized. Regarding the compounds containing 2-phenylpyridine-ligands, mono- and disubstituted dyes were isolated.

Secondly, platinum precursor that showed to be promising for either platination or cyclometalation reactions were synthesized. Various platination reactions for  $\pi$ -extended porphyrins were conducted. Reaction conditions could be improved compared to literature procedures for the platination of benzoporphyrins [91–93].

Regarding the synthesis of cyclometalated complexes, various difficulties were encountered. After addition of Pt-precursors to a solution of dyes suitable for cyclometalation, often a complex mixture of products was obtained that could not be separated via column chromatography or other purification methods. A challenging task was the attachment of the desired acetylacetonate ligand to the introduced heavy atom (Pt). After various unsuccessful attempts, finally, one cyclometalated porphyrin dye (compound 18) could be isolated. This synthesis could be performed successfully due to the usage of a newly synthesized platinum precursor (compound 4). This precursor contained a chlorine, a DMSO and an acetylacetonate ligand, wherefore additional attachment of acetylacetonate after introduction of the heavy atom was not required. After several purification steps, it was possible to yield the pure cyclometalated dye, which structure was confirmed by  $^1\text{H-NMR}$  (figure 10.11) and MS-spectroscopy (figure 10.12).

## 5.1.1 Synthesis of new platinum-precursors for platination reactions

Typically, platination of  $\pi$ -extended porphyrins requires very harsh reaction conditions. Often,  $\text{PtCl}_2$  or  $\text{Pt}(\text{BN})_2\text{Cl}_2$  are used as Pt-precursors, which require temperatures up to 200 °C, in order to achieve successful insertion of the Pt central atom [75, 90, 91]. However, such drastic reaction conditions bear the risk of decomposition of the porphyrin ligand, leading to rather moderate yields and long reaction times. Therefore, the synthesis of new precursors was performed, which were promising to improve the currently applied reaction conditions for the synthesis of Pt-porphyrins. The idea hereby was, to isolate precursors with ligands that can easily be removed and at the same time do not produce acidic species, such as chlorine containing complexes.

Two different precursors were synthesized according to literature procedure [102, 103, 105] (figure 5.1).

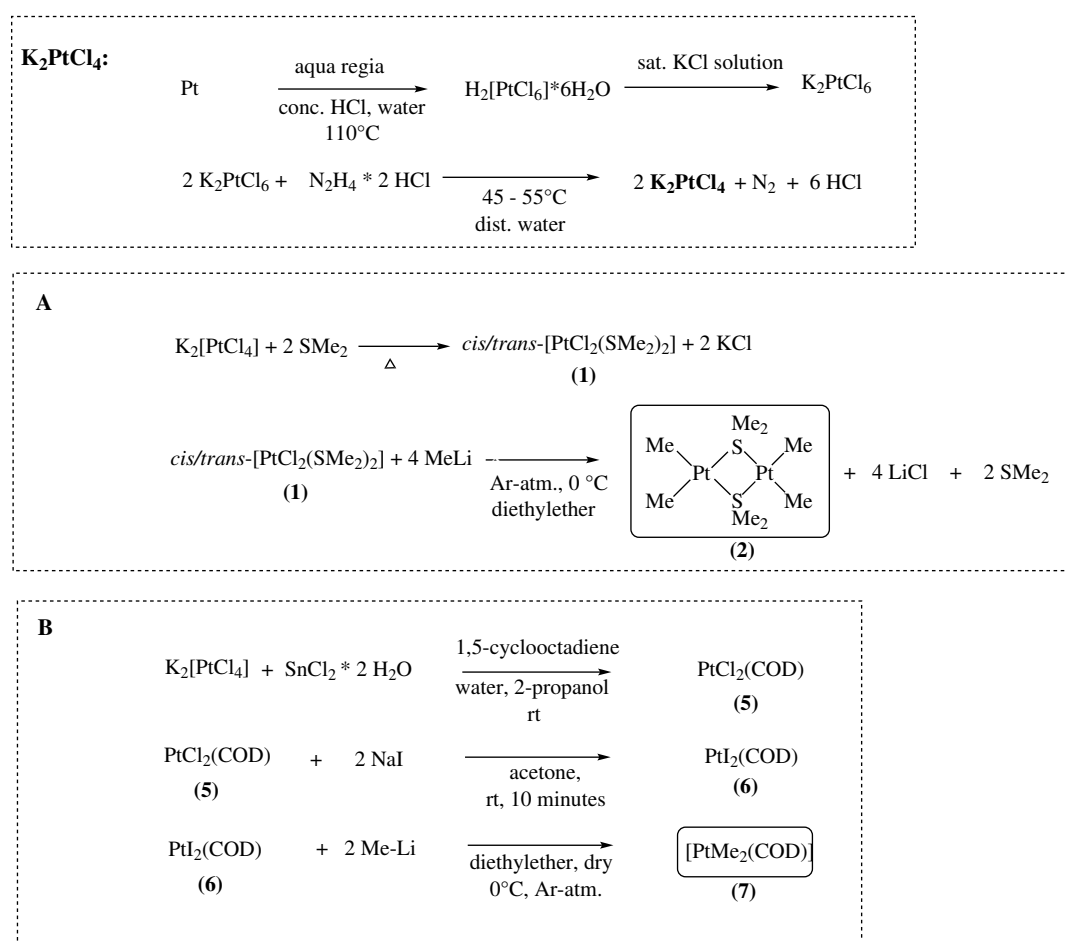


**Figure 5.1:** Synthesis of compound 2 following pathway A and of compound 7 following pathway B

Due to the reason that potassium tetrachloroplatinate(II) was the starting material for both platinum precursors, this compound was synthesized beforehand. The preparation of  $\text{K}_2\text{PtCl}_4$  followed a literature procedure [102]; pure platinum was dissolved at high temperature in aqua regia, leading to potassium hexachloroplatinate after addition of saturated KCl solution. The

final step was a reduction by hydrazine to the desired product. Although  $K_2PtCl_4$  is readily available from commercial sources, this synthesis was a much cheaper alternative, leading to pure potassium tetrachloroplatinate(II) crystals in a high yield (81 %).

The first platinum-precursor (compound **2**) was obtained after a 2-step synthesis (**A**). The first step of this reaction pathway, including the addition of dimethylsulfide to  $K_2PtCl_4$  while heating, was performed without any problems. *Cis/trans*-dichlorobis(dimethyl sulfide)platinum(II) (compound **1**), was isolated as a yellow solid in a high yield (86 %). The next step of the synthesis, leading to the desired compound **2**, turned out to be challenging due to the temperature and air-instability of the methyl-lithium reagent and the dimeric product. Therefore, the reaction had to be carried out in dried diethylether under argon atmosphere at 0 °C. Furthermore, solvent evaporation on the rotary evaporator had to be performed without using the hot water bath, due to the risk of decomposition of the product. Although handled carefully, the product was obtained with a rather moderate yield of 25 %; it was stored in a Schlenk under Ar-atmosphere in the freezer.

The second platinum-precursor (**7**) was isolated after conducting a three-step synthesis (**B**). The first two steps of this synthesis yielding compound **5** and compound **6** were carried out without facing any difficulties. Compound **5** was received by addition of 1,5-cyclooctadiene and tin chloride to a solution of  $K_2PtCl_4$  as a light brown precipitate, which could be isolated by filtration with a yield of 77 %. Compound **6** was then synthesized by addition of NaI in acetone after 10 minutes as a bright yellow solid; again a yield of 77 % could be achieved. The third step of the synthesis, leading to the desired precursor  $[PtMe_2(COD)]$ , had to be carried out with the exclusion of any traces of moisture or oxygen. Therefore, dry diethylether and a Schlenk flask under Ar-atmosphere cooled to 0 °C were required for this synthesis. The product (**7**) could be obtained after addition of methyl lithium and extraction with cold diethylether as a light brown solid with a yield of 44 %. It was assumed that due to the presence of methyl groups which could be easily eliminated by formation of methane, this precursor would be highly suitable for platination reactions.

### 5.1.2 Improvement of the reaction conditions for platination reactions of benzoporphyrins

The performance of the two newly synthesized precursors (described in section 5.1.1) for the platination of benzoporphyrins was investigated.

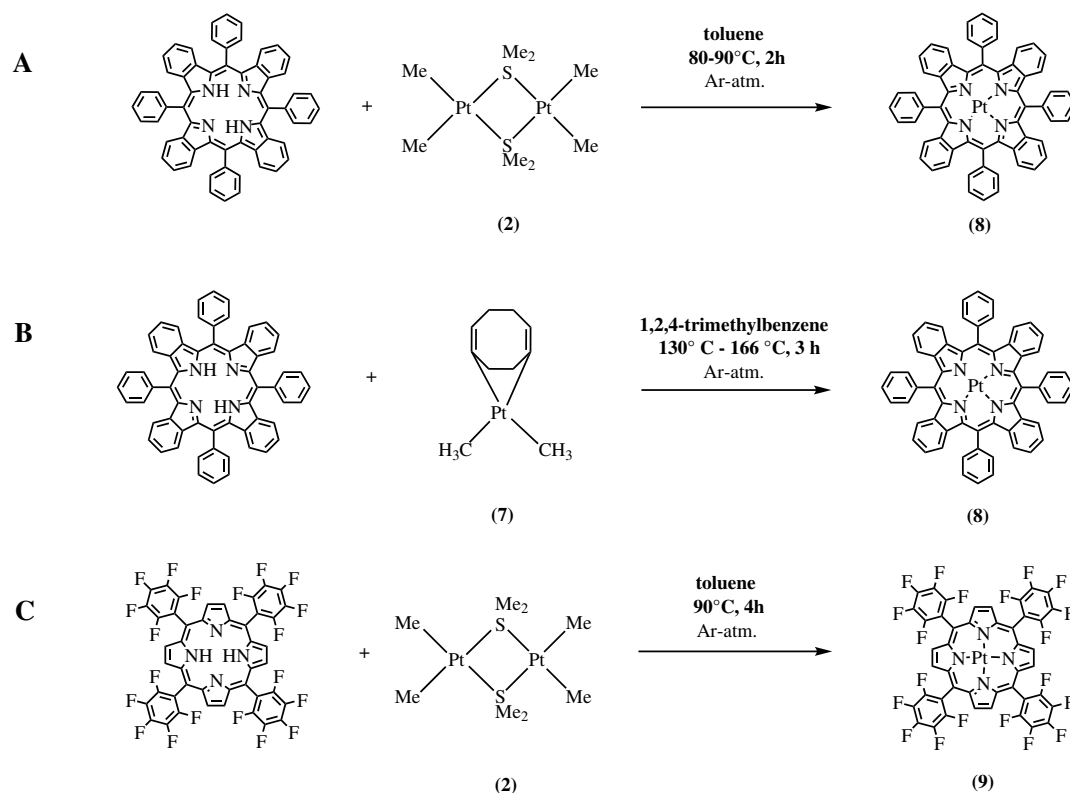


**Figure 5.2:** Optimized platination reactions using new Pt-precursors (2) and (7)

As already mentioned above, typically platination reactions of  $\pi$ -extended porphyrins require the use of high boiling point solvents such as benzonitrile or diphenylether and temperatures up to 200 °C [93]. It was tried to use less harsh reaction conditions by usage of different precursors. At first, the porphyrin ligand H<sub>2</sub>TPTBP was reacted with the previously synthesized bis[ $\mu$ -dimethyl sulfide]platinum(II) (2) (pathway A). Toluene was used as a solvent and the reaction was heated to 80 °C. Even after 10 minutes, a first progress of the reaction could be observed in the UV-VIS spectrum and the temperature was increased to 90 °C. After a reaction time of two hours, quantitative conversion of the educt to the Pt-complex PtTPTBP was shown (figure 5.3). Using the same dilution of the educt and the reaction mixture showed that full conversion could be achieved and no dye was decomposed. In conclusion, bis[ $\mu$ -dimethyl sulfide]platinum(II) (2) seems to be a highly preferable alternative to currently used precursors such as Pt(BN)<sub>2</sub>Cl<sub>2</sub>, as usage of toluene and low temperatures such as 90 °C lead to the huge advantage that no decomposition of the porphyrin dye takes place.

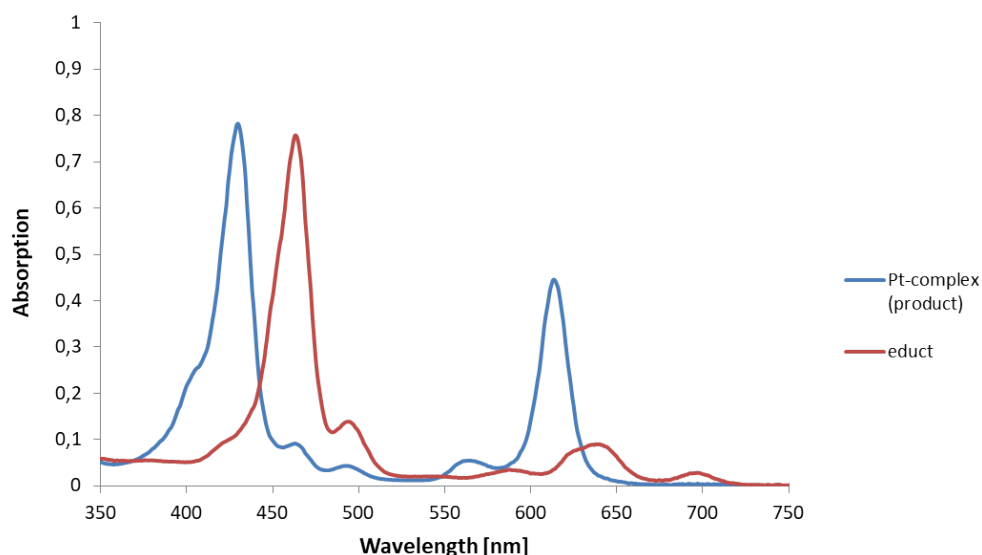


**Figure 5.3:** UV-VIS spectra of the conversion of H<sub>2</sub>TPTBP to PtTPTBP by compound 2

The next platination attempt included the conversion of H<sub>2</sub>TPTBP with the precursor (**7**) Pt(CH<sub>3</sub>)<sub>2</sub>(COD) (pathway **B**). It was assumed that this precursor could lead to fast platination by elimination of methane from the reagent, wherefore an opened reaction system using a bubbler was required. For this reaction, the higher boiling point solvent 1,2,4-trimethylbenzene (bp: 169 °C) was utilized. At first, the reaction mixture consisting of the solvent, the porphyrin ligand and the precursor was heated up to 130 °C, however no progress could be observed. After increasing the temperature to 166 °C, leading to refluxing of 1,2,4-trimethylbenzene, full conversion to PtTPTBP (**9**) was shown in the UV-VIS spectrum (figure 5.4).

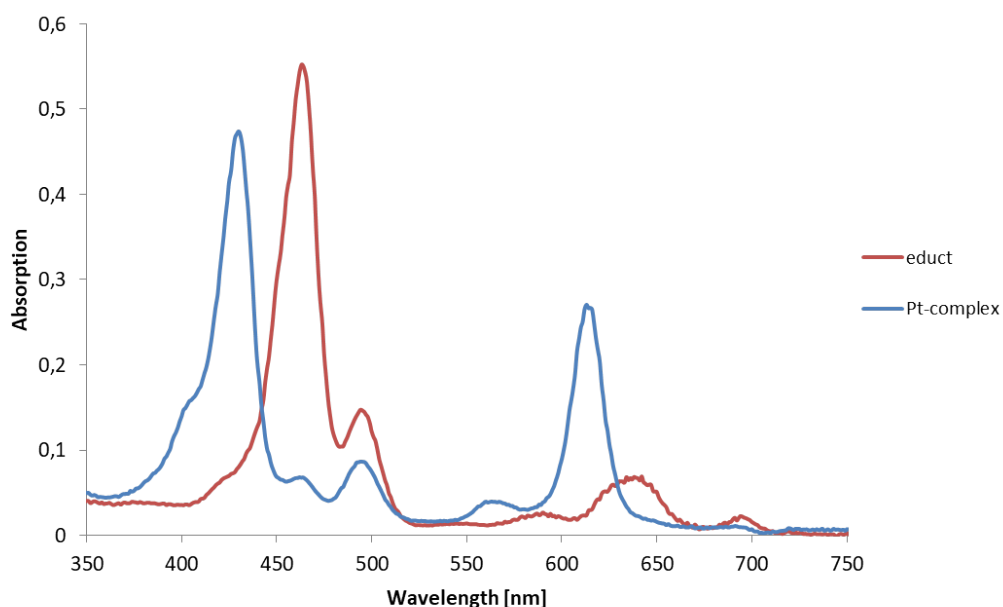


**Figure 5.4:** UV-VIS spectra of the conversion of H<sub>2</sub>TPTBP to PtTPTBP by compound 7

Same dilution of the educt and product mixture, which were measured in DCM via UV-VIS-spectroscopy, showed that the intensity of the Soret-band of the Pt-complex was slightly lower than of the porphyrin ligand. Therefore, it can be assumed that some decomposition of the porphyrin dye took place, however the amount of decomposition is still significantly lower than for commonly used precursors such as  $\text{Pt}(\text{BN})_2\text{Cl}_2$ . Compared to pathway **A**, using bis[dimethyl( $\mu$ -dimethyl sulfide)platinum(II)] (**2**) as the reagent, more drastic reaction conditions were required for pathway **B**. While the dimeric precursor (**2**) required toluene as a solvent, 90 °C and 2 hours of reaction time,  $\text{PtMe}_2(\text{COD})$  only led to full conversion using the higher boiling point solvent 1,2,4-trimethylbenzene, 166 °C and 3 hours of reaction time. All in all, both compounds lead to efficient platination of benzoporphyrins at moderate reaction conditions, however the dimeric Pt-precursor (**2**) appears to be the preferred compound in order to achieve quantitative conversion without decomposition of the dye. On the other hand it needs to be pointed out that compound **7** is more stable and allows easier handling and storage compared to the dimeric compound **2**.

Due to the reason that compound **2** only required very mild conditions for the platination of  $\text{H}_2\text{TPTBP}$ , it was tested again with another fluorinated porphyrin ligand  $\text{H}_2\text{TFPP}$  (pathway **C**). It could be observed in the UV-VIS spectrum that conversion took place in toluene at only 90 °C (figure 5.5). Addition of 2.5 equivalents led to formation of the Pt-complex after 10 minutes; increasing the equivalents of the precursor to 4.5 equivalents resulted in a conversion rate of more than 50 %. It was expected that addition of further equivalents would result in full conversion of the porphyrin ligand, however due to a limited synthesized amount of the Pt-precursor no more equivalents were added.

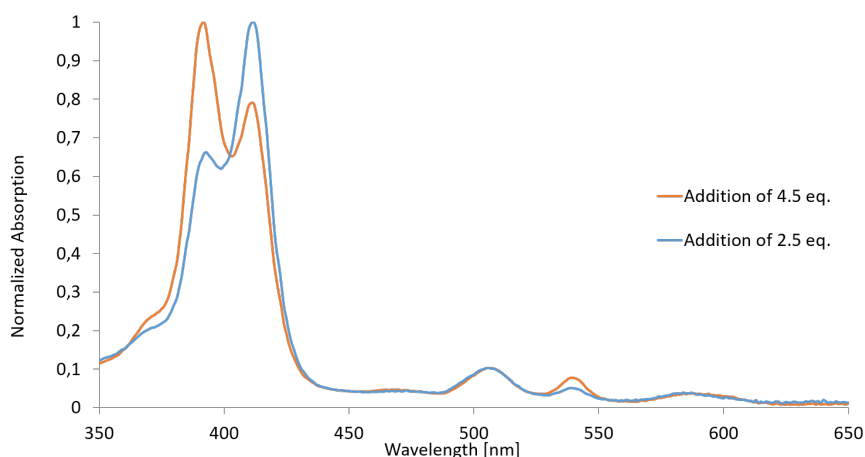


**Figure 5.5:** UV-VIS spectra of the conversion of  $\text{H}_2\text{TFPP}$  to  $\text{PtTFPP}$  by compound **2** after addition of several equivalents of the precursor

In general, it can be said that it was possible to enhance the reaction conditions for the platination of benzoporphyrins. Two suitable compounds were synthesized, whereby especially bis[dimethyl( $\mu$ -dimethyl sulfide)platinum(II)] (**2**) required significantly milder conditions than precursors presented in literature so far. For example, a typical platination procedure for porphyrins includes the  $\text{PtCl}_2$  precursor and PhCN as a solvent at reflux at approximately 200 °C [75, 90, 92]. Using compound **2** it was possible to perform this reaction in toluene at only 90 °C. Easy removal of the solvent and no decomposition of the dyes are exceptional advantages of these newly discovered reaction conditions.

## 5.1.3 Dyes with structures suitable for cyclometalation

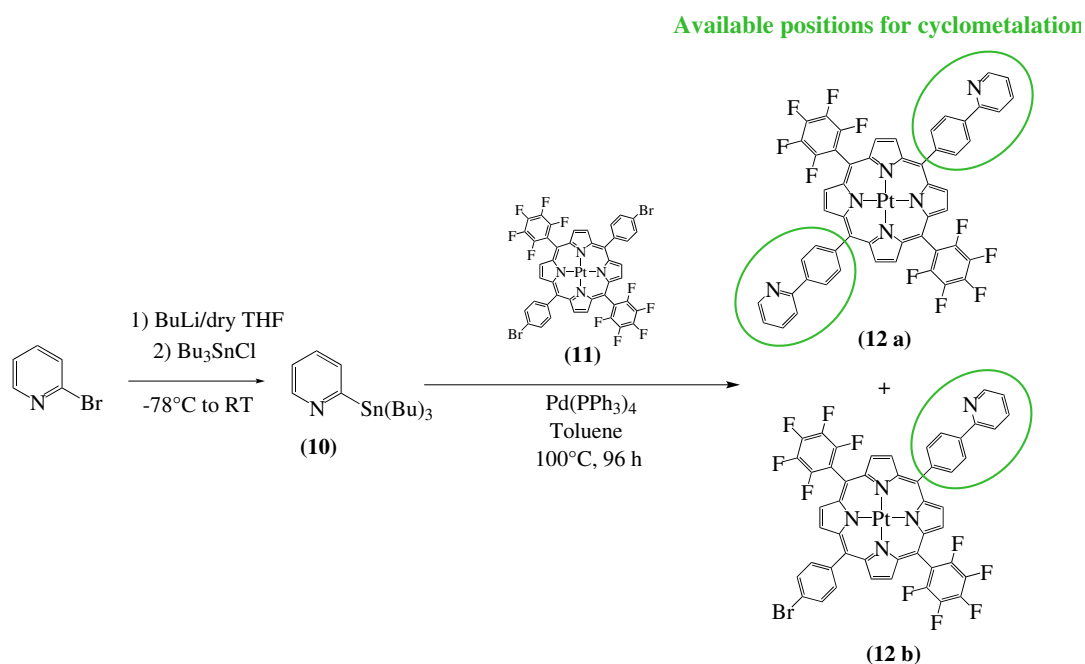


**Figure 5.6:** Pathway for the synthesis of porphyrin structures suitable for peripheral cyclometalation

In the first attempt, Pt-porphyrins with the cyclometalating (C<sup>^</sup>N) ligand 2-phenylpyridine were synthesized. The organo-tin compound 2-(tributylstannyl)pyridine (**10**) was prepared according to literature procedure. Tributyltin chloride was the starting material and *n*-Buli was added as a reagent. The product was obtained as a brown liquid in a high yield and <sup>1</sup>H-NMR data were in accordance with literature.

In the next step, a palladium-catalysed Stille-coupling involving the organotin compound (**10**) and the electrophilic bromine atoms at the Pt-porphyrin complex (**11**) was performed. After a reaction time of 96 hours the mixture showed still traces of educt on the TLC, however as no more progress was observed, the reaction mixture was worked-up. After purification via column chromatography the expected mono- (**12 b**) and disubstituted (**12 a**) products were isolated. Although 2.5 equivalents of the 2-(tributylstannyl)pyridine compound (**10**) were added, the mono- and disubstituted products were obtained in a ratio of 5:1, respectively.

A <sup>1</sup>H-NMR of the two products was performed, which tended to be difficult to analyse. Although not every peak could be assigned with certainty, it was still confirmed that the mono- and disubstituted products of the Pt-complex had formed. The 2-phenylpyridine ligands on the porphyrin dye (figure 5.6) were thought to be suitable structures for further peripheral cyclometalation experiments.

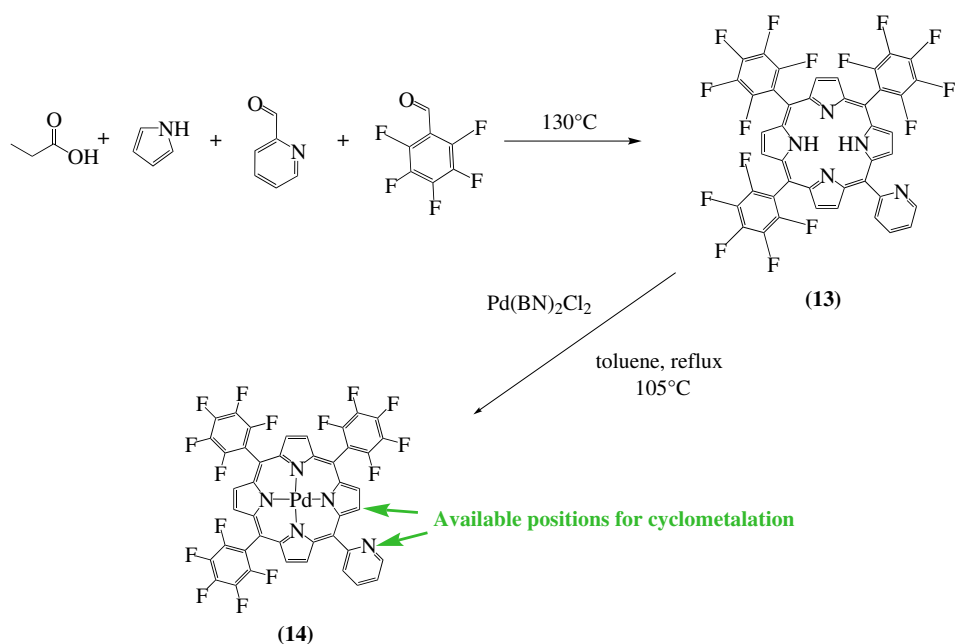


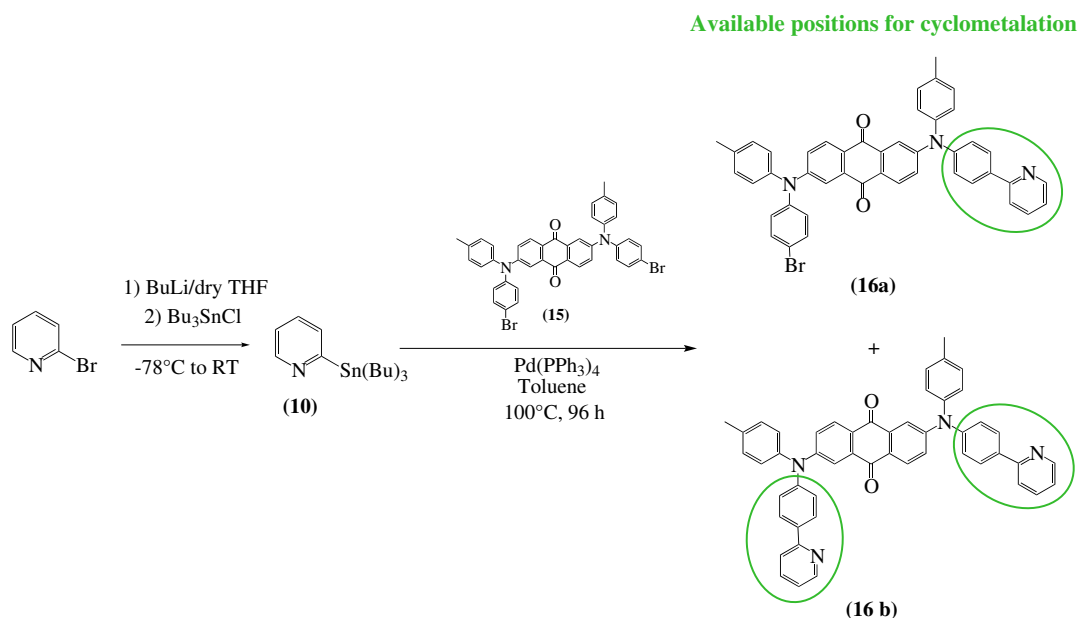
**Figure 5.7:** Pathway for the synthesis of complexes suitable for cyclometalation at the porphyrin core

Besides peripheral cyclometalation of porphyrin dyes, also cyclometalation at the porphyrin core was a reaction attempt of high interest for this thesis (figure 5.7). The porphyrin ligand (compound 13) was synthesized by condensation of pyrrole, 2-pyridinecarboxaldehyde and pentafluorobenzaldehyde dissolved in propionic acid under air at 130 °C. In order to achieve the substitution of the porphyrin ligand by pyridine at only one of the four meso-positions, various preliminary experiments were conducted. It was shown that a ratio of 5:1 of the pentafluorobenzaldehyde to the 2-pyridinecarboxaldehyde yielded the highest amount of the desired product compared to other side-products. The reaction was monitored via UV-VIS spectroscopy that showed the formation of the porphyrin compound. Via TLC the formation of different products containing one, two, three or four pyridine substituents was observed, whereby the desired product containing only one pyridine-substituent was shown to be the main product. The dye was separated from the reaction mixture and purified via column chromatography; afterwards the porphyrin ligand was precipitated from a mixture of cyclohexane and DCM, leading to a violet clean solid product. Precipitation showed to be a challenging task due to very high solubility of the product in various solvents. Dissolution of the dye in a mixture of CH<sub>2</sub>Cl<sub>2</sub>, DCM and 3M Novec 7200 finally led to precipitation after evaporation of the DCM. The structure of the isolated ligand (13) was confirmed via <sup>1</sup>H-NMR-spectroscopy.

In the next step, the analogous Pd-complex (14) had to be synthesized by addition of Pd(BN)<sub>2</sub>Cl<sub>2</sub> in toluene under reflux. Full conversion of the educt to the respective Pd-complex was confirmed by UV-VIS spectroscopy after 3 hours. The product was cleaned by column chromatography and appeared to be clean without any side products; however <sup>1</sup>H-NMR spectroscopy showed that benzonitrile was still coordinated, most likely via Pd of the precursor to the pyridine substituent of the product.

Removal of benzonitrile turned out to be a challenging task. The product was washed and centrifuged with pyridine, ethanol and distilled water; subsequently several washing steps with pure distilled water had to be performed in order to remove traces of pyridine. Then, another

column chromatography was performed. Finally,  $^1\text{H-NMR}$  confirmed successful removal of benzonitrile and a pure Pd-porphyrin-complex (**14**). However, due to the challenging purification steps a rather low yield of 24 % was obtained.

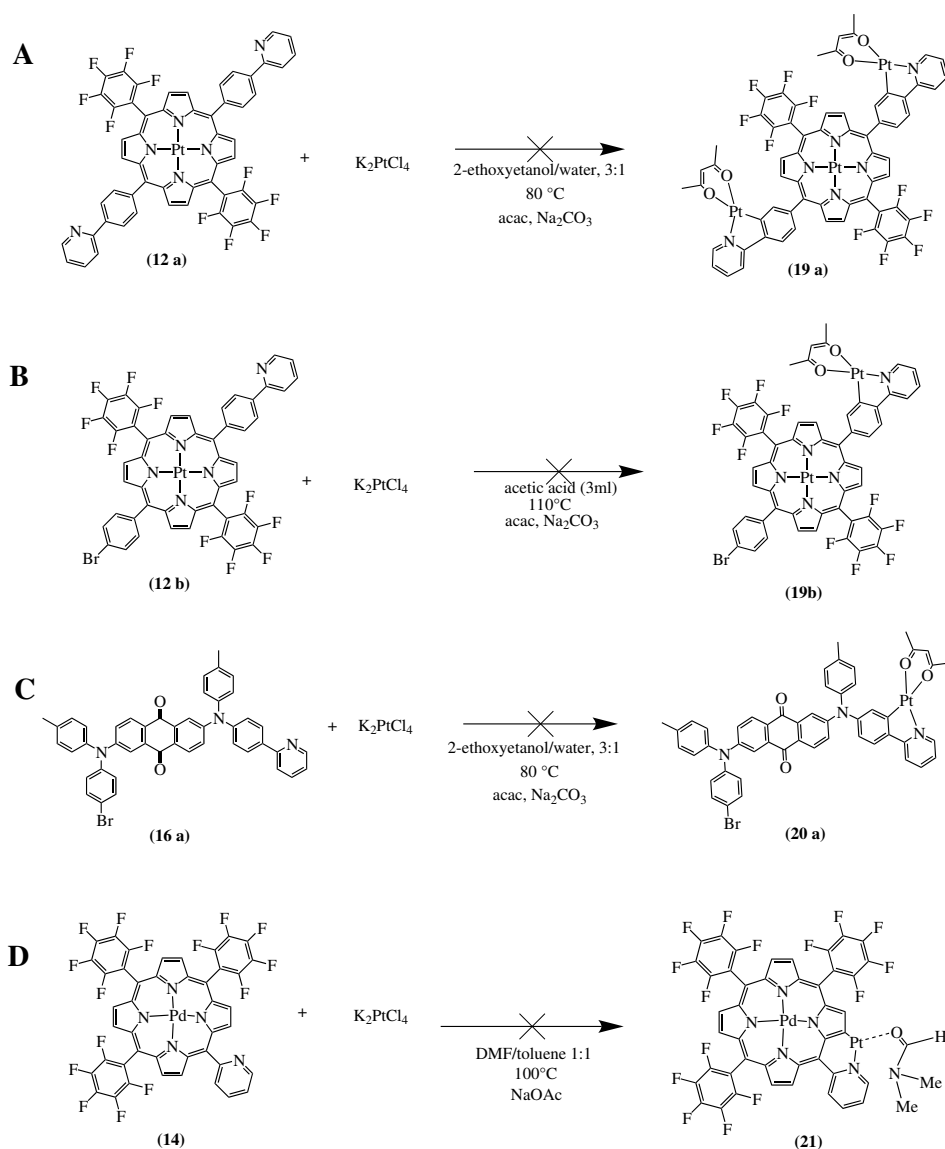


**Figure 5.8:** Pathway for the synthesis of anthraquinone-based dyes suitable for cyclometalation reactions

Besides porphyrins, also the effect of cyclometalation on anthraquinone-based-dyes had to be investigated, wherefore suitable structures containing 2-phenylpyridine-groups were synthesized. Compound (**10**) was prepared without any problems according to literature as described above on page 50. The organotin-compound was then coupled with the bromine-atoms of the anthraquinone dye via Stille-reaction. After 24 hours traces of educt could still be detected via TLC, nevertheless the reaction work-up was proceeded. The mono- and disubstituted compound were obtained after purification via column chromatography. Due to the fact that only 1.2 equivalents of the organotin compound were used, a higher amount of the monosubstituted product was isolated. The ratio of synthesized mono- to disubstituted product was 2:1, respectively. Both structures could be confirmed via  $^1\text{H-NMR}$ -spectroscopy, although again a certain assignment of each peak was not possible.

## 5.1.4 Cyclometalation reactions

The concept of cyclometalation was tried out for different substrates and using different precursors. While at first known precursors such as  $K_2PtCl_4$  or  $Pt(BN_2)Cl_2$  were used, the efficiency of self-synthesized precursors for cyclometalation reactions was studied later on. In the following section the various attempts and the successful cyclometalation synthesis that were carried out within the scope of this thesis will be discussed.

Cyclometalation attempts using  $K_2PtCl_4$ 

**Figure 5.9:** Attempted cyclometalation reactions using  $K_2PtCl_4$  as a precursor

$K_2PtCl_4$  is a common reagent in literature for the preparation of cyclometalated complexes [108–111]. Therefore, the suitability of this precursor for substrates such as porphyrins and anthraquinone-based dyes was investigated, whereby reaction conditions were varied for different

substrates. The detailed experimental procedures for these reaction attempts can be found in the appendix of this thesis.

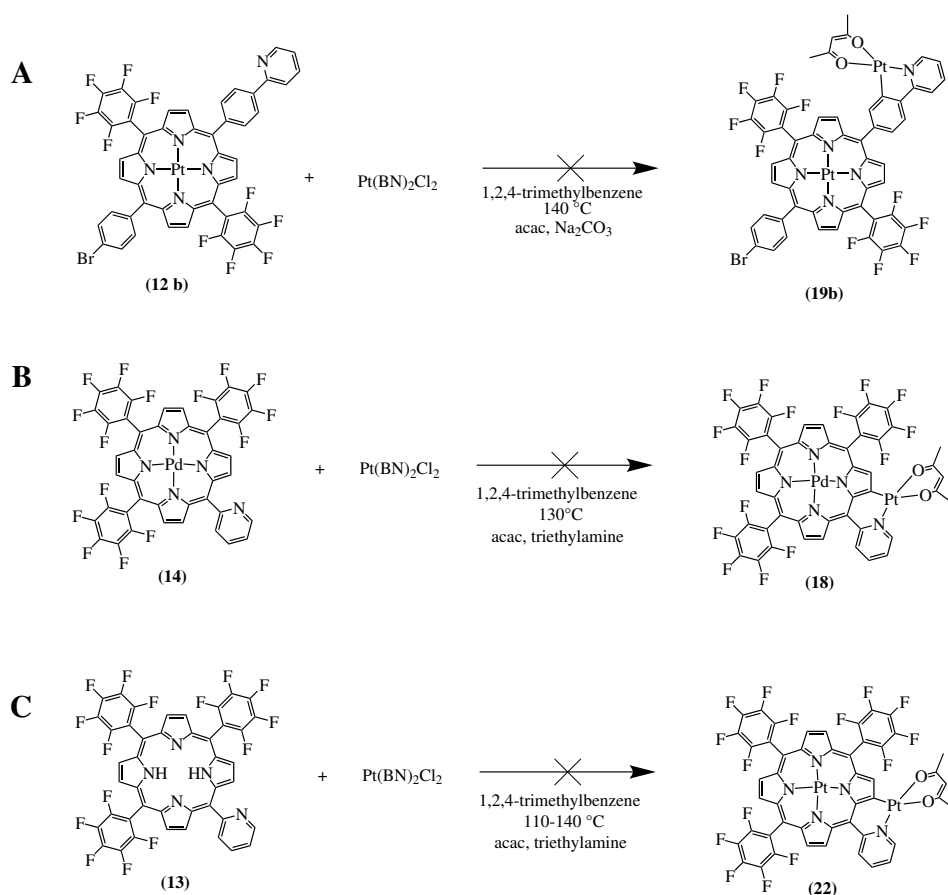
Regarding pathway **A**, it was attempted to achieve peripheral cyclometalation of the porphyrin at the 2-phenylpyridine ligands by reaction with  $K_2PtCl_4$ . According to literature, the cyclometalated product should precipitate during the reaction [110]. The Pt-porphyrin complex (**12 a**) was dissolved in 2-ethoxyethanol/water in a ratio of 3:1,  $K_2PtCl_4$  was added and the solution was heated up to 80 °C and stirred for 12 hours. After this reaction time a black precipitate had formed that could not be dissolved. It was assumed that no product but elemental platinum had formed. The precipitate was filtered and the filtrate was heated up again to 100 °C after addition of acetylacetone and sodium carbonate. This step was performed in order to receive an acetylacetone-ligand on the potentially introduced Pt-atom (**19 a**). However, the UV-VIS spectrum of the reaction mixture did not show any shifts compared to the spectrum of the educt. Therefore, it was assumed, regarding the cyclometalation reaction of the di-pyridyl-substituted dye that probably an insoluble polymeric compound had formed.

The next cyclometalation attempt included the use of  $K_2PtCl_4$  under acidic conditions (pathway **B**) and the use of the mono-substituted dye instead of the di-substituted compound. The Pt-porphyrin (**12 a**) was dissolved in acetic acid,  $K_2PtCl_4$  was added and the mixture was heated to 110 °C for 67 hours. This time a red-brown precipitate could be observed which was filtered off and was reacted with acetylacetone and sodium carbonate. However, the UV-VIS spectrum showed no reaction progress compared to the spectrum of the educt. Also, the performed TLC did not show the formation of a new cyclometalated product. Although the cyclometalation of complexes in acetic acid was reported to be successful in literature [112], these conditions seem to be not suitable for the peripheral cyclometalation of porphyrins.

Furthermore, cyclometalation of anthraquinone-based dyes using  $K_2PtCl_4$  was attempted (pathway **C**). The same method, using ethoxyethanol/water (3:1) as a solvent, as in pathway **A** was used. This time however, no precipitate was formed. UV-VIS spectra showed no reaction progress; centrifugation in order to obtain a precipitate was not successful.

The last reaction attempt using  $K_2PtCl_4$  as a precursor included cyclometalation at the porphyrin core (pathway **D**). DMF and toluene were used as the solvent mixture, and sodium acetate was added additionally. After stirring at 100 °C for 24 hours the UV-VIS spectrum still did not show a shift to longer wavelengths, that would indicate the formation of the cyclometalated product.

All in all it was shown that  $K_2PtCl_4$  was not a suitable precursor for the cyclometalation of porphyrins or anthraquinone-based dyes. Also, alteration of the reaction conditions such as acidic conditions or different solvents did not lead to any sign of conversion in the measured UV-VIS-spectra. It was expected that a successful cyclometalated complex would have led to a significant bathochromic shift of the absorption spectrum. Therefore, these attempts were regarded as not successful and it was decided to test different precursors for their suitability for cyclometalation.

Cyclometalation attempts using  $\text{Pt}(\text{BN})_2\text{Cl}_2$ 

**Figure 5.10:** Attempted cyclometalation reactions using  $\text{Pt}(\text{BN})_2\text{Cl}_2$  as a precursor

Another precursor, which was promising to be suitable for cyclometalation is  $\text{Pt}(\text{BN})_2\text{Cl}_2$ . For all three different reactions shown above (figure 5.10) the high boiling point solvent 1,2,4-trimethylbenzene, acetylacetonate and  $\text{Na}_2\text{CO}_3$  or triethylamine were utilized. Regarding pathway **A**, again peripheral cyclometalation of a Pt-porphyrin (**12 b**) was attempted. After addition of the  $\text{Pt}(\text{BN})_2\text{Cl}_2$  precursor, the solution was heated to 140 °C for two hours, however no shift could be observed in the UV-VIS spectrum. Addition of acetylacetonate and sodium carbonate neither led to a conversion of the educt to the desired cyclometalated compound.

The next attempt was cyclometalation at the porphyrin core (**14**) using the same precursor and reaction conditions, whereby this time triethylamine was used for attachment of the acetylacetonate ligand instead of sodium carbonate (pathway **B**). After addition of the precursor and stirring for 3 hours at 130 °C the reaction mixture turned from a pink to a green brownish colour and a strong shift of the absorption to higher wavelengths (435 nm) compared to the educt (408 nm) was observed. Acetylacetonate and triethylamine were added; after stirring for several more hours at room temperature a TLC of the reaction mixture showed that a complex mixture of many products had formed. It was tried to separate the different products by column chromatography, however all fractions showed very similar absorption spectra and still several spots on the TLC plates. Therefore, it was not possible to achieve separation of the reaction mixture by column chromatography. It was assumed that a cyclometalation reaction took place;

however it might be possible that the acetylacetonone ligand was not attached to the introduced Pt-atom, but other ligands such as chlorine atoms or no ligands at all.

The last cyclometalation attempt with  $\text{Pt}(\text{BN})_2\text{Cl}_2$  as a precursor included the use of the porphyrin ligand (**13**) without a central metal atom (pathway **C**). It was tried to achieve both insertion of the central Pt-atom and cyclometalation at the porphyrin core at the same time. A shift of the educt spectrum could be observed after stirring at 140 °C and two new peaks were observed. While both peaks were present at a reaction temperature of 110 °C (426 nm and 446 nm), only the peak at 426 nm was left when increasing the temperature to 140 °C. The TLC again showed a mixture of several products; purification via column chromatography was attempted, however the UV-VIS spectrum of all fractions showed both peaks that were observed during the reaction. Therefore, it was shown that it was not possible to separate these formed compounds by column chromatography. Furthermore, the spots on the TLC did not show any phosphorescence which would be highly expected for a Pt-cyclometalated complex. All in all, it was assumed that the reaction was not carried out successfully.

In general it can be said that cyclometalation at the porphyrin core using  $\text{Pt}(\text{BN})_2\text{Cl}_2$  can take place; however complex product mixtures are a result of this precursor, which can not be separated via column chromatography. A problem might be to achieve attachment of the acetylacetonone ligand to the introduced Pt-atom; presence of chlorine atoms instead of acetylacetonone would explain poor movement of the different product on silica gel. Further precursors, which might lead to more selective product formation were therefore investigated.

## Cyclometalation attempts using newly synthesized Pt-precursors

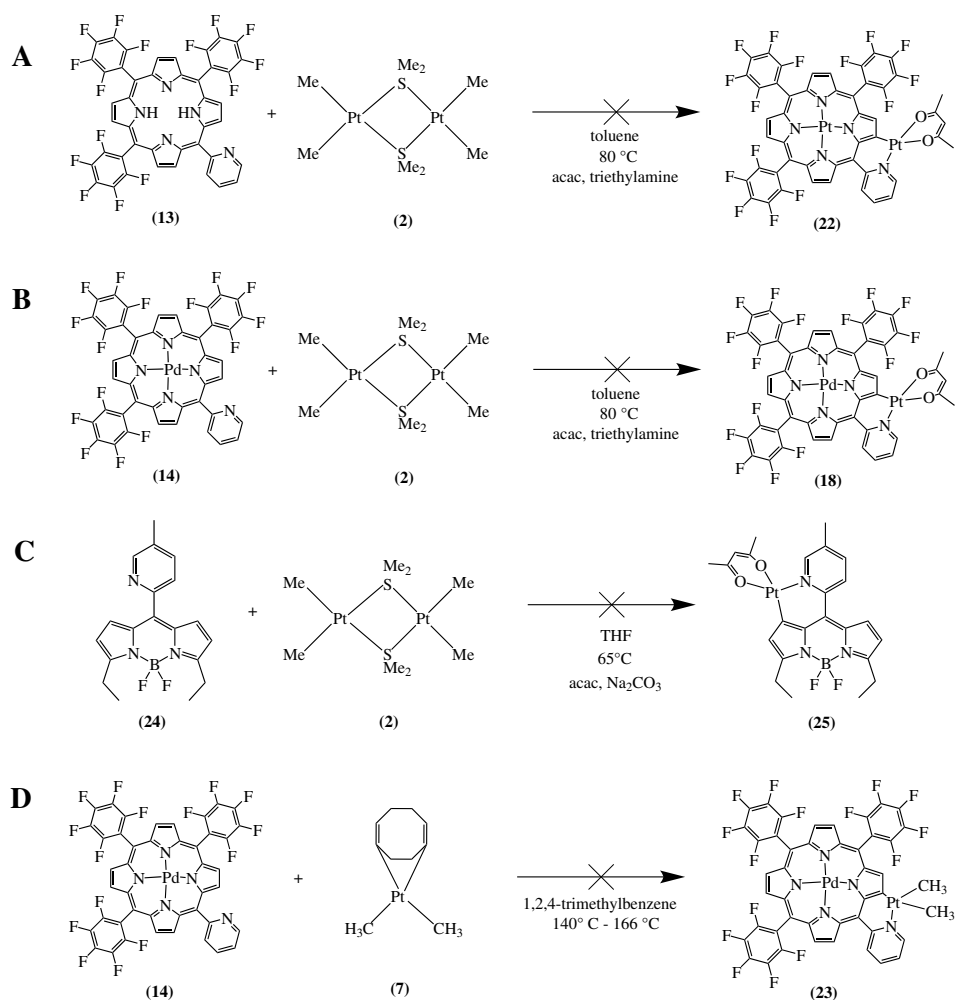


**Figure 5.11:** Attempted cyclometalation reactions using newly synthesized Pt-precursors (2) and (7)

The synthesized Pt-precursors (2) and (7) that were excellently suitable for platination of  $\pi$ -extended porphyrins were investigated regarding their suitability for cyclometalation reactions. At first, it was tried to achieve cyclometalation of the porphyrin ligand (13) by using the dimeric Pt-precursor bis[dimethyl( $\mu$ -dimethyl sulfide)platinum(II)] (pathway A). The porphyrin ligand was dissolved in toluene and after addition of the precursor, the mixture was heated to 80 °C. After several hours of stirring another peak beside the educt peak could be observed in the UV-VIS spectrum. However, this peak was shifted to lower wavelengths, which indicated that a platinum central atom was inserted into the porphyrin ligand, but no cyclometalation of the compound took place. Purification via column chromatography confirmed that only the non-cyclometalated Pt-complex had formed.

Due to the reason that reaction of the porphyrin ligand with the dimeric compound only led to insertion of the Pt-central atom, the same reaction was repeated using a Pd-complex (14) instead of the ligand (pathway B). Unfortunately, stirring at 80 °C for several hours did not lead to any conversion of the educt as was shown in the UV-VIS spectrum. Also addition of

more equivalents of the precursor did not lead to further reaction progress.

Furthermore, cyclometalation of a BODIPY dye (**24**) was attempted using the dimeric precursor (**2**) (pathway **C**). The dye and the Pt-precursor were heated to 65°C in THF under Ar-atmosphere. After 5 hours, absorption spectra showed a peak at higher wavelengths, however the educt peak was still strongly present. Acetylacetone and sodium carbonate were added; the mixture was stirred for 1 hour at room temperature. Then, it was attempted to separate the reaction mixture via column chromatography. However, it was shown on TLCs that a large variety of different compounds had formed and it was not possible to separate this complex mixture of products via column chromatography.

Finally, the newly synthesized PtMe<sub>2</sub>(COD) (**7**) precursor was tested regarding its suitability for cyclometalation reactions (pathway **D**). It was assumed that the methyl groups might stay attached to the introduced Pt-atom upon cyclometalation. The palladium porphyrin was dissolved in trimethylbenzene and PtMe<sub>2</sub>(COD) was added. The mixture was heated to reflux of 1,2,4-trimethylbenzene, however the UV-VIS spectrum showed no conversion of the educt even at 166 °C.

All in all it can be said that compounds **2** and **7** seem to be excellent alternatives for the platination of benzoporphyrins, however they are not suitable for the formation of cyclometalated porphyrins. The UV-VIS spectra showed no conversion using these two Pt-precursors. Also regarding the cyclometalation attempt of the BODIPY dye, only a complex mixture of compounds was obtained, which could not be separated via column chromatography. Again, it was tried to find new alternative precursors which might lead to selective cyclometalation of porphyrins.

## Cyclometalation with precursor containing an acac-ligand

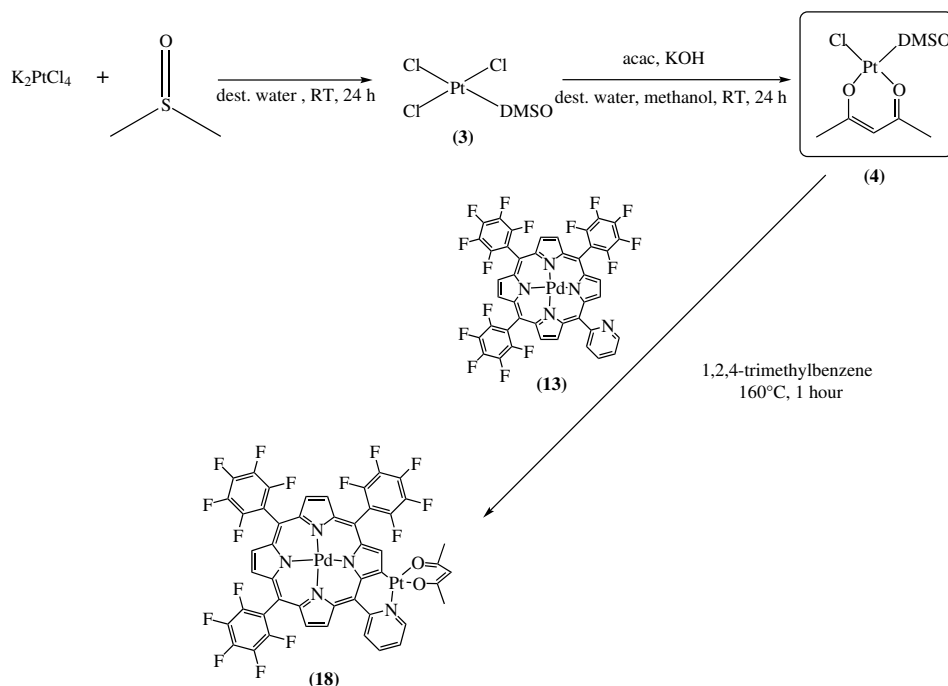


**Figure 5.12:** Cyclometalation reaction at the porphyrin core with a newly synthesized precursor **(4)**

Due to the reason that attachment of the acetylacetonone ligand to the introduced Pt-atom seemed to be a challenging task, it was thought that it might be possible to prevent this problem by using a precursor which already contains an acetylacetonone ligand. At the same time the other groups of the precursor had to be attached rather weakly, in order to achieve release of those groups but keeping the acetylacetonone group attached upon cyclometalation. Therefore, a Pt-precursor containing a chlorine, a DMSO and an acetylacetonone ligand **(4)** was synthesized (figure 5.12).

The synthesis of compound **4** was a straightforward 2-step reaction. In the first step  $K_2PtCl_4$  was reacted with DMSO in distilled water and stirred for 24 hours at room temperature. A yellow colour of the solution appeared, and after solvent evaporation the product **(3)** was received as a yellow solid. Despite stated in the literature procedure [104] the product **(3)** was insoluble in acetone, wherefore it was not further purified and directly used for the next reaction step. It was then reacted with acetylacetonone and KOH in distilled water, leading to formation of the final precursor as a pale yellow solid **(4)**.

The suitability of this new precursor for cyclometalation at the porphyrin core was investigated. The Pd-porphyrin dye **(14)** and the Pt-precursor **(4)** were therefore reacted in 1,2,4-trimethylbenzene at 160 °C. After 60 minutes full conversion of the educt was visible in the UV-VIS spectrum. A TLC showed a much less complex product mixture compared to using  $Pt(BN)_2Cl_2$  as a precursor. A column chromatography with CH+EE 3+1 was performed and two different fractions which showed a different absorption spectrum were obtained. After washing with cyclohexane both fractions were analyzed via MS-spectroscopy.

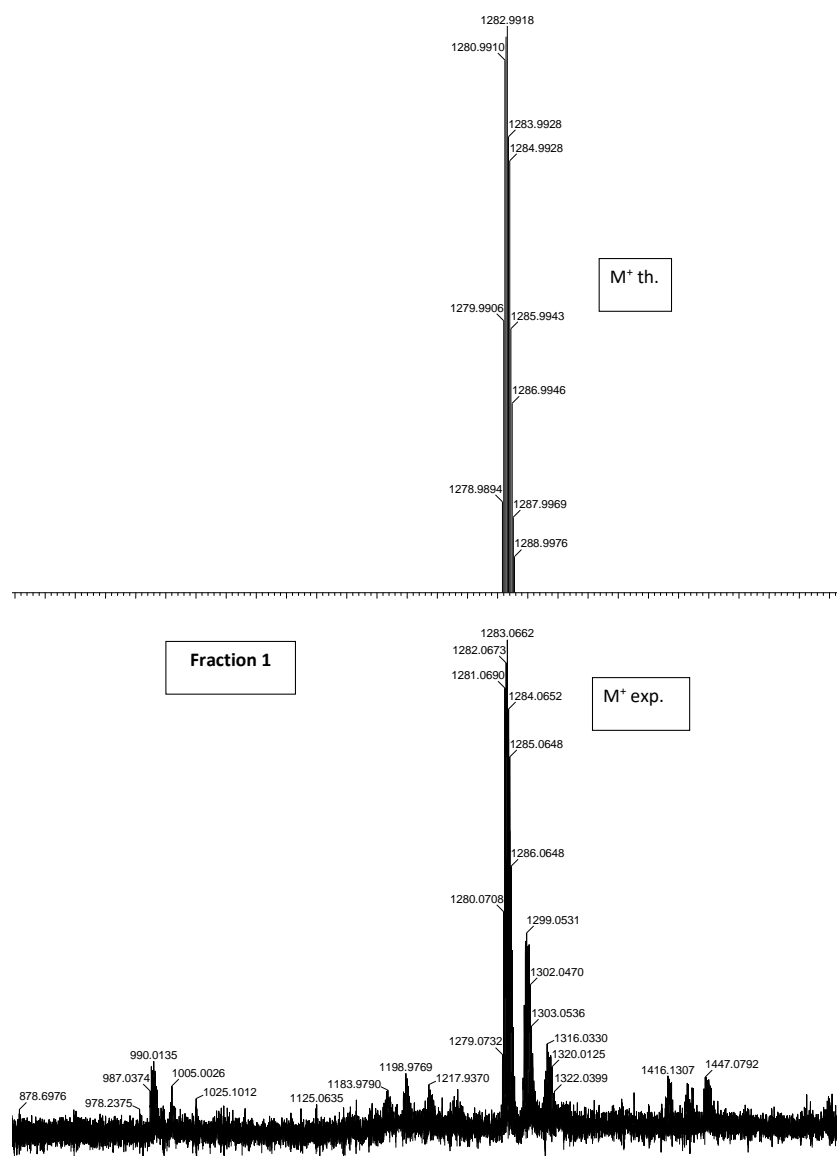


**Figure 5.13:** MS-spectrum of fraction 1 showing the desired cyclometalated complex beside other side-products

The MS-spectrum of the first fraction (figure 5.13) showed that the desired cyclometalated complex (**18**) ( $m/z$ :  $[M^+]$  calc.: 1282.99, found: 1283.07) was definitely present in this isolated fraction. However, it can be seen that despite the purification steps still some impurities are present in this spectrum.

The second fraction however, did not show the desired cyclometalated product at all; instead this fraction contained side products such as the cyclometalated product without acac or with chlorine atoms instead of the acac.

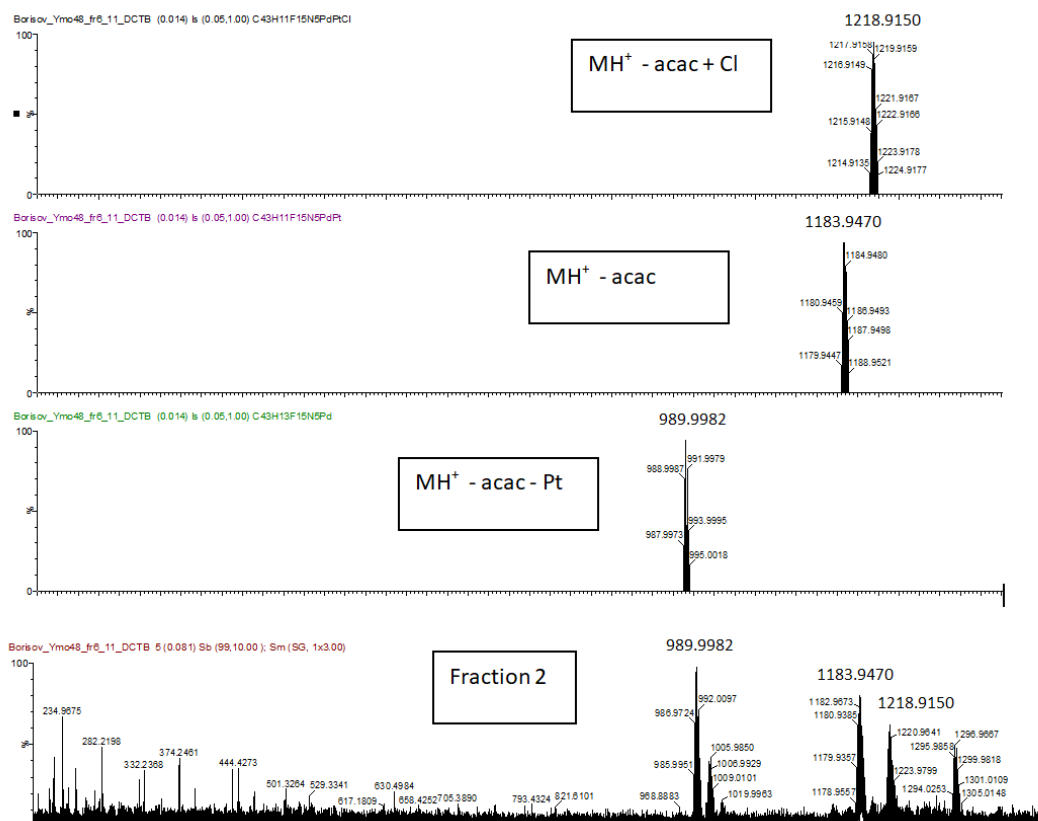


**Figure 5.14:** MS-spectrum of fraction 2 showing side-products but not the desired cyclometalated compound

Looking at figure 5.14 it can be seen that one component of this fraction was the protonated non-cyclometalated Pd-complex with an  $m/z$  ratio of 989.9 ( $MH^+ - acac - Pt$ ). Furthermore, the protonated cyclometalated compound without acetylacetonone ( $MH^+ - acac$ ) and without acac but with chlorine atoms ( $MH^+ - acac + Cl$ ) was shown in the spectrum.

After all it can be said that this Pt-precursor (**4**) made it possible to achieve cyclometalation to the desired compound. However, the obtained yields were very low and the MS-spectrum still showed impurities and the formation of various side-products containing no acetylacetonone-ligand. Therefore, it was attempted to optimize the reaction conditions for this synthesis by variation of the used solvents and temperature, in order to obtain higher yields of the desired cyclometalated complex (**18**).

### Attempted optimization of reaction conditions for cyclometalation of compound 14

The detailed experimental procedures for these attempted optimization reactions can be found in the appendix of this thesis.

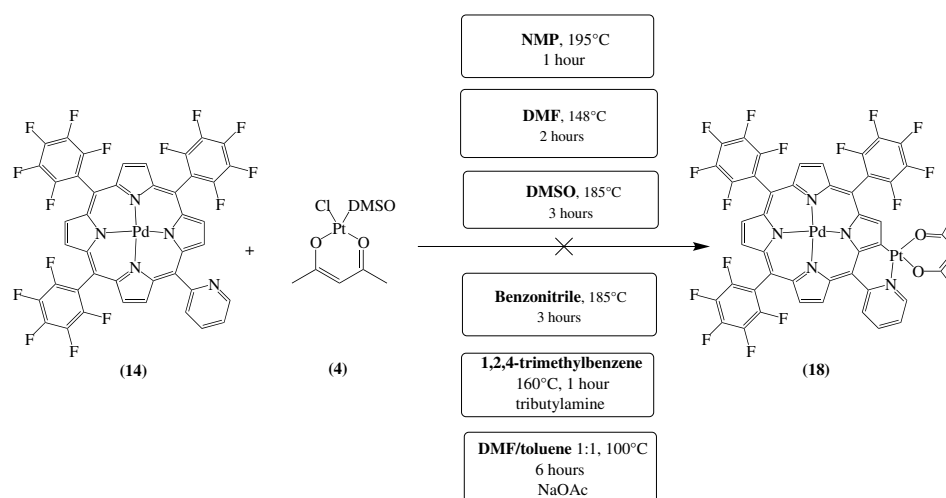


**Figure 5.15:** Attempted optimization of reaction conditions for cyclometalation at the porphyrin core

In order to try to optimize the conversion of the Pd-porphyrin complex (**14**) with the Pt-precursor (**4**) to the cyclometalated compound (**18**), different solvent mixtures were tested. For the standard procedure (described in the previous section), that yielded the desired compound in low yields, 1,2,4 trimethylbenzene and a temperature of 160 °C were used. The optimization attempt included the use of NMP, DMF, DMSO, benzonitrile, 1,2,4-trimethylbenzene with addition of tributylamine and a mixture of DMF/toluene with addition of NaOAc. The progress of these reactions was determined simultaneously by UV-VIS spectroscopy.

If the reaction was carried out in DMF at 148°C, in DMSO at 185 °C or in NMP at 195 °C, no conversion of the educt could be observed in the spectrum. Regarding the use of benzonitrile and a temperature of 185 °C, full conversion could be obtained after three hours. The UV-VIS spectrum looked similar to the UV-VIS-spectrum of the standard procedure in 1,2,4-trimethylbenzene. In order to estimate the amount of desired product that had formed, a TLC of the reaction mixture in BN was performed, whereby the already successfully cyclometalated compound (**18**) was used as a reference. It was shown that only very little of the desired compound containing an acac-ligand had formed, which was probably due to the higher temperature of 185 °C in benzonitrile compared to the 160 °C in trimethylbenzene. Therefore, also benzonitrile was not regarded a suitable alternative to 1,2,4-trimethylbenzene.

Another optimization attempt included the use of DMF/toluene in a ratio of 1:1 under addition of NaOAc at 100 °C. It was stated in literature [109, 111] that these reaction conditions are suitable for the cyclometalation of porphyrin dyes. However, it was shown that under these conditions no conversion of the Pd-porphyrin (**14**) could be achieved. Therefore, it was assumed that these mild conditions are not suitable for the formation of this specific cyclometalated porphyrin complex (**18**).

The last optimization procedure was the use of 1,2,4-trimethylbenzene in combination with an additional base tributylamine. Tributylamine was used analogously to triethylamine due to

its higher boiling point of 214 °C. After heating the reaction mixture to 160 °C, formation of elemental Pt was observed. It was assumed that the Pt-precursor was decomposed under these basic conditions. Therefore, the use of tributylamine was also not regarded as suitable for this specific cyclometalation reaction, although it is stated in literature that Et<sub>3</sub>N is a suitable base for the synthesis of various cyclometalated complexes.

In summary, no optimization of the previously used reaction conditions (1,2,4-trimethylbenzene, 160 °C) could be found. Several solvents and temperatures were tested for their suitability for the synthesis of compound 18, however mostly no conversion of the educt was observed. Benzonitrile was the only solvent also leading to full conversion according to the UV-VIS spectrum, however TLCs showed that only a very small amount of the cyclometalated complex bearing the acetylacetonate ligand was formed. Therefore, it was decided to stick to the original reaction conditions and try to achieve a clean product by scale-up of this cyclometalation reaction.

### Scale-up of the synthesis leading to pure compound 18

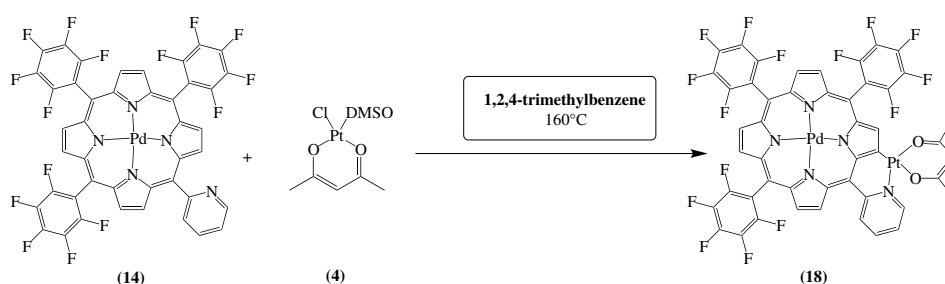


**Figure 5.16:** Scale-up of the cyclometalation reaction leading to a pure compound 18

The synthesis of compound 18 was repeated using 25 mg of the educt (14), in order to be able to achieve a reasonable amount of a pure product after several purification steps. The procedure was carried out the same way as the previous synthesis by dissolving the Pd-complex in trimethylbenzene, adding the Pt-precursor and stirring for 2 hours at 160 °C. Then, a column chromatography was performed, where the desired product could be isolated in one fraction. Another fraction consisted of the cyclometalated product without acetylacetonate, which was concluded by TLC. It was tried to convert these fractions into the product with acac ligand by dissolving them in THF and treating them with acetylacetonate and triethylamine. However, this attempt was not successful and the performed TLCs showed no different spots before and after the treatment.

Therefore, only the fraction of the desired product which was received after column chromatography was further purified by washing steps with CH<sub>2</sub>Cl<sub>2</sub>, heptane and 3M Novec 7200. A <sup>1</sup>H NMR (figure 10.11) of the product was performed, which confirmed the formation of the cyclometalated Pd-complex (18). Also MS-spectroscopy (figure 10.12) showed that the isolated fraction contained the pure desired product. Even though it was possible to isolate the pure product it was unfortunately only achieved in a very low yield of 10 %. The main problem of this synthesis was the successful attachment of the acetylacetonate ligand to the Pt-atom. In spite of the fact that the acac was already attached to the used Pt-precursor (4), many side products containing chlorine atoms instead of acac or no ligand at all were obtained.

## Further attempted cyclometalation reactions using compound 4 as a precursor

The detailed experimental procedure of these two reactions is shown in the appendix.

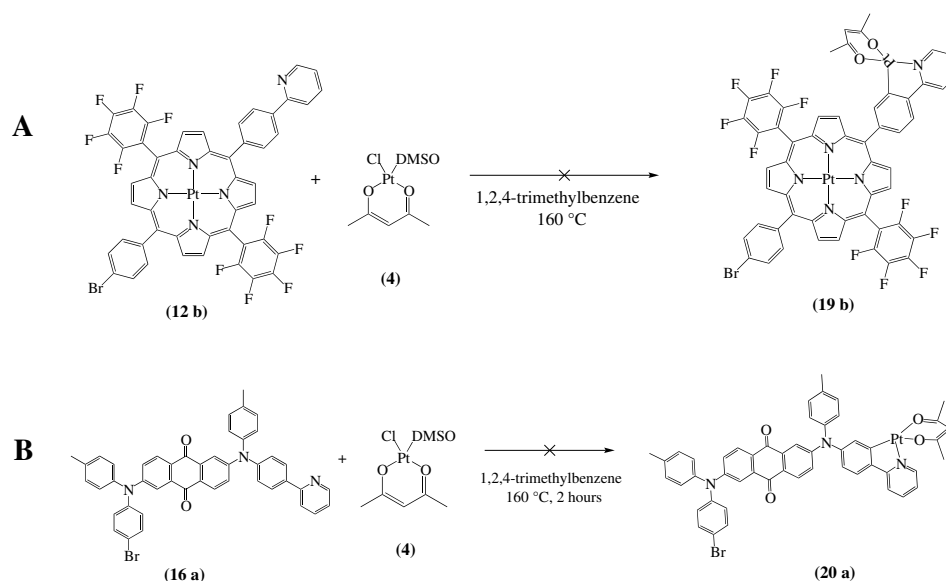


**Figure 5.17:** Testing the suitability of precursor (4) for cyclometalation of various substrates

As it was possible to obtain the cyclometalated compound 18 using the newly synthesized precursor (4), the suitability of this precursor for other substrates was tested.

First, it was tried to achieve peripheral cyclometalation of the Pt-porphyrin compound 12 b (pathway A). The porphyrin educt and the precursor were reacted in trimethylbenzene at 160 °C for 2 hours. UV-VIS spectra showed no shift of the absorption, however TLCs confirmed that new products had formed. Many spots were visible on the TLC plate that could not be separated properly in various solvent mixtures. It was not possible to obtain pure fractions via column chromatography (CH+EE 3+1). It was assumed that a cyclometalation reaction had taken place, whereby peripheral cyclometalation of the porphyrin seems to not affect the shift of the absorption spectrum. Unfortunately, it was not possible to isolate the product from the complex mixture, wherefore no further characterization was possible.

The other attempt included the cyclometalation of an anthraquinone-based dye (16 a) via compound 4 (pathway B). The same reaction conditions as for pathway A were used. Again, no change in the absorption spectrum was observed, but the performed TLCs indicated the formation of new compounds. A column chromatography was performed, however the obtained fractions still showed several spots on the TLC and showed very bad movement on the silica-gel. Therefore, also regarding pathway B it was not possible to isolate the desired cyclometalated compound from the reaction mixture.

Unfortunately, it was shown that compound 4 did not lead to selective cyclometalation of the Pt-porphyrin complex (12 b) or the anthraquinone-based dye (16 a). Several side-products were obtained that could not be separated via column chromatography. Optimization of the reaction conditions such as solvents or temperature might be required in order to obtain the desired cyclometalated complexes.

### 5.1.5 Characterization of the cyclometalated Pd-porphyrin-dye (18)

In order to determine the photophysical properties of the cyclometalated dye, excitation and emission spectra as well as the lifetime and quantum yield were determined. The aim was to compare the properties of the non-cyclometalated educt to the cyclometalated compound.

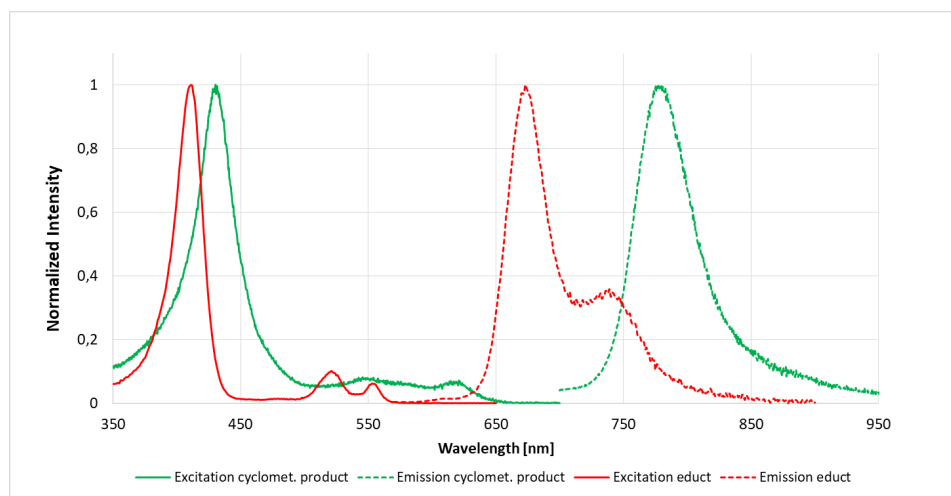


**Figure 5.18:** Excitation and emission spectra ( $\lambda_{exc} = 395$  nm,  $\lambda_{em.} = 652$  nm) of the Pd-porphyrin-dye (**14**) (red); and excitation and emission spectra ( $\lambda_{exc} = 430$  nm,  $\lambda_{em.} = 765$  nm) of the cyclometalated analogous porphyrin (**18**) (green) in toluene under anoxic conditions

In figure 5.18 the excitation and emission spectra of the Pd-porphyrin complex (**14**) (red) and the cyclometalated analogous complex (**18**) (green) are shown. It can be observed, that the emission and excitation of the cyclometalated compound is strongly shifted to higher wavelengths. This observation can be explained by planarization of the porphyrin system by the meso-positioned phenyl ring, leading to an extended  $\pi$ -conjugation. Compared to the Pd-porphyrin educt, the Soret band is slightly shifted by 20 nm (412/432 nm), whereas the Q-band is strongly red-shifted from 553 nm to 621 nm. The emission maximum of the cyclometalated dye is shifted bathochromically by 105 nm (675/780 nm).

In figure 5.19 the absorption and excitation spectrum of the cyclometalated compound is shown. It can be seen that both spectra are as expected virtually identical.

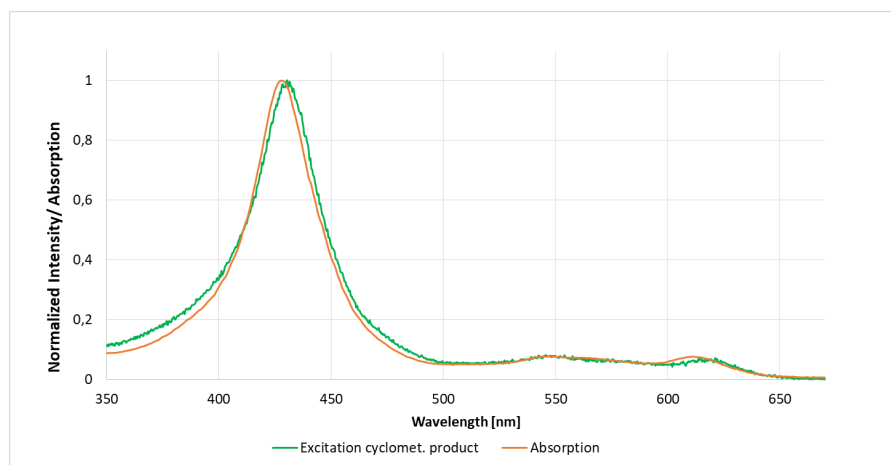


**Figure 5.19:** Excitation ( $\lambda_{exc} = 430$  nm,  $\lambda_{em.} = 765$  nm) and absorption spectrum of the cyclometalated dye (**18**) in toluene under anoxic conditions

Unfortunately, it was not possible to determine a molar absorption coefficient of the dye due to the small amount available of the pure compound **18**. For further dye characterization the relative quantum yields and the lifetimes of compound **14** and **18** were determined. In order to obtain the relative quantum yields, the emission spectrum of a reference was measured for each dye. Hereby, PtOEP was used as a reference for the Pd-porphyrin educt and PtTBTBP was used as a reference for the synthesized cyclometalated complex. Furthermore, the lifetime  $\tau$  of the two compounds was determined via single-photon counting.

**Table 5.1:** Relative quantum yields of compound **14**, the cyclometalated compound **18** and of the respective reference dyes and determined lifetimes

Data	Compound <b>14</b>	PtOEP	Compound <b>18</b>	PtTPTBP
QY [%]	21	41	0.5	21
$\tau$ [s]	6.85E-04		9.83E-06	

In table 5.1 it is shown that the relative quantum yield of the Pd-porphyrin educt achieves a value of 21 %, while the cyclometalated analogue only shows a quantum yield of 0.5 %. Unfortunately, the effect of cyclometalation leads to a drastic decrease in QY regarding compound **18**. The porphyrin dye PtTPTBP (table 5.1) shows similar spectral properties as the cyclometalated dye, however its quantum yield is significantly higher with 21 % compared to the 0.5 % of compound **18**. Looking at the measured lifetimes it can be observed that the lifetime of the cyclometalated complex decreased by a factor of 100 to a value of 9.8  $\mu$ s. This tendency was expected due to the introduction of the heavy atom and the resulting increased spin-orbit coupling.

In conclusion, it can be said that the effect of cyclometalation leads to drastically altered photophysical properties of the porphyrin dye. Absorption and emission were shifted significantly to higher wavelengths, generating a new red-light excitable NIR emitting phosphorescent dye. The lifetime of the cyclometalated complex was reduced by a factor of 100; unfortunately also the quantum yield was very low with 0.5 %.

---

## 6 Conclusion and Outlook

One aim of this thesis was the improvement of the reaction conditions for the platination of  $\pi$ -extended porphyrins. This task was completed by synthesis of two new Pt-precursors, namely PtMe<sub>2</sub>(COD) (compound 7) and bis[dimethyl( $\mu$ -dimethyl sulfide)platinum(II)] (compound 2). Both precursors allowed quantitative conversion of H<sub>2</sub>TPTBP to the Pt-complex, whereby the dimeric precursor (**2**) already led to full conversion in toluene at only 90 °C. Typically very high boiling point solvents and harsh conditions are required for the platination of  $\pi$ -extended porphyrins; however when using the newly synthesized Pt-precursors, platination is possible at milder conditions. Easy removal of the utilized solvent and no decomposition of the dyes are therefore excellent advantages of these newly discovered reaction conditions.

Another aim of this thesis was the synthesis of cyclometalated porphyrin compounds. The effect of the cyclometalation on the photophysical properties of these dyes should then be investigated. Therefore, dyes with structures suitable for cyclometalation were synthesized. Pt-porphyrins bearing 2-phenylpyridine groups for peripheral cyclometalation (**12**), a Pd-porphyrin with a pyridine introduced at the meso-position for cyclometalation at the porphyrin core (**14**) and anthraquinone-based dyes containing 2-phenylpyridine ligands (**16**) were successfully isolated. Cyclometalation of these compound was investigated via different synthetic routes. The first attempt included use of the precursors K<sub>2</sub>PtCl<sub>4</sub> and Pt(BN)<sub>2</sub>Cl<sub>2</sub>, which are commonly known to be suitable for cyclometalation reactions. No conversion of the educt compounds could be observed using K<sub>2</sub>PtCl<sub>4</sub> as a precursor; however when adding Pt(BN)<sub>2</sub>Cl<sub>2</sub> to the complexes suitable for cyclometalation, a reaction progress could be observed regarding the Pd-porphyrin dye suitable for cyclometalation at the porphyrin core (**14**). It was shown that the reaction resulted in a complex mixture of various products (shown on TLC) that could not be separated via column chromatography. One possible problem was the attachment of an acetylacetonate ligand to the introduced Pt-atom. Therefore, a new precursor (**4**) which already contained an acac ligand was synthesized. By addition of this precursor to the Pd-porphyrin complex it was possible to obtain a porphyrin that was cyclometalated at the porphyrin core (**18**). The reaction that was carried out in 1,2,4-trimethylbenzene at 160 °C led to low yields of 10 %, wherefore it was attempted to optimize the reaction conditions by variation of solvents and temperature. Unfortunately, no other suitable reaction conditions were found for this specific synthesis.

The cyclometalated porphyrin complex (**18**) was characterized regarding its photophysical properties. It was observed that absorption and emission spectra compared to the non-cyclometalated educt were shifted significantly to higher wavelengths, which is due to the planarization of the porphyrin system by the meso-positioned phenyl ring, leading to an extended  $\pi$ -conjugation. In relation to the Pd-porphyrin educt, the Soret band was slightly shifted by 20 nm (412/432 nm), whereas the Q-band was strongly red-shifted from 553 to 621 nm. The emission maximum of the cyclometalated dye was shifted bathochromically by 105 nm (675/780 nm). The lifetime of the cyclometalated complex was reduced as expected, due to introduction of heavy atoms by a factor of 100 to a value of 9.8  $\mu$ s; unfortunately quantum yield were very low with 0.5 %, while the non-cyclometalated Pd-porphyrin complex showed quantum yields of 21 %.

For future research the synthesis of other cyclometalated porphyrin complexes will be attempted. Thereby, synthesis of porphyrins with different central atoms such as Zn, Pt or Ir will be an interesting task. Other central atoms might lead to higher quantum yields than those that were obtained by the cyclometalated Pd-complex. After synthesis of a larger variety of cyclometalated complexes it will be possible to establish a detailed structure-property relationship for the effect of cyclometalation on porphyrin dyes. .

---

## 7 Bibliography

1. McDonagh, C., Burke, C. S. & MacCraith, B. D. Optical Chemical Sensors. *Chemical Reviews* **108**, 400–422 (Feb. 2008).
2. Wolfbeis, O. S. Analytical chemistry with optical sensors. *Fresenius' Zeitschrift fuer Analytische Chemie* **325**, 387–392 (1986).
3. Schaeferling, M. The Art of Fluorescence Imaging with Chemical Sensors. *Angewandte Chemie International Edition* **51**, 3532–3554.
4. Chu, C.-S. & Lin, C.-A. Optical fiber sensor for dual sensing of temperature and oxygen based on PtTFPP/CF embedded in sol-gel matrix. *Sensors and Actuators B: Chemical* **195**, 259–265 (May 2014).
5. Sun, S., Ungerböck, B. & Mayr, T. Imaging of oxygen in microreactors and microfluidic systems. *Methods and Applications in Fluorescence* **3**, 034002 (Apr. 21, 2015).
6. Clark, L. C., Wolf, R., Granger, D. & Taylor, Z. Continuous recording of blood oxygen tensions by polarography. *Journal of Applied Physiology* **6**, 189–193 (Sept. 1953).
7. Quaranta, M., Borisov, S. M. & Klimant, I. Indicators for optical oxygen sensors. *Bioanalytical Reviews* **4**, 115–157 (Dec. 2012).
8. McDonagh, C., Kolle, C., McEvoy, A. K., Dowling, D. L., Cafolla, A. A., Cullen, S. J. & MacCraith, B. D. Phase fluorometric dissolved oxygen sensor, 7 (2001).
9. Bedlek-Anslow, J. M., Hubner, J. P., Carroll, B. F. & Schanze, K. S. Micro-heterogeneous Oxygen Response in Luminescence Sensor Films. *Langmuir* **16**, 9137–9141 (Nov. 2000).
10. Mills, A. & Thomas, M. Fluorescence-based Thin Plastic Film Ion-pair Sensors for Oxygen. *The Analyst* **122**, 63–68 (1997).
11. Klimant, I. & Wolfbeis, O. S. Oxygen-Sensitive Luminescent Materials Based on Silicone-Soluble Ruthenium Diimine Complexes. *Analytical Chemistry* **67**, 3160–3166 (Sept. 15, 1995).
12. Cox, M. E. & Dunn, B. Detection of oxygen by fluorescence quenching. *Applied Optics* **24**, 2114 (July 15, 1985).
13. Kroneis, H. & Marsoner, H. A fluorescence-based sterilizable oxygen probe for use in bioreactors. *Sensors and Actuators* **4**, 587–592 (Jan. 1983).
14. Okura, I. & Kamachi, T. in Kadish, K. M., Smith, K. M. & Guillard, R. *Handbook of Porphyrin Science (Volume 12)* 297–348 (World Scientific Publishing Company, Feb. 2011).
15. Gillanders, R., Tedford, M., Crilly, P. & Bailey, R. Thin film dissolved oxygen sensor based on platinum octaethylporphyrin encapsulated in an elastic fluorinated polymer. *Analytica Chimica Acta* **502**, 1–6 (Jan. 2004).
16. Amao, Y., Miyashita, T. & Okura, I. Platinum tetrakis(pentafluorophenyl)porphyrin immobilized in polytrifluoroethylmethacrylate film as a photostable optical oxygen detection material. *Journal of Fluorine Chemistry* **107**, 101–106 (Jan. 2001).

17. Koren, K., Borisov, S. M. & Klimant, I. Stable optical oxygen sensing materials based on click-coupling of fluorinated platinum(II) and palladium(II) porphyrins—A convenient way to eliminate dye migration and leaching. *Sensors and Actuators B: Chemical* **169**, 173–181 (July 2012).
18. Soultati, A., Papadimitropoulos, G., Davazoglou, D., Argitis, P., Alexandropoulos, D., Politi, C. T., Vainos, N., Pistolis, G., Coutsolelos, A. G. & Vasilopoulou, M. *Near-IR organic light emitting diodes based on porphyrin compounds* in (IEEE, July 2015), 1–4.
19. Huang, L., Park, C. D., Fleetham, T. & Li, J. Platinum (II) azatetrabenzoporphyrins for near-infrared organic light emitting diodes. *Applied Physics Letters* **109**, 233302 (Dec. 5, 2016).
20. Graham, K. R., Yang, Y., Sommer, J. R., Shelton, A. H., Schanze, K. S., Xue, J. & Reynolds, J. R. Extended Conjugation Platinum(II) Porphyrins for use in Near-Infrared Emitting Organic Light Emitting Diodes. *Chemistry of Materials* **23**, 5305–5312 (Dec. 27, 2011).
21. Xiang, H., Cheng, J., Ma, X., Zhou, X. & Chruma, J. J. Near-infrared phosphorescence: materials and applications. *Chemical Society Reviews* **42**, 6128 (2013).
22. Zach, P. W., Maierhofer, M., Püschmann, S. D., Klimant, I. & Borisov, S. M. Tuning photophysical properties of phosphorescent benzoporphyrin complexes via 1-step pi-extension. *Dyes and Pigments* **159**, 610–618 (Dec. 2018).
23. Mueller, B. J., Burger, T., Borisov, S. M. & Klimant, I. High performance optical trace oxygen sensors based on NIR-emitting benzoporphyrins covalently coupled to silicone matrixes. *Sensors and Actuators B: Chemical* **216**, 527–534 (Sept. 2015).
24. Hutter, L. H., Müller, B. J., Koren, K., Borisov, S. M. & Klimant, I. Robust optical oxygen sensors based on polymer-bound NIR-emitting platinum(II)–benzoporphyrins. *J. Mater. Chem. C* **2**, 7589–7598 (2014).
25. Papkovsky, D. B., Ponomarev, G. V., Trettnak, W. & O’Leary, P. Phosphorescent Complexes of Porphyrin Ketones: Optical Properties and Application to Oxygen Sensing. *Analytical Chemistry* **67**, 4112–4117 (Nov. 1995).
26. Khalil, G. *et al.* Synthesis and spectroscopic characterization of Ni , Zn , Pd and Pt tetra(pentafluorophenyl)porpholactone with comparisons to Mg , Zn , Y , Pd and Pt metal complexes of tetra(pentafluorophenyl)porphine. *Journal of Porphyrins and Phthalocyanines* **06**, 135–145 (Feb. 2002).
27. Amao, Y., Ishikawa, Y. & Okura, I. Green luminescent iridium(III) complex immobilized in fluoropolymer film as optical oxygen-sensing material. *Analytica Chimica Acta* **445**, 177–182 (Oct. 2001).
28. Borisov, S. M. & Klimant, I. Ultrabright Oxygen Optodes Based on Cyclometalated Iridium(III) Coumarin Complexes. *Analytical Chemistry* **79**, 7501–7509 (Oct. 2007).
29. Lamansky, S., Djurovich, P., Murphy, D., Abdel-Razzaq, F., Lee, H.-E., Adachi, C., Burrows, P. E., Forrest, S. R. & Thompson, M. E. Highly Phosphorescent Bis-Cyclometalated Iridium Complexes: Synthesis, Photophysical Characterization, and Use in Organic Light Emitting Diodes. *Journal of the American Chemical Society* **123**, 4304–4312 (May 2001).
30. Vander Donckt, E., Camerman, B., Herne, R. & Vandeloise, R. Fibre-optic oxygen sensor based on luminescence quenching of a Pt(II) complex embedded in polymer matrices. *Sensors and Actuators B: Chemical* **32**, 121–127 (May 1996).

31. Wu, W., Wu, W., Ji, S., Guo, H., Song, P., Han, K., Chi, L., Shao, J. & Zhao, J. Tuning the emission properties of cyclometalated platinum(II) complexes by intramolecular electron-sink/arylethynylated ligands and its application for enhanced luminescent oxygen sensing. *Journal of Materials Chemistry* **20**, 9775 (2010).
32. Valeur, B. *Molecular fluorescence: principles and applications* OCLC: ocm45541665. 387 pp. (Wiley-VCH, Weinheim ; New York, 2002).
33. Atkins, P. W. & De Paula, J. *Atkins' Physical chemistry* 8th ed. 1064 pp. (Oxford University Press, Oxford ; New York, 2006).
34. Lakowicz, J. R. *Principles of fluorescence spectroscopy* 3rd ed. 954 pp. (Springer, New York, 2006).
35. Wakasa, M., Yago, T., Sonoda, Y. & Katoh, R. Structure and dynamics of triplet-exciton pairs generated from singlet fission studied via magnetic field effects. *Communications Chemistry* **1** (Dec. 2018).
36. Santos, J. L. & Farahi, F. *Handbook of Optical Sensors* Google-Books-ID: yY7aBAAAQBAJ. 722 pp. (CRC Press, Oct. 29, 2014).
37. Yoshihara, T., Yamaguchi, Y., Hosaka, M., Takeuchi, T. & Tobita, S. Ratiometric Molecular Sensor for Monitoring Oxygen Levels in Living Cells. *Angewandte Chemie International Edition* **51**, 4148–4151 (Apr. 23, 2012).
38. Zhang, G., Chen, J., Payne, S. J., Kooi, S. E., Demas, J. N. & Fraser, C. L. Multi-Emissive Difluoroboron Dibenzoylmethane Polylactide Exhibiting Intense Fluorescence and Oxygen-Sensitive Room-Temperature Phosphorescence. *Journal of the American Chemical Society* **129**, 8942–8943 (July 2007).
39. Koo Lee, Y.-E., Ulbrich, E. E., Kim, G., Hah, H., Strollo, C., Fan, W., Gurjar, R., Koo, S. & Kopelman, R. Near Infrared Luminescent Oxygen Nanosensors with Nanoparticle Matrix Tailored Sensitivity. *Analytical Chemistry* **82**, 8446–8455 (Oct. 15, 2010).
40. Schmaelzlin, E., van Dongen, J. T., Klimant, I., Marmodée, B., Steup, M., Fisahn, J., Geigenberger, P. & Löhmansröben, H.-G. An Optical Multifrequency Phase-Modulation Method Using Microbeads for Measuring Intracellular Oxygen Concentrations in Plants. *Biophysical Journal* **89**, 1339–1345 (Aug. 2005).
41. Majumdar, P., Nomula, R. & Zhao, J. Activatable triplet photosensitizers: magic bullets for targeted photodynamic therapy. *J. Mater. Chem. C* **2**, 5982–5997 (2014).
42. Jiskoot, W. & Crommelin, D. *Methods for Structural Analysis of Protein Pharmaceuticals* Google-Books-ID: CyeilBm5az8C. 694 pp. (Springer Science & Business Media, Dec. 5, 2005).
43. Buxbaum, E. *Biophysical Chemistry of Proteins: An Introduction to Laboratory Methods* Google-Books-ID: gqK\_S5\_7rrAC. 490 pp. (Springer Science & Business Media, Nov. 18, 2010).
44. Wu, M.-H., Lin, J.-L., Wang, J., Cui, Z. & Cui, Z. Development of high throughput optical sensor array for on-line pH monitoring in micro-scale cell culture environment. *Biomedical Microdevices* **11**, 265–273 (Feb. 2009).
45. Zhou, J., Zhang, L. & Tian, Y. Micro Electrochemical pH Sensor Applicable for Real-Time Ratiometric Monitoring of pH Values in Rat Brains. *Analytical Chemistry* **88**, 2113–2118 (Feb. 16, 2016).

46. Strobl, M., Rappitsch, T., Borisov, S. M., Mayr, T. & Klimant, I. NIR-emitting aza-BODIPY dyes – new building blocks for broad-range optical pH sensors. *The Analyst* **140**, 7150–7153 (2015).
47. Wolfbeis, O. S. & Weidgans, B. M. in *Optical Chemical Sensors* (eds Baldini, F., Chester, A., Homola, J. & Martellucci, S.) 17–44 (Kluwer Academic Publishers, Dordrecht, 2006).
48. Wencel, D., Abel, T. & McDonagh, C. Optical Chemical pH Sensors. *Analytical Chemistry* **86**, 15–29 (Jan. 7, 2014).
49. Liu, Z., Luo, F. & Chen, T. Phenolphthalein immobilized membrane for an optical pH sensor. *Analytica Chimica Acta* **510**, 189–194 (May 2004).
50. Wang, E., Chow, K.-F., Wang, W., Wong, C., Yee, C., Persad, A., Mann, J. & Bocarsly, A. Optical sensing of HCl with phenol red doped sol–gels. *Analytica Chimica Acta* **534**, 301–306 (Apr. 2005).
51. Orellana, G. Luminescent optical sensors. *Analytical and Bioanalytical Chemistry* **379**, 344–346 (June 1, 2004).
52. Cajlakovic, M., Lobnik, A. & Werner, T. Stability of new optical pH sensing material based on cross-linked poly(vinyl alcohol) copolymer. *Analytica Chimica Acta* **455**, 207–213 (Mar. 2002).
53. Weidgans, B. M., Krause, C., Klimant, I. & Wolfbeis, O. S. Fluorescent pH sensors with negligible sensitivity to ionic strength. *The Analyst* **129**, 645 (2004).
54. Vasylevska, A. S., Karasyov, A. A., Borisov, S. M. & Krause, C. Novel coumarin-based fluorescent pH indicators, probes and membranes covering a broad pH range. *Analytical and Bioanalytical Chemistry* **387**, 2131–2141 (Feb. 26, 2007).
55. Hulth, S., Aller, R. C., Engström, P. & Selander, E. A pH plate fluorosensor (optode) for early diagenetic studies of marine sediments. *Limnology and Oceanography* **47**, 212–220 (Jan. 2002).
56. Kermis, H. R., Kostov, Y. & Rao, G. Rapid method for the preparation of a robust optical pH sensor. *The Analyst* **128**, 1181 (2003).
57. Aslan, K., Lakowicz, J. R., Szmackinski, H. & Geddes, C. D. Enhanced Ratiometric pH Sensing Using SNAFL-2 on Silver Island Films: Metal-enhanced Fluorescence Sensing. *Journal of Fluorescence* **15**, 37–40 (Jan. 2005).
58. Pal, R. & Parker, D. A ratiometric optical imaging probe for intracellular pH based on modulation of europium emission. *Organic & Biomolecular Chemistry* **6**, 1020 (2008).
59. Liu, M., Ye, Z., Xin, C. & Yuan, J. Development of a ratiometric time-resolved luminescence sensor for pH based on lanthanide complexes. *Analytica Chimica Acta* **761**, 149–156 (Jan. 2013).
60. Goncalves, H. M., Maule, C. D., Jorge, P. A. & Esteves da Silva, J. C. Fiber optic lifetime pH sensing based on ruthenium(II) complexes with dicarboxybipyridine. *Analytica Chimica Acta* **626**, 62–70 (Sept. 2008).
61. Malins, C., Glever, H., Keyes, T., Vos, J., Dressick, W. & MacCraith, B. Sol–gel immobilised ruthenium(II) polypyridyl complexes as chemical transducers for optical pH sensing. *Sensors and Actuators B: Chemical* **67**, 89–95 (Aug. 2000).
62. Tuffy, B. *Porphyrin Materials for Organic Light Emitting Diodes* Google-Books-ID: vX9kD9FFg9sC. 98 pp. (Brian Tuffy, Oct. 2011).

63. Borisov, S. M., Zenkl, G. & Klimant, I. Phosphorescent Platinum(II) and Palladium(II) Complexes with Azatetrabenzoporphyrins—New Red Laser Diode-Compatible Indicators for Optical Oxygen Sensing. *ACS Applied Materials & Interfaces* **2**, 366–374 (Feb. 24, 2010).
64. Amao, Y. & Okura, I. An oxygen sensing system based on the phosphorescence quenching of metalloporphyrin thin film on alumina plates. *The Analyst* **125**, 1601–1604 (2000).
65. Borisov, S. M., Lehner, P. & Klimant, I. Novel optical trace oxygen sensors based on platinum(II) and palladium(II) complexes with 5,10,15,20-meso-tetrakis-(2,3,4,5,6-pentafluorophenyl)-porphyrin covalently immobilized on silica-gel particles. *Analytica Chimica Acta* **690**, 108–115 (Mar. 2011).
66. Zaitsev, N., Melnikov, P., Alferov, V., Kopytin, A. & German, K. Stable Optical Oxygen Sensing Material Based on Perfluorinated Polymer and Fluorinated Platinum(II) and Palladium(II) Porphyrins. *Procedia Engineering* **168**, 309–312 (2016).
67. Eastwood, D. & Gouterman, M. Porphyrins. *Journal of Molecular Spectroscopy* **35**, 359–375 (Sept. 1970).
68. Amao, Y., Okura, I., Shinohara, H. & Nishide, H. An Optical Sensing Material for Trace Analysis of Oxygen. Metalloporphyrin Dispersed in Poly(1-trimethylsilyl-1-propyne) Film. *Polymer Journal* **34**, 411–417 (June 2002).
69. Shinar, R., Zhou, Z., Choudhury, B. & Shinar, J. Structurally integrated organic light emitting device-based sensors for gas phase and dissolved oxygen. *Analytica Chimica Acta* **568**, 190–199 (May 24, 2006).
70. Amao, Y., Tabuchi, Y., Yamashita, Y. & Kimura, K. Novel optical oxygen sensing material: metalloporphyrin dispersed in fluorinated poly(aryl ether ketone) films. *European Polymer Journal* **38**, 675–681 (Apr. 2002).
71. Cui, W., Liu, R., Manna, E., Park, J.-M., Fungura, F., Shinar, J. & Shinar, R. Oxygen and relative humidity monitoring with films tailored for enhanced photoluminescence. *Analytica Chimica Acta* **853**, 563–571 (Jan. 1, 2015).
72. Lee, S.-K. & Okura, I. Photostable Optical Oxygen Sensing Material: Platinum Tetrakis-(pentafluorophenyl)porphyrin Immobilized in Polystyrene. *Analytical Communications* **34**, 185–188 (1997).
73. Borisov, S., Nuss, G., Haas, W., Saf, R., Schmuck, M. & Klimant, I. New NIR-emitting complexes of platinum(II) and palladium(II) with fluorinated benzoporphyrins. *Journal of Photochemistry and Photobiology A: Chemistry* **201**, 128–135 (Jan. 2009).
74. Borisov, S. M., Nuss, G. & Klimant, I. Red Light-Excitable Oxygen Sensing Materials Based on Platinum(II) and Palladium(II) Benzoporphyrins. *Analytical Chemistry* **80**, 9435–9442 (Dec. 15, 2008).
75. Finikova, O. S., Cheprakov, A. V. & Vinogradov, S. A. Synthesis and Luminescence of Soluble *meso*-Unsubstituted Tetrabenzo- and Tetranaphtho[2,3]porphyrins. *The Journal of Organic Chemistry* **70**, 9562–9572 (Nov. 2005).
76. Sommer, J. R., Shelton, A. H., Parthasarathy, A., Ghiviriga, I., Reynolds, J. R. & Schanze, K. S. Photophysical Properties of Near-Infrared Phosphorescent Pi-Extended Platinum Porphyrins. *Chemistry of Materials* **23**, 5296–5304 (Dec. 27, 2011).

77. Lebedev, A. Y., Cheprakov, A. V., Sakadžić, S., Boas, D. A., Wilson, D. F. & Vinogradov, S. A. Dendritic Phosphorescent Probes for Oxygen Imaging in Biological Systems. *ACS Applied Materials & Interfaces* **1**, 1292–1304 (June 24, 2009).
78. Niedermair, F., Borisov, S. M., Zenkl, G., Hofmann, O. T., Weber, H., Saf, R. & Klimant, I. Tunable Phosphorescent NIR Oxygen Indicators Based on Mixed Benzo- and Naphthoporphyrin Complexes. *Inorganic Chemistry* **49**, 9333–9342 (Oct. 18, 2010).
79. Sommer, J. R., Farley, R. T., Graham, K. R., Yang, Y., Reynolds, J. R., Xue, J. & Schanze, K. S. Efficient Near-Infrared Polymer and Organic Light-Emitting Diodes Based on Electrophosphorescence from (Tetraphenyltetranaphtho[2,3]porphyrin)platinum(II). *ACS Applied Materials & Interfaces* **1**, 274–278 (Feb. 25, 2009).
80. Finikova, O. S., Cheprakov, A. V., Carroll, P. J. & Vinogradov, S. A. Novel Route to Functionalized Tetraaryltetra[2,3]naphthaloporphyrins via Oxidative Aromatization. *The Journal of Organic Chemistry* **68**, 7517–7520 (Sept. 2003).
81. Caicedo, C., Zaragoza-Galán, G., Crusats, J., El-Hachemi, Z., Martínez, A. & Rivera, E. Design of novel luminescent porphyrins bearing donor–acceptor groups. *Journal of Porphyrins and Phthalocyanines* **18**, 209–220 (Mar. 2014).
82. Josefsen, L. B. & Boyle, R. W. Photodynamic Therapy and the Development of Metal-Based Photosensitisers. *Metal-Based Drugs* **2008**, 1–23 (2008).
83. Gouterman, M. Study of the Effects of Substitution on the Absorption Spectra of Porphin. *The Journal of Chemical Physics* **30**, 1139–1161 (May 1959).
84. Gouterman, M. A Theory for the Triplet-Triplet Absorption Spectra of Porphyrins. *The Journal of Chemical Physics* **33**, 1523–1529 (Nov. 1960).
85. Gouterman, M. Spectra of porphyrins. *Journal of Molecular Spectroscopy* **6**, 138–163 (Jan. 1961).
86. Giovannetti, R. in *Macro To Nano Spectroscopy* (ed Uddin, J.) (InTech, June 29, 2012).
87. Carvalho, C. M. B., Brocksom, T. J. & de Oliveira, K. T. Tetrabenzoporphyrins: synthetic developments and applications. *Chemical Society Reviews* **42**, 3302 (2013).
88. Borek, C. *et al.* Highly Efficient, Near-Infrared Electrophosphorescence from a Pt–Metalloporphyrin Complex. *Angewandte Chemie International Edition* **46**, 1109–1112.
89. Zach, P. W., Freunberger, S. A., Klimant, I. & Borisov, S. M. Electron-Deficient Near-Infrared Pt(II) and Pd(II) Benzoporphyrins with Dual Phosphorescence and Unusually Efficient Thermally Activated Delayed Fluorescence: First Demonstration of Simultaneous Oxygen and Temperature Sensing with a Single Emitter. *ACS Applied Materials & Interfaces* **9**, 38008–38023 (Nov. 2017).
90. Perez, M. D., Borek, C., Forrest, S. R. & Thompson, M. E. Molecular and Morphological Influences on the Open Circuit Voltages of Organic Photovoltaic Devices. *Journal of the American Chemical Society* **131**, 9281–9286 (July 8, 2009).
91. Zems, Y., Moiseev, A. G. & Perepichka, D. F. Convenient Synthesis of a Highly Soluble and Stable Phosphorescent Platinum Porphyrin Dye. *Organic Letters* **15**, 5330–5333 (Oct. 18, 2013).
92. Aartsma, T. J., Gouterman, M., Jochum, C., Kwiram, A. L., Pepich, B. V. & Williams, L. D. Porphyrins. 43. Triplet sublevel emission of platinum tetrabenzoporphyrin by spectrothermal principal component decomposition. *Journal of the American Chemical Society* **104**, 6278–6283 (Nov. 1982).

93. Borisov, S. M. & Klimant, I. Efficient metallation in diphenylether – A convenient route to luminescent platinum(II) complexes. *Dyes and Pigments* **83**, 312–316 (Dec. 2009).
94. Yamashita, K.-i., Katsumata, N., Tomita, S., Fuwa, M., Fujimaki, K., Yoda, T., Hirano, D. & Sugiura, K.-i. Facile and Practical Synthesis of Platinum(II) Porphyrins under Mild Conditions. *Chemistry Letters* **44**, 492–494 (Apr. 5, 2015).
95. Wang, X.-d. & Wolfbeis, O. S. Optical methods for sensing and imaging oxygen: materials, spectroscopies and applications. *Chem. Soc. Rev.* **43**, 3666–3761 (2014).
96. Liu, Y., Guo, H. & Zhao, J. Ratiometric luminescent molecular oxygen sensors based on uni-luminophores of CN Pt(II)(acac) complexes that show intense visible-light absorption and balanced fluorescence/phosphorescence dual emission. *Chemical Communications* **47**, 11471 (2011).
97. Huo, S., Carroll, J. & Vezzu, D. A. K. Design, Synthesis, and Applications of Highly Phosphorescent Cyclometalated Platinum Complexes. *Asian Journal of Organic Chemistry* **4**, 1210–1245 (Nov. 2015).
98. Levine, I. N. *Quantum Chemistry* 2. ed., 10 print. OCLC: 249253184. 506 pp. (Allyn and Bacon, Boston, 1980).
99. Koziar, J. C. & Cowan, D. O. Photochemical heavy-atom effects. *Accounts of Chemical Research* **11**, 334–341 (Sept. 1978).
100. McClure, D. S. Triplet-Singlet Transitions in Organic Molecules. Lifetime Measurements of the Triplet State. *The Journal of Chemical Physics* **17**, 905–913 (Oct. 1949).
101. Crosby, G. A. & Demas, J. N. Measurement of photoluminescence quantum yields. Review. *The Journal of Physical Chemistry* **75**, 991–1024 (Apr. 1971).
102. Brauer, G. *Handbook of Preparative Inorganic Chemistry* Google-Books-ID: Pef47TK5NfkC. 882 pp. (Elsevier, Dec. 2, 2012).
103. Hill, G. S., Irwin, M. J., Levy, C. J., Rendina, L. M., Puddephatt, R. J., Andersen, R. A. & Mclean, L. in *Inorganic Syntheses* (ed Darensbourg, M. Y.) 149–153 (John Wiley & Sons, Inc., Hoboken, NJ, USA, Jan. 5, 2007).
104. De Pascali, S. A., Lugoli, F., De Donno, A. & Fanizzi, F. P. Mutagenic Tests Confirm That New Acetylacetonate Pt(II) Complexes Induce Apoptosis in Cancer Cells Interacting with Nongenomic Biological Targets. *Metal-Based Drugs* **2011**, 1–10 (2011).
105. Clark, H. & Manzer, L. Reactions of ( $\pi$ -1,5-cyclooctadiene) organoplatinum(II) compounds and the synthesis of perfluoroalkylplatinum complexes. *Journal of Organometallic Chemistry* **59**, 411–428 (Oct. 1973).
106. Hoang, T. N. Y., Humbert-Droz, M., Dutronc, T., Guénée, L., Besnard, C. & Piguet, C. A Polyaromatic Terdentate Binding Unit with Fused 5,6-Membered Chelates for Complexing s-, p-, d-, and f-Block Cations. *Inorganic Chemistry* **52**, 5570–5580 (May 6, 2013).
107. Sergeeva, N. N., Scala, A., Bakar, M. A., O’Riordan, G., O’Brien, J., Grassi, G. & Senge, M. O. Synthesis of Stannyl Porphyrins and Porphyrin Dimers via Stille Coupling and Their 119 Sn NMR and Fluorescence Properties. *The Journal of Organic Chemistry* **74**, 7140–7147 (Sept. 18, 2009).
108. Hudson, Z. M., Blight, B. A. & Wang, S. Efficient and High Yield One-Pot Synthesis of Cyclometalated Platinum(II) beta-Diketonates at Ambient Temperature. *Organic Letters* **14**, 1700–1703 (Apr. 6, 2012).

109. Yamaguchi, S., Shinokubo, H. & Osuka, A. Double Cleavage of sp<sup>2</sup> C-H and sp<sup>3</sup> C-H Bonds on One Metal Center: DMF-Appended Cyclometalated Platinum(II) and (IV) Porphyrins. *Inorganic Chemistry* **48**, 795–797 (Feb. 2, 2009).
110. Ho, C.-L., Wong, W.-Y., Yao, B., Xie, Z., Wang, L. & Lin, Z. Synthesis, characterization, photophysics and electrophosphorescent applications of phosphorescent platinum cyclometalated complexes with 9-arylcarbazole moieties. *Journal of Organometallic Chemistry* **694**, 2735–2749 (Aug. 2009).
111. Yorimitsu, H. & Osuka, A. Organometallic Approaches for Direct Modification of Peripheral C-H Bonds in Porphyrin Cores. *Asian Journal of Organic Chemistry* **2**, 356–373 (May 2013).
112. Culham, S., Lanoe, P.-H., Whittle, V. L., Durrant, M. C., Williams, J. A. G. & Kozhevnikov, V. N. Highly Luminescent Dinuclear Platinum(II) Complexes Incorporating Bis-Cyclometallating Pyrazine-Based Ligands: A Versatile Approach to Efficient Red Phosphors. *Inorganic Chemistry* **52**, 10992–11003 (Oct. 7, 2013).

---

## 8 List of Figures

2.1	Possible de-excitation processes for excited molecules . . . . .	3
2.2	Difference in spin orientation for excited singlet or triplet states . . . . .	4
2.3	Potential energy diagrams for different vertical transitions . . . . .	5
2.4	Jablonski-diagram for radiative and non-radiative processes . . . . .	6
2.5	Simplified Jablonski-diagram showing the emissive rate of a fluorophore and the rate of non-radiative decay . . . . .	8
2.6	Components of a typical chemical optical sensor . . . . .	9
2.7	Principles of Frequency-Domain and Lifetime-Domain Measurements . . . . .	10
2.8	Mechanisms for dynamic and static quenching . . . . .	12
2.9	Mechanisms of absorption-based (1) and fluorescence-based (2) pH-sensing . . . . .	14
2.10	Typical porphyrin ligand and porphyrin compound including a metal atom in the core . . . . .	15
2.11	Structure of octaethylporphyrin (left) and tetrakis(pentafluorophenylporphyrin) (right) containing a central metal atom (M = Pt(II), Pd(II)) . . . . .	15
2.12	Structure of Pt(II) octaethylporphyrinketone (PtOEPK) (left) and Platinum(II)-5,10,15,20-tetrakis-(2,3,4,5,6-pentafluorophenyl)porpholactone (PtTFPPL) (right)	16
2.13	Structure of TBP (right) and TNP (left) ligands . . . . .	17
2.14	Emission spectra of various $\pi$ -extended porphyrins in toluene [76] . . . . .	17
2.15	Absorption spectrum of a porphyrin without metal ion [82] . . . . .	18
2.16	Typical platination procedure for $\pi$ -extended porphyrins . . . . .	19
2.17	Typical high-boiling point solvents for the platination of porphyrins . . . . .	19
2.18	Recently reported platination reaction using sodium propionate as a base . . . . .	20
2.19	Examples of cyclometalated indicator dyes such as [Ir(ppy) <sub>3</sub> ] (A), acetylacetonato based Pt (II) complex (B), thienylpyridine based Pt(thpy) <sub>2</sub> (C) and iridium complex with coumarin ligands Ir(C <sub>x</sub> ) <sub>2</sub> (acac) (with X = N, O, S-Me or S) (D)	21
2.20	Structures of a binuclear platinum(II) complex (left) and a hybrid trinuclear complex with two Pt and one Ir center (right) . . . . .	22
2.21	Expected advantages for the cyclometalation of porphyrin dyes . . . . .	23
4.1	Synthesis of K <sub>2</sub> PtCl <sub>6</sub> from pure platinum metal . . . . .	28
4.2	Preparation of K <sub>2</sub> PtCl <sub>6</sub> from potassium hexachloroplatinate using hydrazine dihydrochloride . . . . .	29
4.3	Synthesis of compound <b>1</b> . . . . .	29
4.4	Synthesis of compound <b>2</b> . . . . .	30
4.5	Synthesis of compound <b>3</b> . . . . .	31
4.6	Synthesis of compound <b>4</b> . . . . .	31
4.7	Synthesis of compound <b>5</b> . . . . .	32
4.8	Synthesis of compound <b>6</b> . . . . .	32
4.9	Synthesis of compound <b>7</b> . . . . .	33
4.10	Synthesis of compound <b>8</b> . . . . .	34
4.11	Synthesis of compound <b>9</b> . . . . .	34

4.12	Synthesis of compound <b>8</b> using PtMe <sub>2</sub> COD ( <b>7</b> ) as a precursor . . . . .	35
4.13	Synthesis of compound <b>10</b> . . . . .	36
4.14	Synthesis of compound <b>12</b> . . . . .	37
4.15	Synthesis of compound <b>13</b> . . . . .	38
4.16	Synthesis of compound <b>14</b> . . . . .	39
4.17	Synthesis of compound <b>16</b> . . . . .	40
4.18	Synthesis of compound <b>17</b> . . . . .	41
4.19	Synthesis of compound <b>18</b> . . . . .	42
5.1	Synthesis of compound <b>2</b> following pathway <b>A</b> and of compound <b>7</b> following pathway <b>B</b> . . . . .	45
5.2	Optimized platination reactions using new Pt-precursors ( <b>2</b> ) and ( <b>7</b> ) . . . . .	47
5.3	UV-VIS spectra of the conversion of H <sub>2</sub> TPTBP to PtTPTBP by compound <b>2</b> .	48
5.4	UV-VIS spectra of the conversion of H <sub>2</sub> TPTBP to PtTPTBP by compound <b>7</b> .	48
5.5	UV-VIS spectra of the conversion of H <sub>2</sub> TFPP to PtTFPP by compound <b>2</b> after addition of several equivalents of the precursor . . . . .	49
5.6	Pathway for the synthesis of porphyrin structures suitable for peripheral cyclometalation . . . . .	50
5.7	Pathway for the synthesis of complexes suitable for cyclometalation at the porphyrin core . . . . .	51
5.8	Pathway for the synthesis of anthraquinone-based dyes suitable for cyclometalation reactions . . . . .	52
5.9	Attempted cyclometalation reactions using K <sub>2</sub> PtCl <sub>4</sub> as a precursor . . . . .	53
5.10	Attempted cyclometalation reactions using Pt(BN) <sub>2</sub> Cl <sub>2</sub> as a precursor . . . . .	55
5.11	Attempted cyclometalation reactions using newly synthesized Pt-precursors ( <b>2</b> ) and ( <b>7</b> ) . . . . .	57
5.12	Cyclometalation reaction at the porphyrin core with a newly synthesized precursor ( <b>4</b> ) . . . . .	59
5.13	MS-spectrum of fraction 1 showing the desired cyclometalated complex beside other side-products . . . . .	60
5.14	MS-spectrum of fraction 2 showing side-products but not the desired cyclometalated compound . . . . .	61
5.15	Attempted optimization of reaction conditions for cyclometalation at the porphyrin core . . . . .	62
5.16	Scale-up of the cyclometalation reaction leading to a pure compound <b>18</b> . . . . .	63
5.17	Testing the suitability of precursor ( <b>4</b> ) for cyclometalation of various substrates	64
5.18	Excitation and emission spectra ( $\lambda_{exc} = 395$ nm, $\lambda_{em.} = 652$ nm) of the Pd-porphyrin-dye ( <b>14</b> ) (red); and excitation and emission spectra ( $\lambda_{exc} = 430$ nm, $\lambda_{em.} = 765$ nm) of the cyclometalated analogous porphyrin ( <b>18</b> ) (green) in toluene under anoxic conditions . . . . .	65
5.19	Excitation ( $\lambda_{exc} = 430$ nm, $\lambda_{em.} = 765$ nm) and absorption spectrum of the cyclometalated dye ( <b>18</b> ) in toluene under anoxic conditions . . . . .	66
10.1	<sup>1</sup> H-NMR spectrum of <i>cis/trans</i> -dichlorobis(dimethyl sulfide)platinum(II) ( <b>compound 1</b> ) . . . . .	81
10.2	<sup>1</sup> H-NMR spectrum of bis[dimethyl( $\mu$ -dimethyl sulfide)platinum(II)] ( <b>compound 2</b> ) . . . . .	82
10.3	<sup>1</sup> H-NMR spectrum of [PtMe <sub>2</sub> (COD)] ( <b>compound 7</b> ) . . . . .	83

---

10.4	<sup>1</sup> H-NMR spectrum of 2-(Tributylstannyl)pyridine ( <b>compound 10</b> ) . . . . .	84
10.5	<sup>1</sup> H-NMR spectrum of ( <b>compound 12a</b> ) . . . . .	85
10.6	<sup>1</sup> H-NMR spectrum of ( <b>compound 12b</b> ) . . . . .	86
10.7	<sup>1</sup> H-NMR spectrum of ( <b>compound 13</b> ) . . . . .	87
10.8	<sup>1</sup> H-NMR spectrum of ( <b>compound 14</b> ) . . . . .	88
10.9	<sup>1</sup> H-NMR spectrum of ( <b>compound 16 a</b> ) . . . . .	89
10.10	<sup>1</sup> H-NMR spectrum of ( <b>compound 16 b</b> ) . . . . .	90
10.11	<sup>1</sup> H-NMR spectrum of ( <b>compound 18</b> ) . . . . .	91
10.12	MALDI-TOF spectrum of ( <b>compound 18</b> ) in a DCTB matrix and corresponding isotope pattern . . . . .	92

---

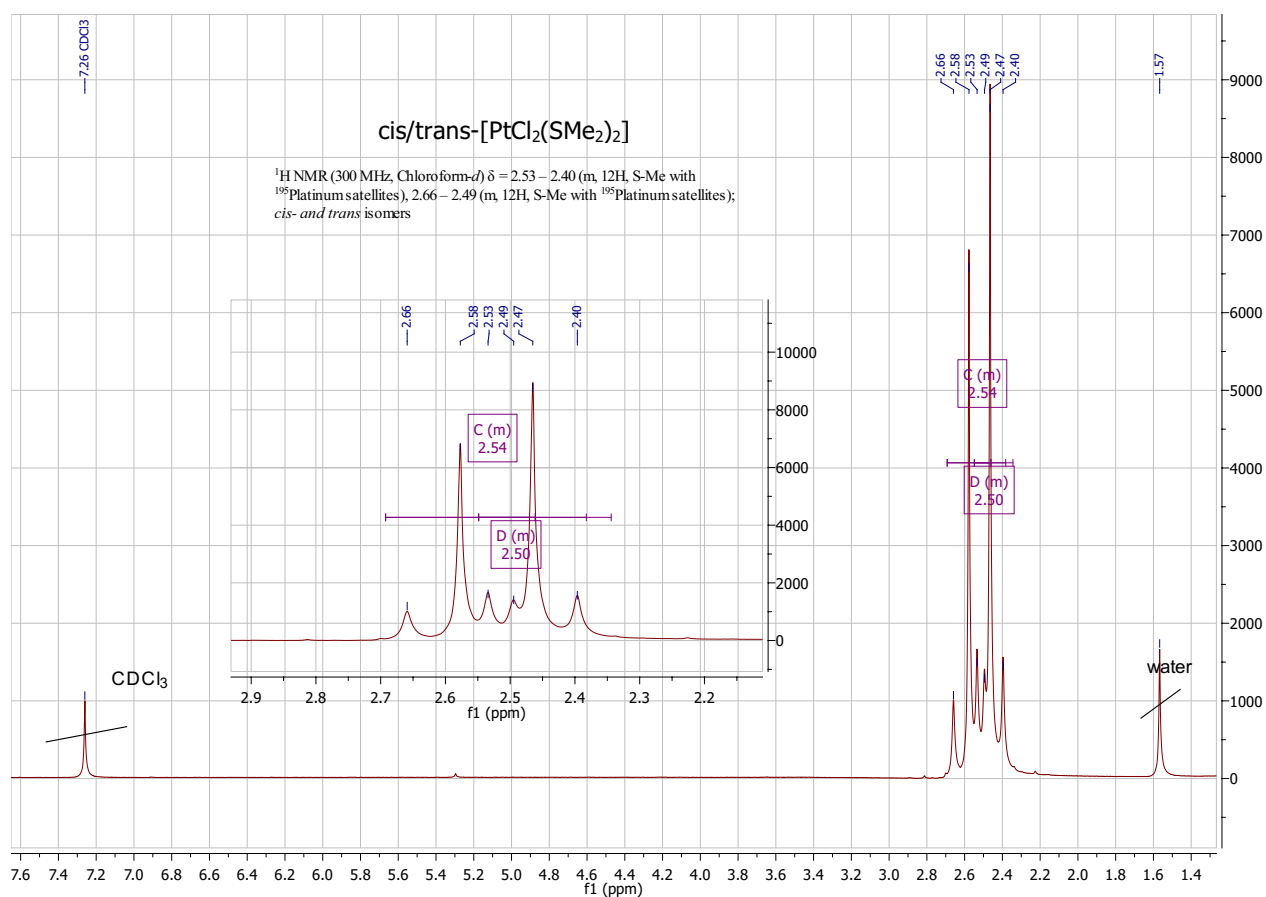
## 9 List of Tables

3.1	List of used chemicals . . . . .	24
3.2	List of used solvents . . . . .	25
5.1	Relative quantum yields of compound 14, the cyclometalated compound 18 and of the respective reference dyes and determined lifetimes . . . . .	66
10.1	List of abbreviations . . . . .	97

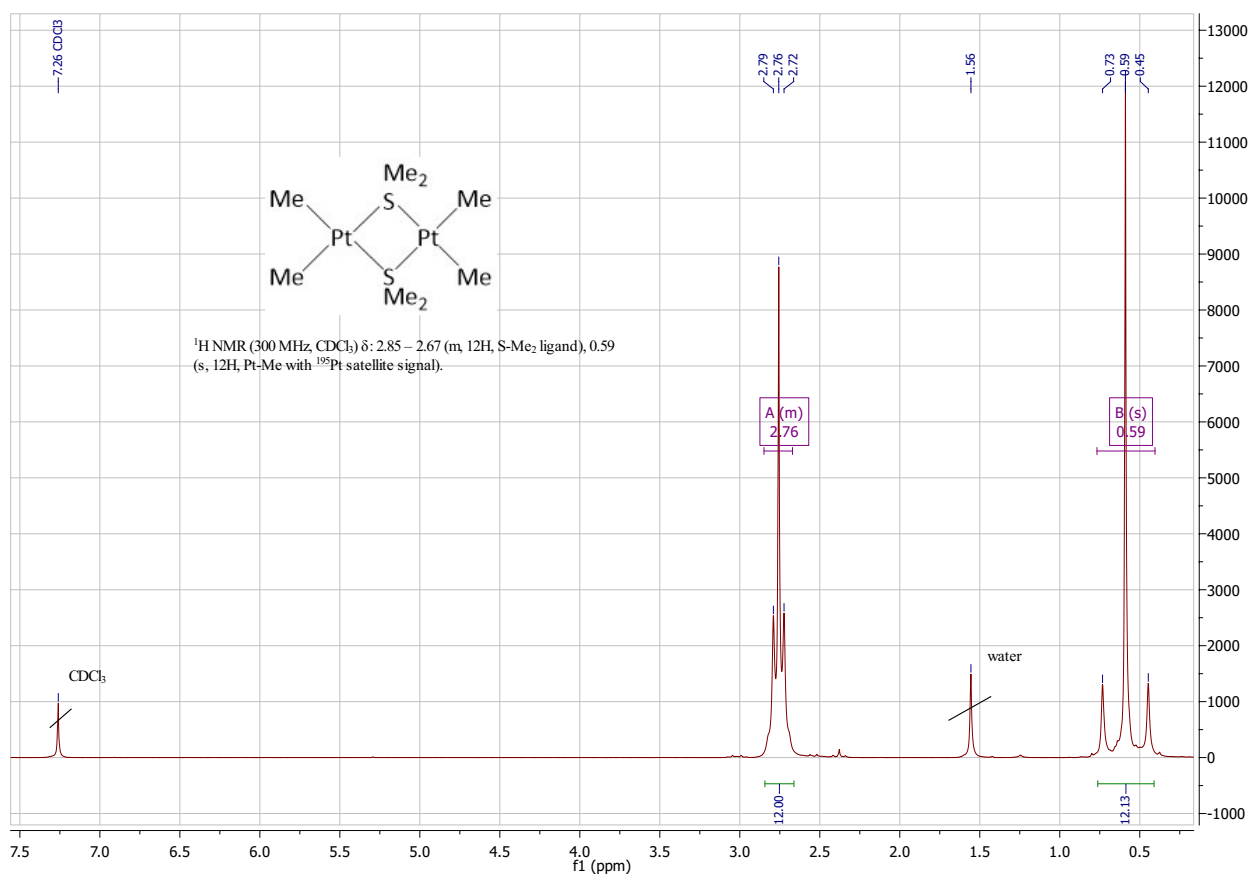
# 10 Appendix

## 10.1 NMR-spectra of synthesized compounds

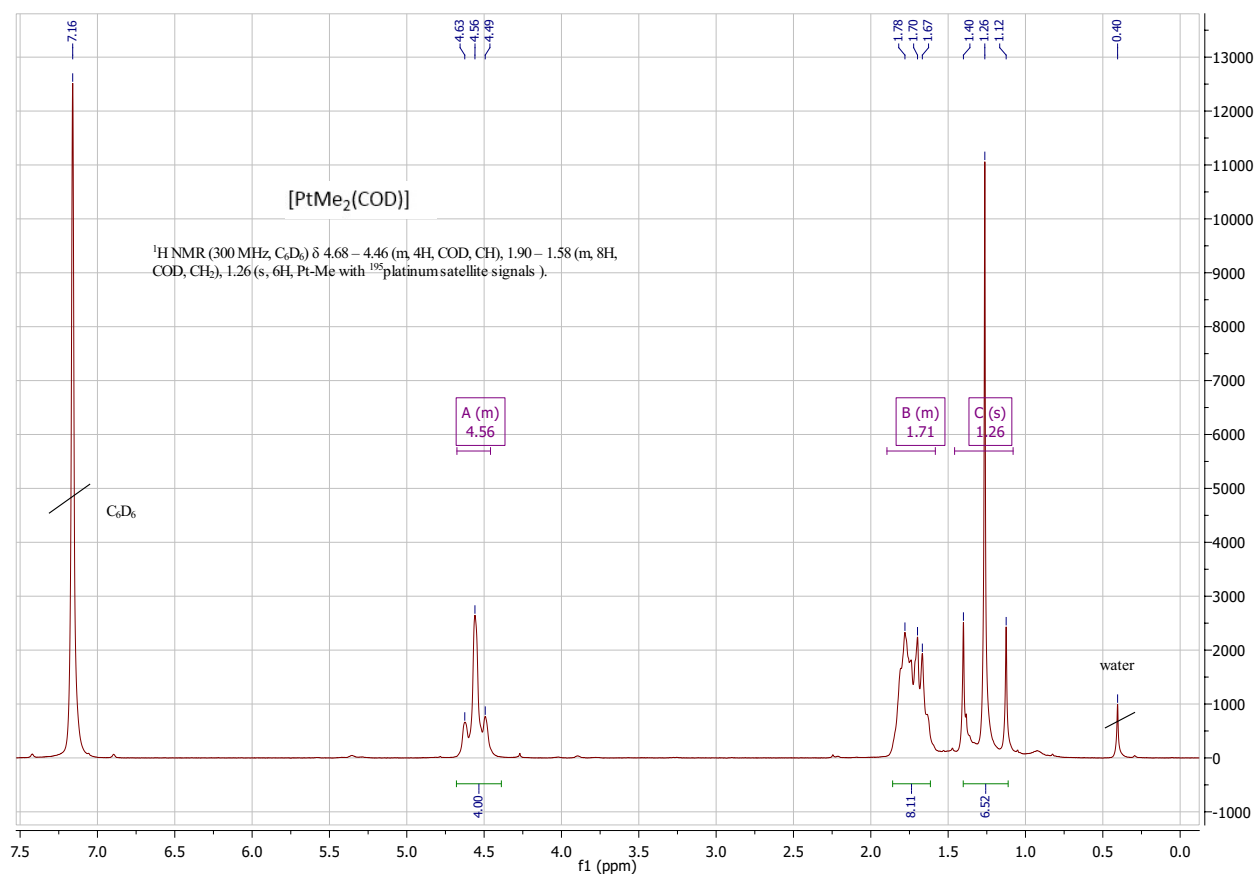
### 10.1.1 *Cis/trans*-dichlorobis(dimethyl sulfide)platinum(II) (compound (1))



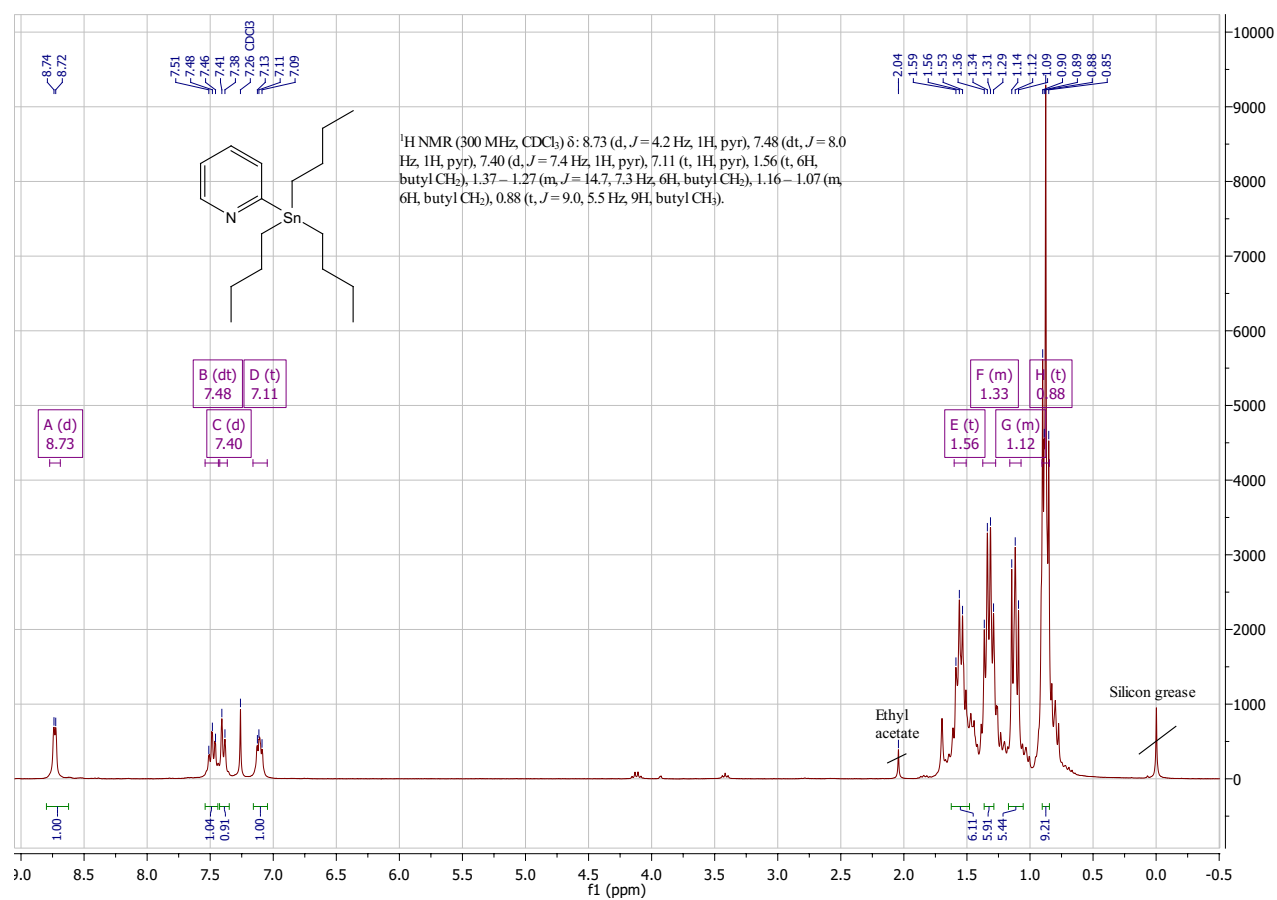
**Figure 10.1:** <sup>1</sup>H-NMR spectrum of *cis/trans*-dichlorobis(dimethyl sulfide)platinum(II) (compound 1)

10.1.2 Bis[dimethyl( $\mu$ -dimethyl sulfide)platinum(II)] (compound 2)

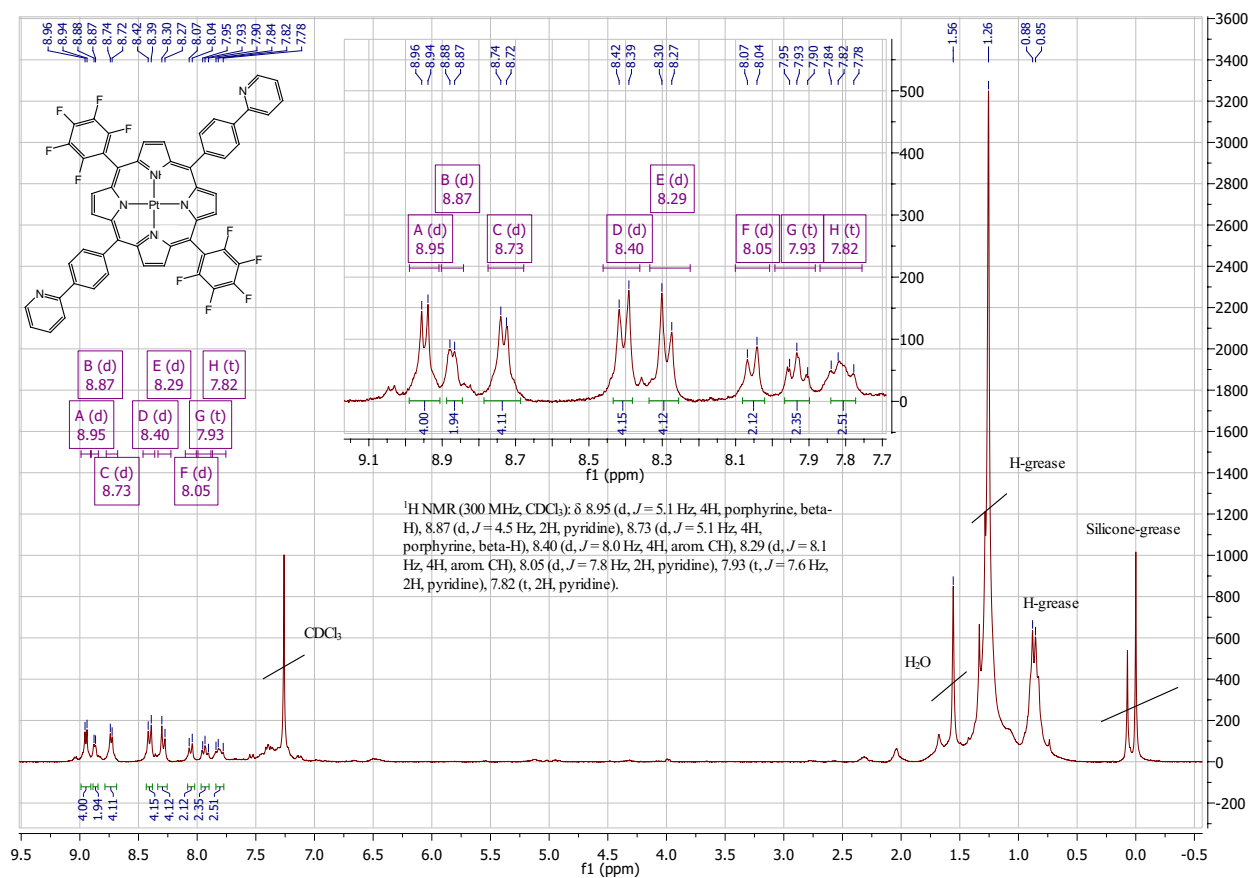
**Figure 10.2:**  $^1\text{H}$ -NMR spectrum of bis[dimethyl( $\mu$ -dimethyl sulfide)platinum(II)] (compound 2)

10.1.3 [PtMe<sub>2</sub>(COD)] (compound (7))**Figure 10.3:** <sup>1</sup>H-NMR spectrum of [PtMe<sub>2</sub>(COD)] (compound 7)

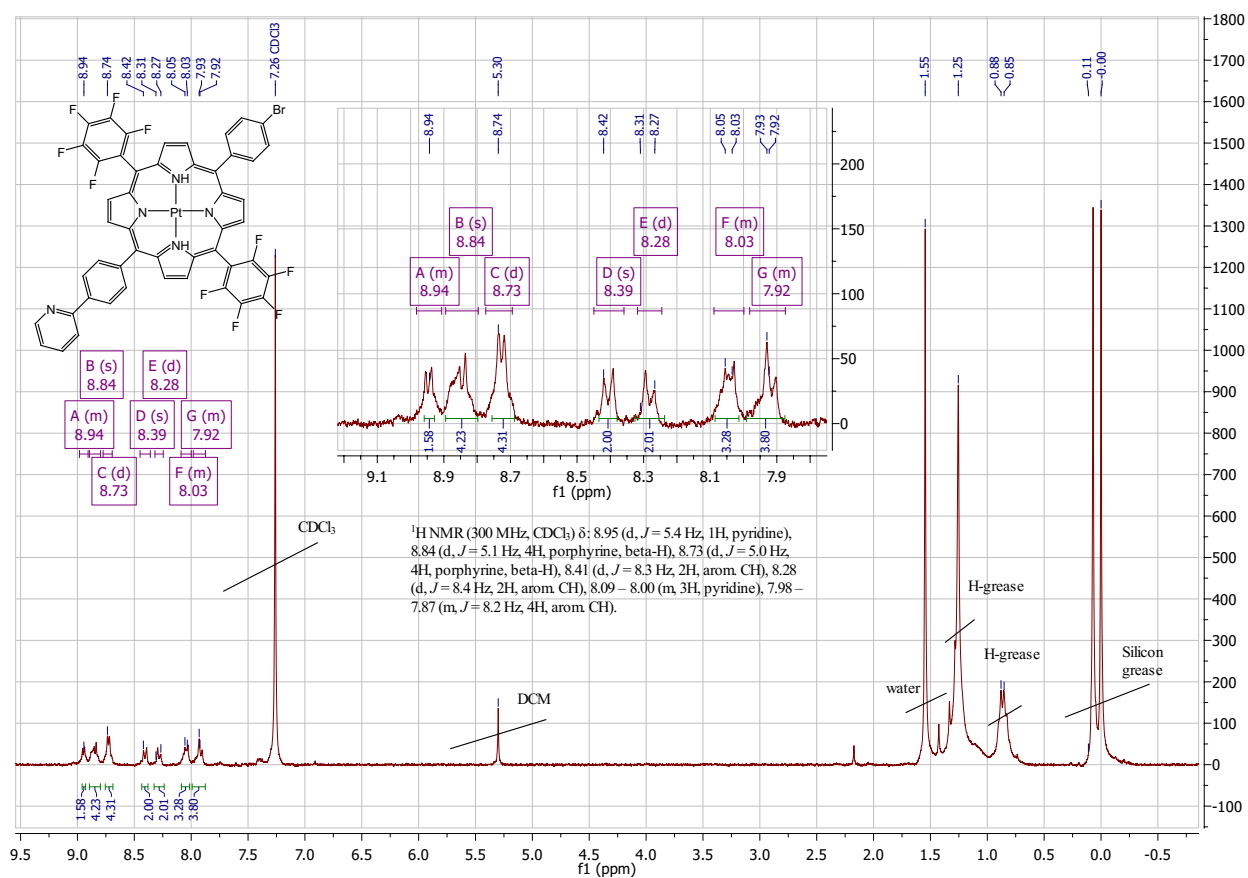
## 10.1.4 2-(Tributylstannyl)pyridine (compound (10))

Figure 10.4: <sup>1</sup>H-NMR spectrum of 2-(Tributylstannyl)pyridine (compound 10)

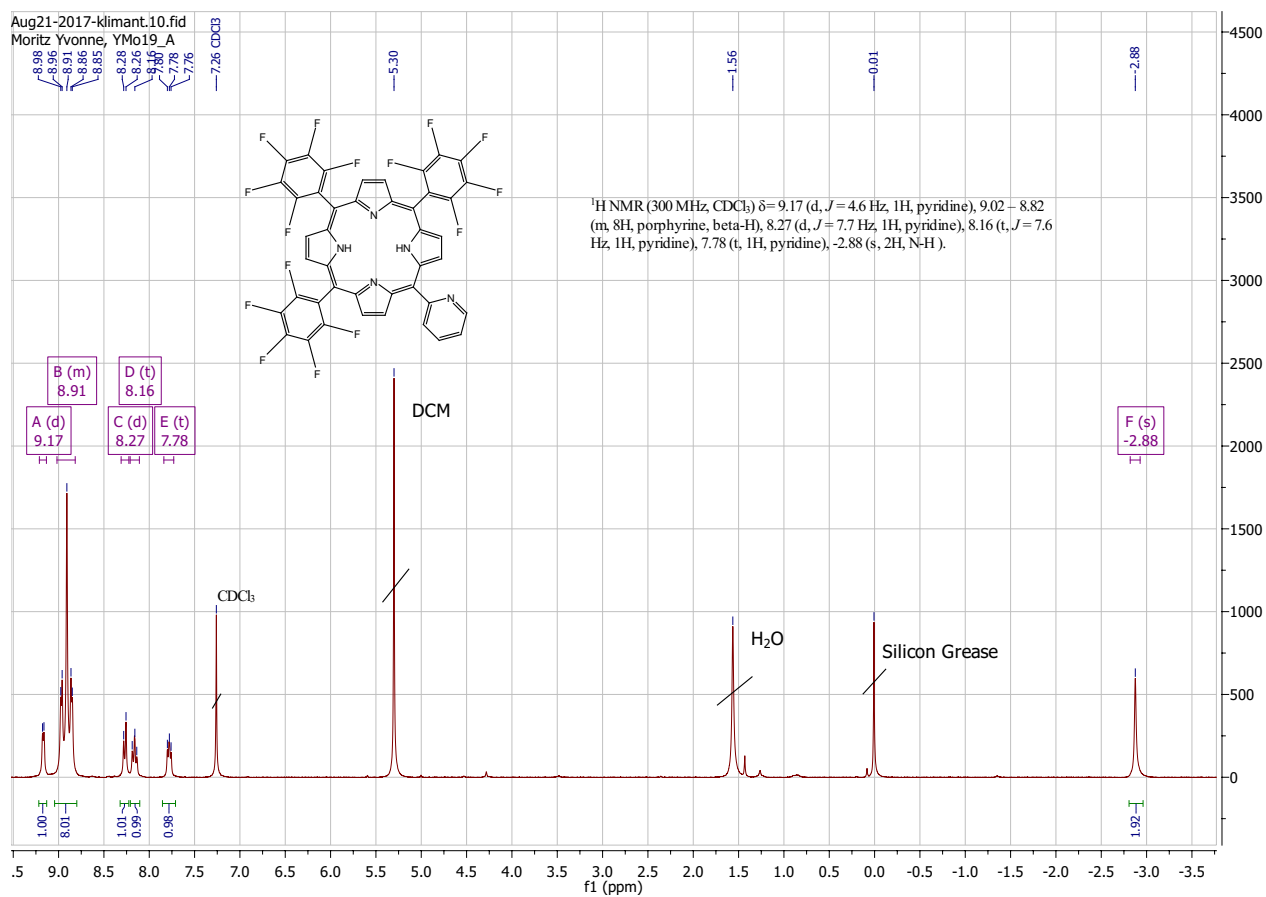
## 10.1.5 Disubstituted compound 12 (compound (12a))

Figure 10.5: <sup>1</sup>H-NMR spectrum of (compound 12a)

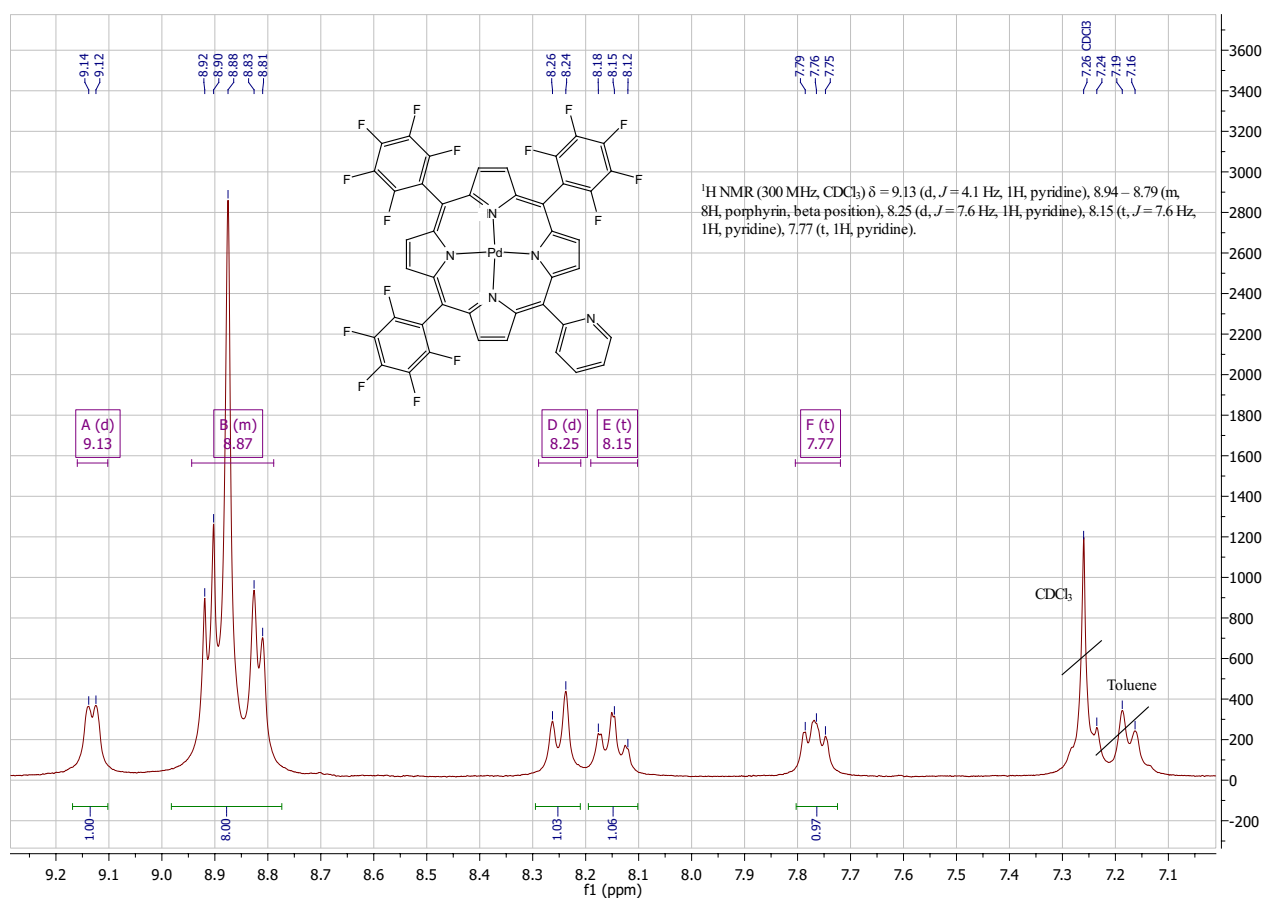
## 10.1.6 Monosubstituted compound 12 (compound (12b))

Figure 10.6: <sup>1</sup>H-NMR spectrum of (compound 12b)

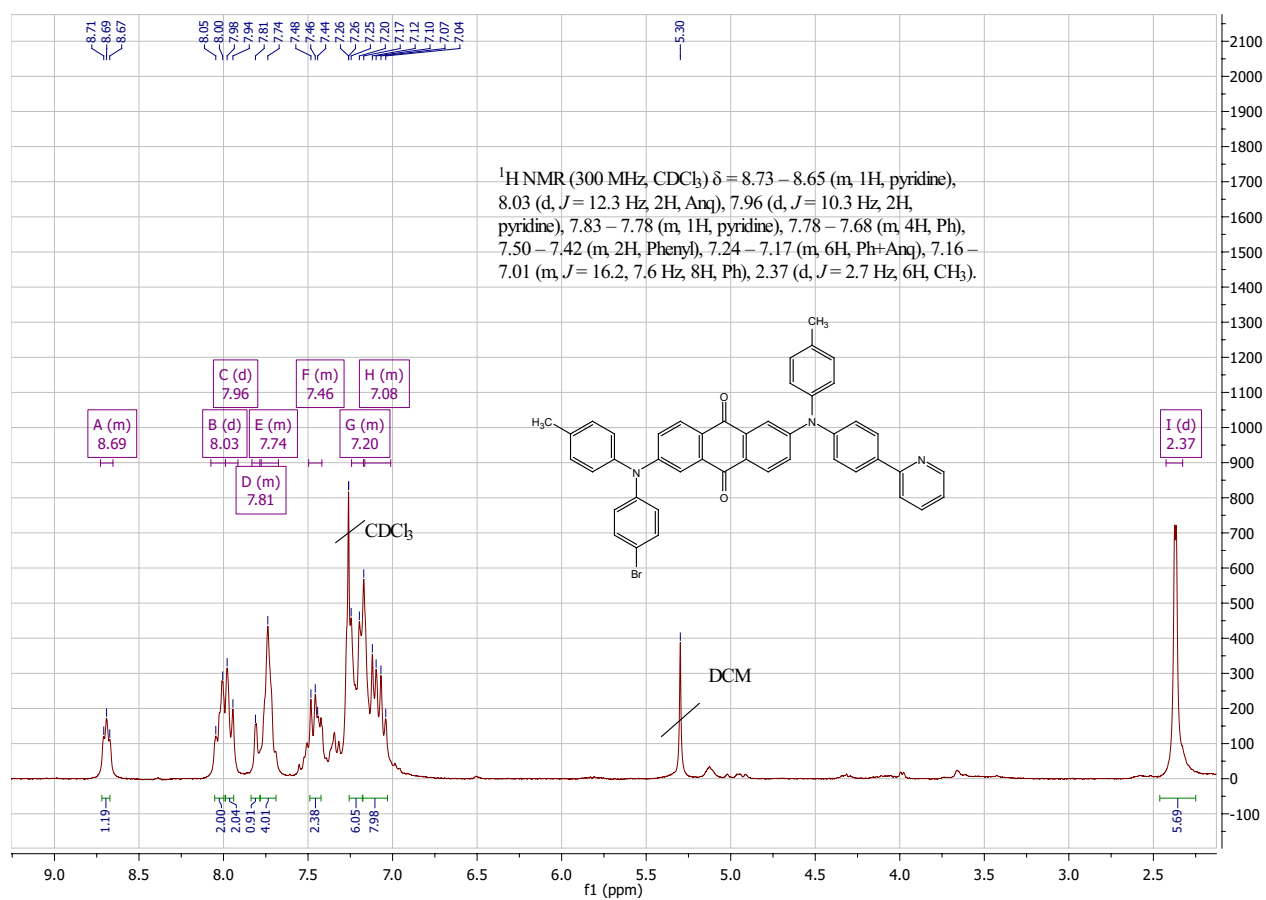
## 10.1.7 Porphyrin ligand (compound (13))

Figure 10.7:  $^1\text{H-NMR}$  spectrum of (compound 13)

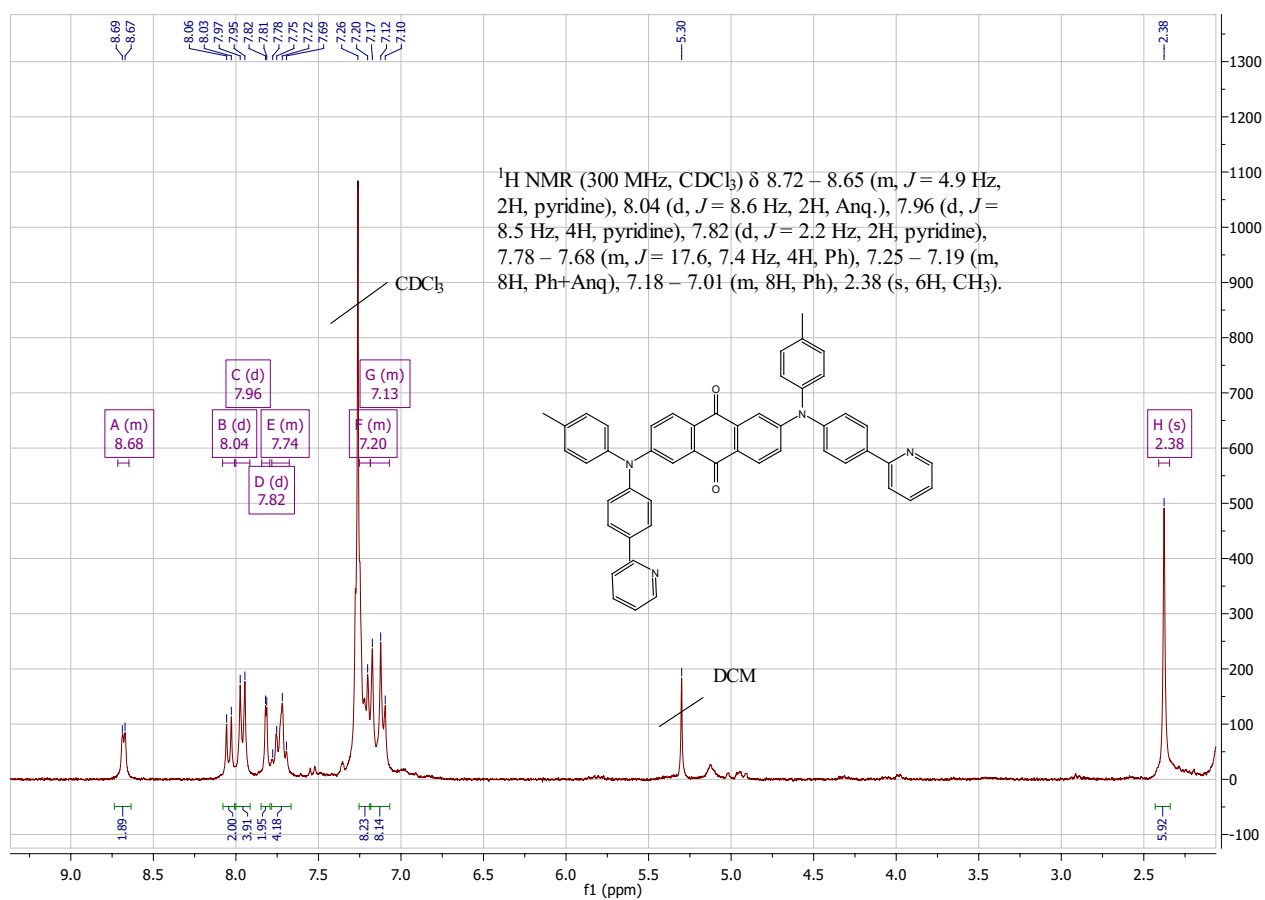
## 10.1.8 Pd-porphyrin-complex (compound 14)

Figure 10.8: <sup>1</sup>H-NMR spectrum of (compound 14)

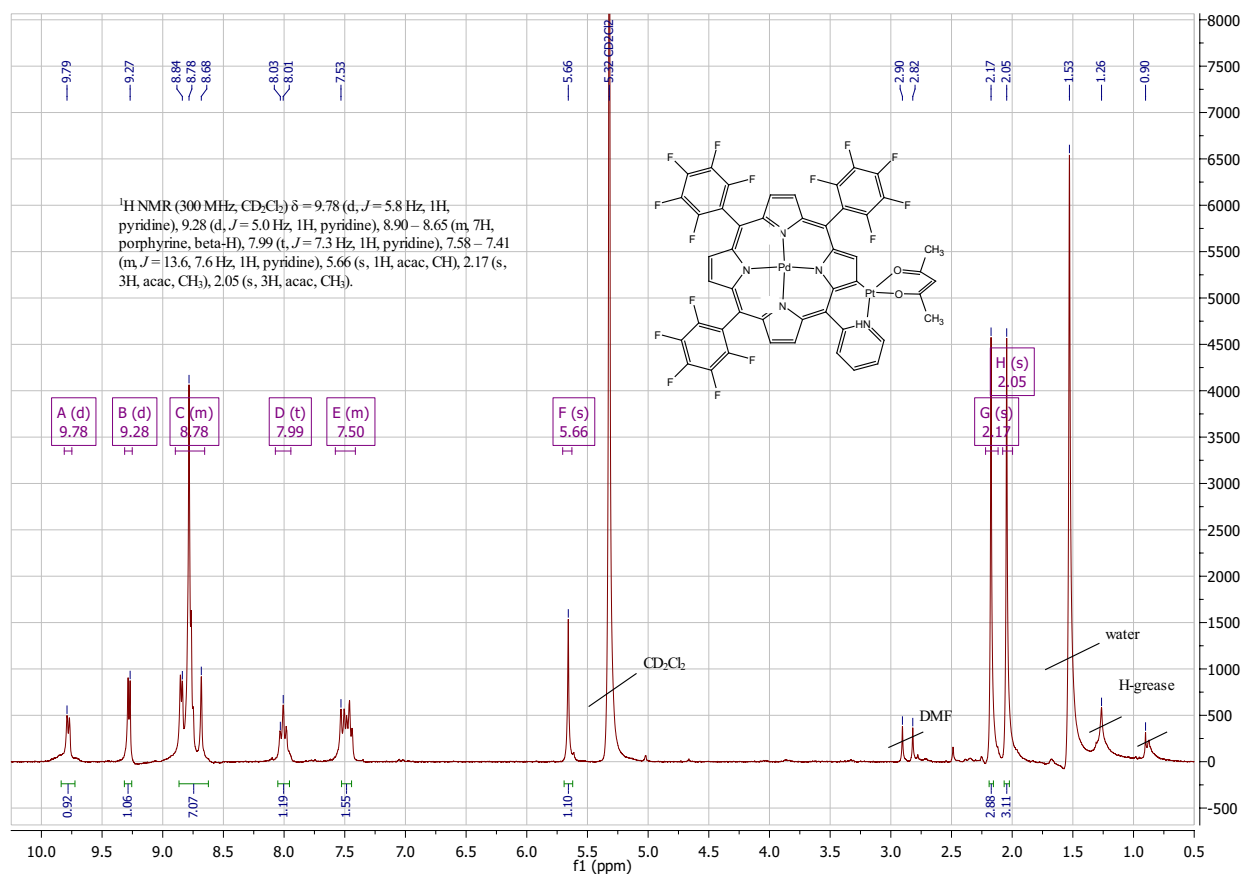
## 10.1.9 Monosubstituted compound (16 a)

Figure 10.9: <sup>1</sup>H-NMR spectrum of (compound 16 a)

## 10.1.10 Disubstituted compound (16 b)

Figure 10.10: <sup>1</sup>H-NMR spectrum of (compound 16 b)

## 10.1.11 Cyclometalated complex (compound 18)

Figure 10.11: <sup>1</sup>H-NMR spectrum of (compound 18)

## 10.2 MS-Data

## 10.2.1 Cyclometalated complex (compound 18)

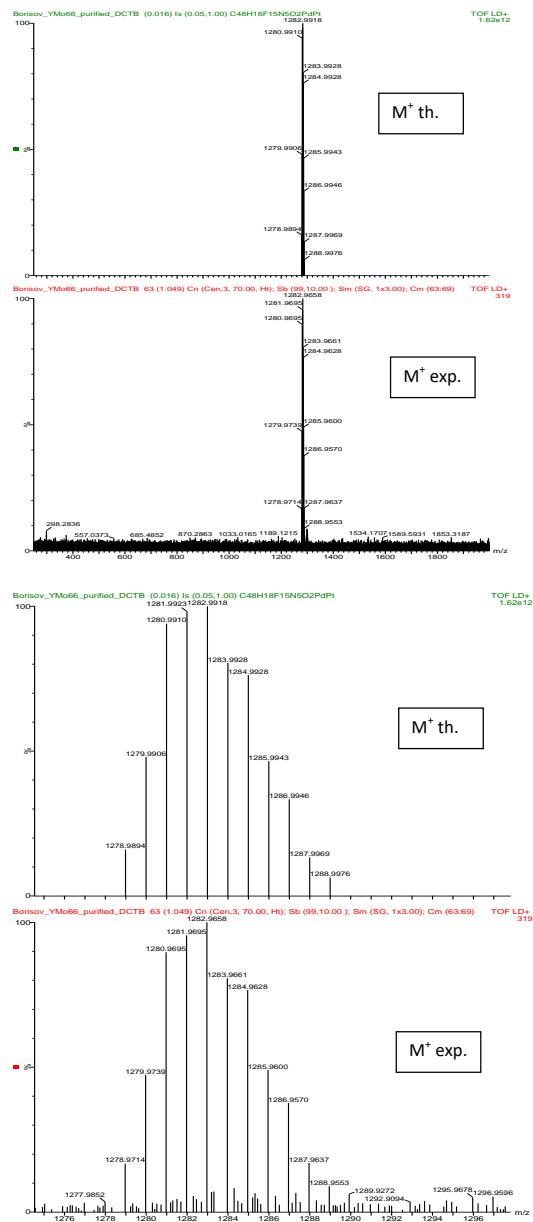


**Figure 10.12:** MALDI-TOF spectrum of (compound 18) in a DCTB matrix and corresponding isotope pattern

## 10.3 Supporting information for synthetic considerations

In this section all experimental procedures that were not carried out successfully will be described in detail.

### 10.3.1 Cyclometalation attempts using $K_2PtCl_4$

#### Pathway A leading to compound 19 a

This synthesis was performed analogously to reference [110].

The disubstituted Pt-complex (compound 12 a) (1 mg, 0.87  $\mu$ mol, 1 eq.) was dissolved in a Schlenk flask in ethoxyethanol/water (3:1) (3 ml) under argon-atmosphere.  $K_2PtCl_4$  (0.9 mg, 2.1  $\mu$ mol, 2.5 eq.) was dissolved in the same solvent mixture (0.5 ml) and added to the reaction vessel. The solution was heated to 80 °C and stirred for 12 hours. A black insoluble precipitate was formed which was filtered off. Acetylacetone (0.3 mg, 2.9  $\mu$ mol, 3.3 eq.) and  $Na_2CO_3$  (0.9 mg, 8.5  $\mu$ mol, 10 eq.) were added to the filtrate and the solution was heated again to 100 °C for 24 hours. However, the peaks in the UV-VIS spectrum of the reaction mixture did not shift compared to the educt mixture, wherefore it was assumed that no reaction took place.

#### Pathway B leading to compound 19 b

This reaction was carried out according to literature procedure [112].

The Pt-porphyrin dye (**12 b**) (2 mg, 1.75  $\mu$ mol, 1 eq.) was dissolved in 3 ml of acetic acid in a Schlenk flask under Ar-atmosphere.  $K_2PtCl_4$  (1.1 mg, 2.63  $\mu$ mol, 1.5 eq.) was dissolved in 50  $\mu$ l of distilled water and added to the mixture. The solution was heated to 110 °C and stirred for 67 hours. A red-brownish precipitate formed which was filtered off and washed with acetic acid (3 ml) and ethanol (3 ml). The precipitate (~0.5 mg) was dissolved in acetone (4 ml) in a Schlenk flask under Ar-atmosphere. Approximately 3 eq. of acetyl acetone (0.2 mg) and 10 eq. of sodium carbonate (1 mg) were added and the solution was refluxed at 50 °C for 24 hours. The UV-VIS spectrum that was measured afterwards did not show any different shifts compared to the educt spectrum. Nonetheless, the solvent was evaporated by rotary evaporation and the residue was treated with DCM and filtered. The solvent of the filtrate was removed again and a TLC of the porphyrin educt and the dry residue of the filtrate was performed. The TLC showed that no new cyclometalated product had formed.

#### Pathway C leading to compound 20 a

This synthesis was also performed analogously to reference [110].

The anthraquinone-based dye (**16 a**) (0.5 mg, 0.69  $\mu$ mol, 1 eq.) was dissolved in a Schlenk flask in ethoxyethanol/water (3:1) (3 ml) under Ar-atmosphere.  $K_2PtCl_4$  (1 mg, 1.7  $\mu$ mol, 2.5 eq.) was added and the solution was heated to 80 °C and stirred for 2 hours. After addition of distilled water (20 ml) no precipitated was obtained. Also centrifugation did not lead to isolation of a precipitate; the UV-VIS spectrum did not show any reaction progress.

#### Pathway D leading to compound 21

The Pd-porphyrin-complex (**14**) (1 mg, 1.0  $\mu$ mol, 1 eq.) was dissolved in a Schlenk flask in DMF/toluene (1:1) (3 ml).  $K_2PtCl_4$  (0.6 mg, 1.5  $\mu$ mol, 1.5 eq.) and NaOAc (0.8 mg, 7.3  $\mu$ mol, 7 eq.) were added and the solution was heated to 100 °C and stirred for 24 hours. UV-VIS spectra did not show formation of the cyclometalated compound (21).

### 10.3.2 Cyclometalation attempts using Pt(BN)<sub>2</sub>Cl<sub>2</sub>

#### Pathway A leading to compound 19 b

The mono-substituted Pt-porphyrin (**12 b**) (1.5 mg, 1.3  $\mu\text{mol}$ , 1 eq.) was dissolved in 1,2,4-trimethylbenzene (4 ml) in a Schlenk flask under Ar-atmosphere. Pt(BN)<sub>2</sub>Cl<sub>2</sub> (6.2 mg, 13.1  $\mu\text{mol}$ , 10 eq.) was added to the reaction vessel and the mixture was heated to 140 °C and stirred for 60 hours. Measured UV-VIS spectra showed no different shifts compared to the educt spectrum. Nevertheless, acetylacetone (0.39 mg, 3.9  $\mu\text{mol}$ , 3 eq) and sodium carbonate (1.4 mg, 13  $\mu\text{mol}$ , 10 eq.) were added and the solution was stirred at 135 °C overnight. Unfortunately, still no change of the absorption spectrum occurred, wherefore the reaction mixture was discarded.

#### Pathway B leading to compound 18

The Pd porphyrin complex (20 mg, 20.2  $\mu\text{mol}$ , 1 eq.) was dissolved in 1,2,4-trimethylbenzene (12 ml) in a Schlenk flask under Ar-atmosphere. The solution was heated to 120 °C and stirred until the dye was fully dissolved. Then, Pt(BN)<sub>2</sub>Cl<sub>2</sub> (95 mg, 0.20 mmol, 10 eq.) was added and the solution was stirred for three hours, while a green colour appeared. After three hours acetylacetone (25  $\mu\text{l}$ ) and triethylamine (25  $\mu\text{l}$ ) were added. A strong shift of the absorption spectrum of the reaction mixture compared to the educt could be observed. A TLC of the reaction mixture showed the formation of a complex product mixture. Nevertheless, separation via column chromatography (silica gel, DCM, then DCM + THF, then THF + methanol) was attempted. Several different fractions were obtained, however these fractions still showed several spots on the TLC plate and could not be further purified. A <sup>1</sup>H NMR was performed, but could not be interpreted due to severe impurities.

#### Pathway C leading to compound 22

The porphyrin ligand (5 mg, 5.7  $\mu\text{mol}$ , 1 eq.) was dissolved in 1,2,4-trimethylbenzene (8 ml) in a Schlenk flask under Ar-atmosphere. Pt(BN)<sub>2</sub>Cl<sub>2</sub> (27.3 mg, 57  $\mu\text{mol}$ , 10 eq.) was added and the solution was heated to 110 °C and stirred in an oil bath. After an hour an absorption spectrum was measured that showed two peaks (426 nm, 446 nm); after increasing the temperature to 140 °C just the peak at 426 was shown in the spectrum. Acetylacetone (10  $\mu\text{mol}$ ) and triethylamine (10  $\mu\text{mol}$ ) were added at room temperature and the solution was stirred for several minutes. The TLC showed that the reaction solution consisted of a mixture of many products. It was tried to purify the reaction mixture by column chromatography (silica, DCM, then DCM + THF), however all obtained fractions showed both peaks in the UV-VIS spectrum, wherefore it was assumed that these peaks could not be separated and no product was obtained.

### 10.3.3 Cyclometalation attempts using newly synthesized Pt-precursors

#### Pathway A leading to compound 22

The porphyrin ligand (**13**) (5 mg, 5.7  $\mu\text{mol}$ , 1 eq.) was dissolved in toluene (3 ml) in a Schlenk flask under Ar-atmosphere. The dimeric Pt-precursor (3.2 mg, 5.7  $\mu\text{mol}$ , 1 eq.) was added and the mixture was stirred for 4 hours at 90 °C. A shift to lower wavelengths was observed in the UV-VIS spectrum, wherefore 3 more equivalents of the precursor were added, as it was assumed that only insertion of the Pt-central atom took place. Also acetyl acetone (10  $\mu\text{l}$ ) and triethylamine (10  $\mu\text{l}$ ) were added to the reaction mixture and stirring was continued for 2

more hours. A column chromatography (silica, DCM) of the reaction mixture was performed, whereby only the non-cyclometalated Pt-complex could be isolated.

#### Pathway B leading to compound 18

The Pd-porphyrin complex (**14**) (3 mg, 3.0  $\mu\text{mol}$ , 1 eq.) was dissolved in toluene (3 ml) in a Schlenk flask under Ar-atmosphere. The dimeric Pt-precursor (**2**) was added and the solution heated to 80 °C. Absorption spectra were measured after 2 hours, however no conversion of the educt was visible. Even after addition of 3 more equivalents of the precursor no reaction progress could be obtained.

#### Pathway C leading to compound 25

The BODIPY dye (**24**) (3.0 mg, 8.84  $\mu\text{mol}$ , 1 eq.) was dissolved in THF (3 ml) in a Schlenk flask under Ar-atmosphere. The dimeric Pt precursor (**2**) (5.1 mg, 8.84  $\mu\text{mol}$ , 1 eq.) was added and the solution was heated to 65 °C and stirred for 5 hours. A shift to higher wavelenghts could be observed in the absorption spectrum, however the educt peak was still present. Addition of more equivalents of the precursor did not lead to further reaction progress. Therefore, acetylacetone (10  $\mu\text{l}$ ) and 1 mg of  $\text{Na}_2\text{CO}_3$  were added. The mixture was then stirred for another hour at room temperature. Afterwards, purification via column chromatography was attempted. However TLCs (silica, DCM+THF) showed that a complex mixture of many products had formed that could not be separated.

#### Pathway D leading to compound 23

The Pd-porphyrin dye (**14**) (1 mg, 1.0  $\mu\text{mol}$ , 1 eq.) was dissolved in 1,2,4-trimethylbenzene (3 ml) in a Schlenk flask under Ar-atmosphere.  $\text{PtMe}_2(\text{COD})$  (**2**) (0.5 mg, 1.5  $\mu\text{mol}$ , 1.5 eq.) was added and the mixture was heated to 166 °C. No conversion could be seen in the UV-VIS spectrum, wherefore it was assumed that no cyclometalation took place.

### 10.3.4 Attempted optimization of reaction conditions for the cyclometalation of compound 14

All optimization reactions followed the same general procedure. The Pd-complex (**14**) (1 mg, 1.0  $\mu\text{mol}$ , 1 eq.) was dissolved in 1 ml of the respective solvent in a subvelco vial equipped with septum and stirring bar. The vial was flooded with argon for approximately 5 minutes. Then the Pt-precursor (**4**) (1.2 mg, 3.0  $\mu\text{mol}$ , 3 eq.) was dissolved in 0.3 ml of the respective solvent and added to the reaction mixture, which was again flooded with argon for 3 minutes. Then, the vials were heated in a heating block and absorption spectra of the different solutions were measured after several hours. The reaction time and temperature for each solvent is shown in the list below.

**DMF:** 148 °C, 2 hours

**DMSO:** 185 °C, 3 hours

**Benzonitrile:** 185 °C, 3 hours

**NMP:** 195 °C, 1 hour

**DMF/toluene:** 100 °C, 6 hours [109, 111]

**1,2,4-trimethylbenzene (tributylamine):** 160 °C, 1 hour

Only regarding the reaction performed in BN, conversion of the educt could be observed in the

spectrum. However, TLCs showed that the amount of formed product was lower than when using the standard procedure in 1,2,4-trimethylbenzene.

### 10.3.5 Further attempted cyclometalation reactions using compound 4 as a precursor

#### Pathway A leading to compound 19 b

The Pt-porphyrin (**12 b**) (4.5 mg, 3.9  $\mu\text{mol}$ , 1 eq.) was dissolved in 1,2,4-trimethylbenzene (3 ml) in a Schlenk flask under Ar-atmosphere. The Pt-precursor (**4**) (2.9 mg, 7.1  $\mu\text{mol}$ , 1.8 eq.) was added and the solution was stirred for 2 hours at 160 °C. No shift of the absorption spectrum could be observed, however the TLC (CH+EE 4+1) showed the formation of new compounds. It was attempted to separate this mixture by column chromatography (silica, CH+EE 4+1), however due to bad movement on the silica gel only mixed fractions could be obtained.

#### Pathway B leading to compound 20 a

The anthraquinone-based dye (**16 a**) (5 mg, 6.9  $\mu\text{mol}$ , 1 eq.) was dissolved in 1,2,4-trimethylbenzene (3 ml) in a Schlenk flask under Ar-atmosphere. The Pt-precursor (**4**) (5.1 mg, 12.4  $\mu\text{mol}$ , 1.8 eq.) was added and the solution was stirred for 2 hours at 160 °C. No shift of the absorption spectrum could be observed, however the TLC (CH+EE 3+1) showed the formation of new compounds. It was attempted to separate this mixture by column chromatography (silica, CH+EE 3+1), however due to bad movement on the silica gel only mixed fractions could be obtained.

## 10.4 Abbreviations

Table 10.1: List of abbreviations

Abbreviation	Name
UV	Ultraviolet
NIR	Near-infrared
OLED	Organic light-emitting diode
ISC	Intersystem crossing
IC	Internal conversion
LUMO	Lowest unoccupied molecular orbital
HOMO	Highest occupied molecular orbital
CAS	Chemical Abstracts Service
R <sub>f</sub> -value	Retention factor
TLC	Thin layer chromatography
KCl	Potassium chloride
Acac	Acetylacetone
Pd(PPh <sub>3</sub> ) <sub>4</sub>	Tetrakis(triphenylphosphine)palladium(0)
N <sub>2</sub>	Nitrogen
Ar	Argon
KOH	Potassium hydroxide
COD	Cyclooctadiene
Et <sub>3</sub> N	Triethylamine
NH <sub>4</sub> Cl	Ammonium chloride
NaOAc	Sodium acetate
Na <sub>2</sub> CO <sub>3</sub>	Sodium carbonate
DCM	Dichloromethane
THF	Tetrahydrofuran
EE	Ethyl acetate
CH	Cyclohexane
Tol	Toluene
DMF	Dimethylformamid
BN	Benzonitrile
NMP	N-Methyl-2-pyrrolidon
DMSO	Dimethylsulfoxide
CDCl <sub>3</sub>	Deuterated chloroform
CD <sub>2</sub> Cl <sub>2</sub>	Deuterated dichloromethane
C <sub>6</sub> D <sub>6</sub>	Deuterated benzene
n-Buli	n-Butyllithium
MeLi	Methylithium
QY	Quantum yield
MS	Mass Spectrometry
MALDI	Matrix Assisted Laser Desorption Ionization
TOF	Time of Flight

